

**Abnormalities in the Testis,
Reduced Sperm Counts
and Decreased Motility Parameters
in Huntingtin-Interacting Protein 1 (HIP1)
Deficient Mice.**

**Abnormalities in the Testis, Reduced Sperm Counts
and Decreased Motility Parameters in
Huntingtin- Interacting Protein 1 (HIP1) Deficient Mice.**

Karine Khatchadourian
Anatomy and Cell Biology
McGill University, Montreal
October, 2005

A thesis submitted to McGill University in partial fulfillment of the requirements of the degree of Masters of Science.

Copyright © Karine Khatchadourian 2005



Library and
Archives Canada

Bibliothèque et
Archives Canada

Published Heritage
Branch

Direction du
Patrimoine de l'édition

395 Wellington Street
Ottawa ON K1A 0N4
Canada

395, rue Wellington
Ottawa ON K1A 0N4
Canada

Your file *Votre référence*
ISBN: 978-0-494-22737-4
Our file *Notre référence*
ISBN: 978-0-494-22737-4

NOTICE:

The author has granted a non-exclusive license allowing Library and Archives Canada to reproduce, publish, archive, preserve, conserve, communicate to the public by telecommunication or on the Internet, loan, distribute and sell theses worldwide, for commercial or non-commercial purposes, in microform, paper, electronic and/or any other formats.

The author retains copyright ownership and moral rights in this thesis. Neither the thesis nor substantial extracts from it may be printed or otherwise reproduced without the author's permission.

AVIS:

L'auteur a accordé une licence non exclusive permettant à la Bibliothèque et Archives Canada de reproduire, publier, archiver, sauvegarder, conserver, transmettre au public par télécommunication ou par l'Internet, prêter, distribuer et vendre des thèses partout dans le monde, à des fins commerciales ou autres, sur support microforme, papier, électronique et/ou autres formats.

L'auteur conserve la propriété du droit d'auteur et des droits moraux qui protègent cette thèse. Ni la thèse ni des extraits substantiels de celle-ci ne doivent être imprimés ou autrement reproduits sans son autorisation.

In compliance with the Canadian Privacy Act some supporting forms may have been removed from this thesis.

Conformément à la loi canadienne sur la protection de la vie privée, quelques formulaires secondaires ont été enlevés de cette thèse.

While these forms may be included in the document page count, their removal does not represent any loss of content from the thesis.

Bien que ces formulaires aient inclus dans la pagination, il n'y aura aucun contenu manquant.


Canada

To Dr. Hermo and the Khatchadourian clan...

Table of Contents

<i>Table of contents</i>	iv
<i>Acknowledgements</i>	vi
<i>Contribution of authors</i>	viii
<i>List of abbreviations</i>	ix
<i>Abstract</i>	x
<i>Résumé</i>	xi

Chapter I: Literature Review

The Male Reproductive System	1
Testis Histology and Function	1
Cell Types of the Testis and Function	2
Leydig cells	2
Myoid cells	3
Sertoli cells	3
Germ cells and Spermatogenesis	6
<i>The Proliferative phase</i>	6
<i>The Meiotic phase</i>	7
<i>The Spermiogenic phase</i>	8
Sperm Head	8
Development of the acrosome	8
Structure of the acrosome	9
Nuclear shaping	10
<i>The Acrosome-Acroplaxome complex</i>	11
<i>The Manchette</i>	12
<i>The Perinuclear theca</i>	13
Reorganization of the cytoplasm and organelles	13
Sperm Flagellum	14
Completion of Spermiogenesis	16
Staging of Spermatogenesis	17

Huntingtin-interacting protein 1	19
Interaction with huntingtin protein	20
Genome	20
Localization	21
Clathrin-Mediated endocytosis	21
Functional significance of HIP1 in Clathrin-mediated endocytosis	22
Function in apoptosis, tumorigenesis and regulation of receptors	26
Huntingtin protein	27
Role for Huntingtin in the testis	28
HIP1-/- Phenotype	28
Objectives of the current study	29
References	32
Chapter II: Abnormalities in the Testis, Reduced Sperm Counts, and Altered Sperm Motility Measures Are All Detected in HIP1-Deficient Mice	
Title page	55
Abstract	56
Introduction	57
Materials and Methods	59
Results	65
Discussion	72
Acknowledgments	80
Figures, Graphs, Table and Legends	81
References	96
Chapter III: Summary	105

Acknowledgements

I would like to take this opportunity to thank all those individuals who provided me invaluable assistance throughout this thesis.

I would first like to express a tremendous amount of gratitude to my supervisor, Dr. Hermo. For your support, guidance, patience, humour and tremendous kindness over the past three years, I am sincerely grateful and lucky. You sparked my interest for research and taught me to keep striving for the best because “the better is the enemy of the good”. Being in Strathcona with you provided me with numerous memorable moments and I will always remember the wonderful conversations we shared on music, movies, sports, family and health.

A very special thanks goes to Dr. Smith and Dr. Morales. The two professors can be considered as assistant supervisors since they both guided me and assisted in my research. Dr. Smith, thank you for teaching me the wonders of statistics; numbers and graphs couldn't have been taught in a more stimulating way!

Thank you to Dr. Hayden and Dr. Metzler from Vancouver. A special thanks to Dr. Metzler for guiding me through my project and answering all questions pertaining to the HIP1 protein.

A thanks to the new professors of Strathcona: Dr. Davis and Dr. Mandato, your energy and enthusiasm for science are much appreciated by students in this department.

A special thank to all members of the department: students, professors, secretaries, for the pleasant working environment.

I would also like to thank Dr. Cyr and Mary Gregory for allowing me to use their lab equipment for parts of my research. Mary, it was a pleasure conducting sperm motility tests with you and munching on dark chocolate...

A special thanks for Susan and Helmut from Neurophotography and for Jeannie Mui. Your technical assistance sure helped my figures look spectacular. Thanks for your patience, advice, and expertise!

Thanks to my fellow graduates, Amit, Ricardo, Kizzy, Nadine, Jacob, Haitham and Faisal along with Robert. Thank you for the wonderful lunches and talks. You made the stay so enjoyable! A special thanks to Nadine for being the head graduate student who was always ready to answer my questions and guide me through my lab work. Thank you to the undergraduates of Dr. Hermo's lab: Soriaya and Lianne.

Haitham, thank you for your drawings and your generous help!

And at last, to my family and friends.

To my family, Mom, Dad, Katia, Rouben, Haig, Wendy and Little Emma and friends Maha, Val, Kat, Alex, Naz, Patil and Sero, God bless you all.

THANK YOU for fueling me with positive energy and love, supporting me through my daily decisions and encouraging me in all my endeavours. Thank you.

Contribution of Authors

The HIP1 knockout mice were generated by the lab of Dr. Michael R. Hayden at the Centre for Molecular Medicine and Therapeutics, Department of Medical Genetics at University of British Columbia in Vancouver British Columbia.

Dr. Louis Hermo, from the Department of Anatomy and Cell Biology at McGill University, provided me guidance and suggestions throughout my years as a master's student and has been very helpful in editing the paper presented in this thesis.

Dr. Charles E. Smith, from the Department of Stomatology at the University of Montreal has conducted the statistical analysis of the many parameters presented in the second chapter and has also been helpful in editing the paper. Thank you.

Dr. Daniel Cyr and Mary Gregory, from the INRS-Institute Armand Frappier in Pointe-Claire, have permitted me to conduct all sperm counts and motility analyses using the CASA system (computer assisted sperm analysis) in their laboratory and have guided me throughout the data acquisition. They also contributed as co-authors for the paper presented in the second chapter.

Dr. Martina Metzler and Dr. Michael Hayden performed the western blots and collected the fertility data presented in the paper of the second chapter. They also appear as co-authors for the paper.

Haitham Badran did the schematic drawing (fig.12) for the paper in the second chapter.

LIST OF ABBREVIATIONS

AP-2: adaptor-binding protein 2
ALH : amplitude of lateral head displacement
ANTH : AP180 N-terminal homology domain
BCF : beat cross frequency
CASA : computer assisted sperm analysis
CCV : clathrin coated vesicles
CLC : clathrin light chain
CHC : clathrin heavy chain
Elong : elongation
ENTH : epsin N-terminal homology domain
HIP1 : huntingtin interacting protein 1
HIP1r : huntingtin interacting protein 1
Htt : huntingtin protein
HD : huntingtin's disease
IAM : inner acrosomal membrane
IVOS : integrated visual optical system
LIN : linearity
OAM : outer acrosomal membrane
PIP : phosphatidylinositol-4,5-bisphosphate
STR : straightness
TGN : trans-Golgi network
VAP : smoothed path velocity
VCL : track velocity
VSL : straight line velocity
WT : wild type
% slow : percentage of slow sperm
% medium : percentage of medium sperm
% rapid : percentage of rapid sperm

ABSTRACT

Huntingtin interacting protein- 1 (HIP1) is an endocytic protein that associates with clathrin on coated vesicles, but it also binds directly to actin and microtubules. Close histological examination of the testis of HIP1 $-/-$ mice from 7-30 wks of age revealed that HIP1-deficiency was particularly detrimental to spermatids. The testis showed a significant decrease in the diameter of seminiferous tubules, a reduction in the number of late spermatids and the sloughing of germ cells, which were evident as round cells in the epididymal lumen. Major abnormalities in spermatids included structural deformations of heads, bent flagella, the presence of proacrosomic vesicles with the complete or partial absence of an acrosome or its detachment from the nucleus, and retention of the cytoplasm enveloping the spermatid head. Abnormalities with respect to the association of elongating spermatids with ectoplasmic specializations of Sertoli cells were noted as well. Sperm counts and sperm motility parameters were significantly decreased in HIP1 $-/-$ mice compared to their wild-type littermates and these differences accounted for reduced fertility levels noted in HIP1 $-/-$ mice.

Taken together, differences in sperm counts, morphology and their motility parameters suggest a functional role for HIP1 in relation to actin and microtubules during sperm development in the testis.

RÉSUMÉ

La protéine qui interagit avec la protéine huntingtin (HIP1) est une protéine impliquée dans l'endocytose qui s'associe aux vésicules enrobées de clathrine et qui se lie aussi avec l'actine et les microtubules.

Un examen histologique plus précis des testicules de souris HIP1^{-/-}, âgées de 7 à 30 semaines, a montré qu'une déficience de HIP1 avait un effet particulièrement néfaste pour les spermatides. Dans les testicules, une baisse significative du diamètre des tubules séminifères a été observée, une réduction du nombre de spermatides en stade avancé et une perte de cellules germinales qui apparaissent comme des cellules rondes dans la lumière epididymaire. Les anomalies principales notées dans les spermatides étaient : déformation structurelle au niveau de la tête, courbure du flagelle, l'absence partielle ou complète d'une acrosome ou sa détachement du noyau, et la rétention de cytoplasme qui englobe la tête du spermatide. Des anomalies ont aussi été observés aux sites de spécialisations ectoplasmiques des cellules de Sertoli qui maintiennent les spermatides qui s'allongent. Une baisse significative du nombre de spermatozoïdes et des paramètres de motilité des spermatozoïdes a été observée dans les souris HIP1^{-/-} en comparaison avec les souris issues de souche sauvage. Ces différences expliquent la baisse du niveau de fertilité notée dans les souris HIP1^{-/-}. L'ensemble de ces effets néfastes sur le nombre de spermatozoïdes, sur la morphologie et sur les paramètres de motilité suggère que HIP1 joue un rôle dans les testicules avec l'actine et les microtubules au niveau de la spermatogenèse.

Chapter I

Literature Review

The Male Reproductive System

The male reproductive tract includes the following organs: two testes, the rete testis, a system of paired genital ducts (efferent ducts, epididymis, vas deferens), the male accessory sex glands (seminal vesicles, prostate, bulbourethral glands) and the penis. Testosterone synthesis along with the production of germ cells occurs in the testis. Germ cells undergo mitotic and meiotic divisions and eventual metamorphose into a specialized haploid cell, the sperm. The immature sperm isn't capable of fertilizing a viable oocyte from the female reproductive tract yet. The sperm first pass through the efferent tubules, where water absorption concentrates the sperm as they enter the epididymis. Sperm then travel through the epididymis where sperm interacts with epididymal secretions of nutrients, hormones, ions and proteins rendering the sperm motile and fertile (Hermo et al., 1994; Robaire and Hermo, 1998).

The rete testis, efferent ducts, epididymis, and vas deferens are collectively termed the excurrent duct system. These structures are embryologically derived from the Wolffian ducts under the influence of androgens produced by fetal testis (Jost, 1973; Wilson et al., 1981). The epididymis is the site of sperm maturation while the vas deferens is responsible for the final transport of sperm to the urethra and the final delivery out of the body (Robaire and Hermo, 1998).

The prostate, bulbourethral glands and seminal vesicles form the accessory sex glands. They contribute to the formation of semen by secreting various substances (Price and Williams-Ashman, 1961; Mann and Lutwak-Mann, 1981; Williams-Ashman, 1983).

Testis Histology and Function

The testes are paired oval structures that, in many species, are located in an out-pocketing of skin known as the scrotum. This location of the testis ensures spermatogenesis to proceed normally at a lower temperature than the rest of the body (Setchell, 1982). The testis are encapsulated by a thick dense connective tissue known as the tunica albuginea (Davis et al., 1970; Leeson and Cookson, 1974).

In some species, like in the human, extensions from thickened areas of the tunica albuginea form septa to divide the substance of the testis into lobules. The tunica vasculosa, a highly vascularized loose tissue layer, is found adjacent to the tunica albuginea.

The testis is made up of numerous highly convoluted seminiferous tubules and interstitial spaces. The seminiferous tubules exist as loops with both ends anastomosing with the network of tubes known as the rete testis (Clermont and Huckins, 1961). The seminiferous tubules are lined by the seminiferous epithelium which consists of two types of cells: germ cells and the supportive Sertoli cells. Germ cells are found at varying stages of development evolving into gametes and include: the stem cells, spermatogonia; the cells of meiosis, primary and secondary spermatocytes; the round and elongated spermatids; as well as the spermatozoa. The supporting Sertoli cells remain at the base of the epithelium with cytoplasmic extensions reaching the tubular lumen. At the periphery of this epithelium, a limiting membrane is found consisting of connective tissue elements and contractile myoid cells (Clermont, 1958; Dym and Fawcett, 1970).

The testicular interstitial spaces, a richly vascularized loose connective tissue located between the seminiferous tubules, contains blood and lymph vessels and nerves of the testicular parenchyma (Fawcett et al., 1973; Clark, 1976). Testosterone secreting Leydig cells, macrophages and mast cells are also located in these spaces (Christensen, 1975; Mori and Christensen, 1980; Nistal et al., 1984).

Cell Types of the Testis and Function

Leydig cells

In the testicular interstitium, Leydig cells constitute the major cell type (Christensen, 1975; Mori and Christensen, 1980). They are often found in clusters or groups around the many vessels of the intertubular space where they have easy access to circulating cholesterol. They can also form isolated clusters surrounding the seminiferous tubules. Leydig cells have an ovoid shape with an eccentrically located nucleus and are

often described as polygonal or fusiform cells (Clark, 1976). Leydig cells are the main androgen-producing cells of the testis and in response to direct stimulation by luteinizing hormone (LH), function in the biosynthesis of testosterone (Zirkin et al., 1980; Wing et al., 1984 and 1985). The testosterone will then diffuse to the seminiferous epithelium where it will bind to androgen receptors in Sertoli cells, which produce signals for proper completion of spermatogenesis (Sanborn et al., 1977; Tindall et al., 1977). Numerous cytoplasmic lipid inclusions serve as storage sites for cholesterol, the substrate for the synthesis of testosterone. An elaborate smooth endoplasmic reticulum (sER) serves as the site of steroidogenesis where numerous enzymes of the steroid biosynthetic pathway are found (Christensen, 1975; de Krester and Kerr, 1988). Leydig cells also contain lysosomes and exhibit both fluid-phase and adsorptive endocytosis (Hermo et al., 1985, Hermo and Lalli, 1988). Leydig cells are also capable of renewing their cytoplasm by autophagocytosis (Tang et al., 1988) a process whereby small portions of cytoplasm are segregated and destroyed by lysosomal enzymes (de Duve and Wattiaux, 1966).

Myoid cells

Myoid cells are modified contractile smooth muscle cells that are found at the base of the seminiferous tubules (Clermont, 1958). With the lymphatic endothelium and acellular elements, myoid cells form the limiting membrane of the tubule and provide structural support for the Sertoli cells and basal compartment cells which rest on it. Myoid cells are long contractile stellate cells that are thought to aid in the movement of tubular fluid and sperm through the seminiferous tubules (Russell et al., 1989).

Sertoli cells

Anchored at the base of the seminiferous epithelium, the Sertoli cell is a supporting or sustentacular cell that is terminally differentiated (Clermont and Perey, 1957; Kluin et al., 1984). It is a tall columnar and stellate cell which contacts the basement membrane and extends its apical plasma membrane to the tubular lumen. The borders of the apical

and lateral membranes extend into numerous veil-like processes that envelope the developing germ cells with the maturing elongating germ cells being embedded in the deep apical crypts (Wong and Russell, 1983; Russell, 1993). The nucleus, often found with frequent infoldings of the nuclear envelope, is basally located (Fawcett, 1975). The cytoplasm contains many organelles such as abundant profiles of smooth endoplasmic reticulum, a well developed Golgi apparatus, numerous mitochondria, membrane bound vesicles belonging to the endocytic machinery such as lysosomes (Fawcett, 1975; Hermo et al., 1994) and cytoskeletal elements such as microtubules, actin filaments and intermediate filaments (Griswold et al., 1988; Oko et al., 1991; Franke et al., 1979; Fawcett, 1975). It's the elaborate and abundant cytoskeleton that permits the Sertoli cell to continuously alter its shape to mobilize germ cells from the base to the lumen and to adjust to the changes to the germ cells' shape along the way. For example, Sertoli cells extend processes beneath spermatogonia, which are located along the basement membrane, and as these cells mature into primary spermatocytes, they are lifted upwards as new inter-Sertoli cell- junctions form beneath (Russell, 1993; Vogl et al., 1993).

A unique feature to the Sertoli cell are the ectoplasmic specializations, which are actin- associated intercellular adhesion junctions (Russell, 1977). These are cytoskeletal complexes composed of bundles of actin filaments and associated actin binding proteins sandwiched between flattened cisternae of endoplasmic reticulum and the plasma membrane (Russell, 1977). These structures are found at basal sites between adjacent Sertoli cells (Dym and Fawcett, 1970) and at regions of close apposition of developing germ cells, specifically step 8 to 19 elongating spermatids of rats (Russell, 1984). The Ectoplasmic specializations at the two sites are structurally similar. Along with the ectoplasmic specializations, tight junctions (zonula occludens) close to the base of the epithelium are found and constitute a barrier to macromolecules known as the blood-testis barrier (Dym and Fawcett, 1970, Byers et al., 1993). This barrier results of two distinct compartments within the seminiferous epithelium: a basal compartment containing spermatogonia and early spermatocytes and an adluminal compartment containing meiotic spermatocytes and spermatids. The basal compartment is accessible to the blood supply however the adluminal compartment is isolated from systemic circulation and depends on the transport of nutrients such as sugars, amino acids, lipids

and metallic elements from the Sertoli Cell (Byers et al., 1993). With the blood testis barrier, a special environment is created for successful germ cell development. It permits Sertoli cells to play an active role in synthesizing and secreting factors necessary for germ cell maturation. However it also acts as an immunological barrier and prevents immunoglobulins and lymphocytes from attacking the haploid germ cells since these cells express distinct antigens from those of somatic cells (Millette and Bellvè, 1977).

Sertoli cells also have a secretory function. It is well known that it secretes a seminiferous tubular fluid that nourishes and serves as a medium for sperm entering the efferent ducts (Setchell, 1970; Hinton and Setchell, 1993). It also secretes a variety of proteins such as transferrin for iron transport (Skinner and Griswold, 1980), androgen-binding protein (ABP) for the transport of testosterone and dihydrotestosterone (Fritz et al., 1974), a variety of proteases and antiproteases, hormones such as inhibin (Steinberger, 1979) and growth factors (Griswold, 1993).

The Sertoli cell also function in endocytosis by phagocytosing residual bodies (excess cytoplasm) from spermatids (Kerr and de Krester, 1974) and uptaking degenerating germ cells (Russell and Clermont, 1977). Fluid-phase endocytosis occurs at the apex (Morales et al., 1985). In fact phagocytosis of residual bodies is integrated with fluid- phase endocytosis leading to the formation of secondary lysosomes within the Sertoli cells and the lysis of these residual bodies (Morales et al., 1985). Receptor-mediated endocytosis occurs along the basal membrane of Sertoli Cells where small coated and uncoated vesicles are noted (Morales et al., 1985 ; Morales and Clermont, 1993).

The multiple functions of the Sertoli cell are highly regulated by hormones produced by the pituitary gland and by the testis itself. Gonadotropin releasing hormone (GnRH) originating from the hypothalamus stimulates the release of luteinizing hormone (LH) and follicle stimulating hormone (FSH). LH induces the interstitial Leydig cells to produce androgens (Christensen, 1975) notably testosterone. FSH acts directly on Sertoli cells and stimulates the synthesis of androgen binding protein (ABP) in the prepubertal testis (French and Ritzen, 1973; Louis and Fritz, 1977). Testosterone released from the Leydig cells then binds to ABP with high affinity forming a complex which is released into the lumen of seminiferous tubules (Munell et al., 2002) where the elevated

testosterone concentrations enhances spermatogenesis (Griswold, 1995). The complex also acts on target cells expressing androgen receptors, like the Sertoli and myoid cells, which subsequently perform their respective functions in promoting spermatogenesis (Sar et al., 1993, Zirkin, 1995). Hormonal regulation of testicular functions is also established by negative feedback mechanisms to the hypothalamus and the pituitary. Inhibin, a protein secreted by Sertoli cells, along with testosterone inhibits the release of GnRH, FSH and LH (Griswold, 1995).

Germ Cells and Spermatogenesis

There are three major germ cell generations present in the testis: spermatogonia, spermatocytes and spermatids. Spermatogenesis is defined as the process by which diploid spermatogonia are converted into maturing haploid spermatozoa. Spermatogenesis is divided into 3 phases: proliferative phase where spermatogonia divide by mitosis to form spermatocytes, a meiotic phase where spermatocytes form haploid spermatids and lastly a differentiation or spermiogenic phase where the spermatids transform into the fully differentiated sperm cell or spermatozoa (Russell et al., 1990).

The proliferative phase

During this phase, the spermatogonial cell population undergoes numerous divisions. These cells have a high mitotic rate in order to renew themselves and also to generate a large population of cells that will undergo meiosis (Clermont and Leblond, 1953). These spermatogonial divisions will increase the population by over two hundred fold while the following steps of meiosis and spermiogenesis will only increase the population of germ cells by four fold (Russell et al., 1990).

Three types of **spermatogonia** exist all residing in the basal compartment of the seminiferous epithelium: stem cell spermatogonia (A_{isolated}) \rightarrow proliferative spermatogonia (A_{paired} , A_{aligned}) \rightarrow differentiating spermatogonia (A_1 , A_2 , A_3 , A_4 , Intermediate, B) (Huckins, 1971). The proliferating spermatogonia are connected to

spermatogonia of the same type by cytoplasmic bridges named intercellular bridges (Weber and Russell, 1987) due to incomplete cytokinesis. Histologically, the spermatogonia can be distinguished from one another by the amount of chromatin in their nuclei.

The Meiotic phase

During this phase, **spermatocytes** (primary and secondary) divide by meiosis. The primary spermatocytes undergo the first meiotic division producing the secondary spermatocytes which will then proceed to the second meiotic division. The first division, also known as the reductional division, halves the chromosomal number thus giving each daughter cell one of the homologous pairs. After DNA synthesis, the diploid primary spermatocytes containing twice the normal DNA content (4N) divide into two secondary spermatocytes containing a haploid number and a full amount of DNA (2N). Then the small, short-lived secondary spermatocytes divide in a mitotic fashion to produce two spermatids (sister chromatids) each with a haploid chromosome number and haploid DNA content (1N) (Gartner and Hiatt, 1997).

At the end of the proliferative phase, the Type B differentiate to primary spermatocytes also known as preleptotene spermatocytes. During this phase, Sertoli cell processes lift the germ cells upwards into the adluminal compartment while new tight junctions are formed beneath them (Morales and Clermont, 1993; Vogl et al., 1993). The preleptotene spermatocytes are the last cells of the spermatogenic sequence to replicate their DNA prior to division. They are also the first cells to undergo prophase of the first meiotic division. Prophase of the first meiotic division is quite long-lasting and therefore it is divided into sequential segments, each named after a different primary spermatocyte (Russell, 1978). Thus during prophase I, the primary spermatocytes which differentiate along the way are preleptotene, leptotene, zygotene, pachytene and diplotene spermatocytes. These cells are characterized by changes in their sizes and by changes in chromosomal condensation. Diplotene spermatocytes are the largest of all germ cells and also display maximal chromosome condensation. Diplotene is the culmination of an extended prophase, however the remainder of the cell division (Meiosis I) proceeds

quickly to produce secondary spermatocytes. Secondary spermatocytes are short-lived cells and are difficult to locate. They can be differentiated from cells of meiosis I by their smaller size. These cells will quickly complete the second meiotic division to produce haploid **spermatids** (Russell and Frank, 1978) which will enter the final stage of spermatogenesis, the spermiogenic phase.

The Spermiogenic phase

Spermiogenesis involves a sequence of steps whereby round spermatids, cells which can no longer divide, will transform into structurally mature spermatozoa and acquiring a propelling flagellum. These series of changes are used to distinguish the various stages of spermatogenesis (Leblond and Clermont, 1952 a, b), as will be described later. These changes include the development of an acrosome, subsequent elongation and condensation of the nucleus, reorganization of the cytoplasm and organelles and the development of the flagellum (Clermont et al., 1993; Russell et al., 1990). Prior to release into the seminiferous tubule, the nonmotile spermatozoa will shed a large mass of discarded cytoplasm known as the residual body which will then be phagocytosed by the Sertoli cell (Kerr and de Krester, 1974).

Sperm Head

The sperm head contains two major structures: the nucleus and the acrosome. The nucleus is almost entirely located in the head while the acrosome covers the anterior half of the head with the covered area varying by species (Toshimori and Ito, 2003).

Development of the acrosome

The acrosome is a sac-like structure with a membrane overlying the anterior part of the sperm nucleus and contains a number of hydrolytic enzymes and functional proteins that are necessary for the induction of the acrosome reaction and penetration of the oocyte (Benoff 1997; Tulsiani 1998; Kim et al, 2001). The acrosome is also a Golgi

derived secretory granule and its formation occurs throughout spermiogenesis and is not complete until late spermiogenesis (Leblond and Clermont, 1952; Thorne-Tjomsland et al., 1988).

The Golgi apparatus forms small condensing vacuoles or proacrosomal vesicles each containing dense material or proacrosomal granules. Eventually the numerous proacrosomal vesicles will coalesce to form a single acrosomal vesicle with a single acrosomal granule thus forming the acrosomal system or acrosome (Russell et al., 1990). The vesicle will contact the nuclear membrane and slowly flatten out over its surface and cover up to 60% of the nucleus forming the acrosomal cap. Once the cap forms, the spermatid nucleus with the bound cap moves to the cell surface and becomes closely apposed to the plasma membrane, polarizing the cell and thus segregating the sperm head from the tail (Russell et al., 1983). A junction between the head and the tail termed the neck region is also formed during this process. The nucleus progressively elongates and condenses along with the acrosome which also increases in density, while the Golgi apparatus migrates away from the acrosomal vesicle towards the developing tail (Moreno et al., 2000). Finally, the acrosome head will undergo shape changes and lose its spherical shape becoming flat and elongated. The changes seen in the sperm head (acrosome and nucleus) provide the means for classifying mouse spermiogenesis into 16 steps (Russell et al., 1990).

Structure of the acrosome

The mature acrosome is enclosed by a single membrane divided regionally into two parts : an inner acrosomal membrane (IAM) bound to the nuclear envelope and an outer acrosomal membrane (OAM) underlying the plasma membrane. The acrosomal region is divided into two major domains : anterior acrosome (acrosomal cap) and an equatorial segment (posterior acrosome) (Yoshinaga and Toshimori 2003; see fig.1). The postacrosomal region spans from the posterior end of the equatorial segment to the posterior ring region and contains the postacrosomal sheath (PAS).

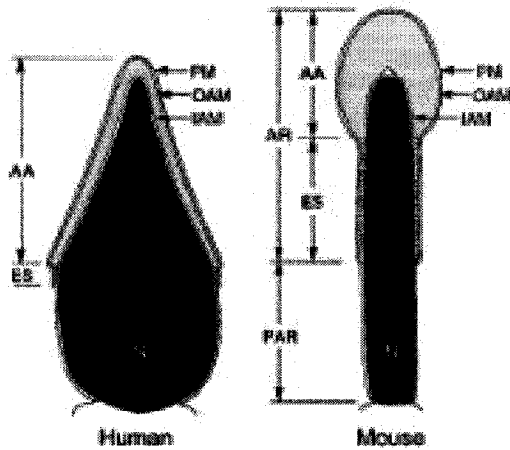


Figure 1: Sagittal-sectional views of the heads of human and mouse spermatozoa. The acrosomal region (AR) is shaded in gray; it consists of the anterior acrosome (AA) and the equatorial segment (ES). IAM, inner acrosomal membrane; N, nucleus; OAM, outer acrosomal membrane; PAR, postacrosomal region; PM, plasma membrane. (Yoshinaga and Toshimori, 2003).

Nuclear shaping

As mentioned before, the round spermatids have a spherical nucleus. With time, the shape and the size of the male germ cell nucleus will undergo complete reorganization. The chromatin condenses due to changes in histones and other proteins associating with DNA (Fawcett et al., 1971; Hecht, 1998; Oko et al., 1996) leading to decreased volumes. Sperm heads attain a characteristic streamlined, elongated shape just before they are released into the lumen. A normal nuclear structure and shape due to proper chromatin remodeling is necessary for fertility. It has been shown that abnormal chromatin remodeling forms abnormal spermatozoa with spherical nuclei and no acrosomes and leads to impaired spermiogenesis and infertility (Wu et al., 2000; Steger et al., 2001). Besides investigating cellular events taking place in the nucleus, researchers have recently been examining the structures surrounding the nucleus in order to comprehend the mechanisms involved in sperm head formation and organization and

shaping. These structures include the acrosome-acroplaxome complex, the manchette and the perinuclear theca.

The Acrosome-Acroplaxome complex

The impact of acrosome biogenesis on spermatid nuclear shaping has recently been studied looking at different mutant mice, particularly in those with deficient acrosome development and round-headed sperm. Hrb-deficient mice display round-headed spermatozoa, lack an acrosome and are infertile (Kang-Decker et al., 2001). Hrb protein is located on the cytosolic surface of proacrosomic transporting vesicles and its absence prevents the fusion of these vesicles and thus the formation of the acrosome. Acrosome formation also fails to develop in GOPC-deficient mice (Yao et al, 2002). GOPC being a Golgi protein necessary for the transport of vesicles from the Golgi apparatus to the acrosomal sac.

Still, very little is known about the targeting and fusion of Golgi vesicles during acrosome vesicle formation. It has been shown in the past that actin filaments are located in the subacrosomal space in round and elongating spermatids (Russell et al., 1986; Vogl, 1989). Recently researchers have investigated the structural and biochemical organization of these actin filament-containing sites in the subacrosomal space and termed these cytoskeletal plates acroplaxomes (Kierszenbaum et al., 2003). The acroplaxome is described as an F-actin-keratin- containing attachment plate present in the subacrosomal space of mammalian spermatozoa anchoring the acrosome to the nucleus (Kierszenbaum et al., 2003). The plate also houses flanking zones termed marginal rings which contain bundles of intermediate filaments with myosin Va located at the leading edge of the acrosome. The size of the acroplaxome changes throughout spermiogenesis with the diameter of the acroplaxome increasing in parallel with the corresponding flattening of the acrosome over the elongating spermatid nucleus. F-actin is the first to appear in early spermiogenesis with the keratin appearing one step later. It is hypothesized that actin polymerization to F-actin is occurring (Kierszenbaum et al., 2003). The F-actin hoops provide a planar scaffold, maintaining the acrosome at the nuclear anchoring site and adjusting to exogenous forces generated by the Sertoli cell ectoplasmic sites to the

nucleus, thus playing a role in nuclear shaping. It has been shown that the acroplaxome is also a nucleation site for Golgi-derived Myosin-Va/Rab27a/b (actin-based motor proteins) containing proacrosomal vesicles (Kierszenbaum et al., 2004) which will coalesce to initiate acrosome biogenesis. Thus two functions have been attributed to acroplaxomes: anchoring the developing acrosome to the elongating spermatid head and providing a mechanical scaffolding plate during the shaping of the spermatid nucleus (Kierszenbaum and Tres, 2004).

The Manchette

The manchette is a transient cytoskeletal element formed around the nucleus as the spermatid nucleus initiates its elongation. More specifically, the manchette begins to appear at step 7, as the Golgi apparatus moves to the opposite pole of the cell and at step 9 of spermatogenesis a fully formed manchette is seen (Moreno et al., 2000). The manchette contains organized bundles of microtubules with the innermost microtubules being linked to the nuclear envelope by rod-like structures during step 8-11 of spermatogenesis (Russell et al., 1991). The microtubules insert at the perinuclear ring, a structure which assembles adjacent to the marginal ring of the acroplaxome. As the sperm enters final steps of spermiogenesis, the manchette will move to the caudal part of the sperm and be eliminated in the cytoplasmic droplet (Goodrowe and Heath, 1984). The timing of the appearance and disappearance of the manchette is very precise: it appears in early elongating spermatids and disappears when elongation and condensation of the spermatid nucleus nears completion (Toshimori and Ito, 2003). Thus, it has long been assumed that the manchette plays a role in the elongation of the spermatid head by deforming part of the nucleus from its spherical shape (Russell et al., 1991). It is now suggested that the manchette along with the acrosome-acroplaxome forms a complex where they act together as an endogenous clutch in sperm head shaping (Kierszenbaum and Tres, 2004).

The Perinuclear theca

Between the outer nuclear membrane and the inner acrosomal membrane resides a cytoskeletal structure known as the perinuclear theca (Longo et al., 1987; Oko and Clermont, 1988). Its many proteins, some which associate with actin (Lecuyer et al., 2000; Heid et al., 2002), condense during development and may be involved in acrosomal binding to nucleus, nuclear head shaping during spermiogenesis and fertilization (Korley et al., 1997; Heid et al., 2002).

Reorganization of the cytoplasm and organelles

Before sperm is released into the lumen, the size of the spermatid is also reduced in volume to approximately 25% of its original size through the elimination of water and cytoplasm (Sprando and Russell, 1987). This reduction in size and shape will permit the spermatids to become hydro-dynamically streamlined and permit them to propel through the fluid environment of the female reproductive tract (Russell et al., 1990). It was mentioned before that the nucleus condenses and elongates during spermiogenesis. During this process, water is eliminated from the nucleus and cytoplasm. Two other methods are available in rendering sperm smaller: the tubulobulbar complexes and the residual cytoplasm. Tubulobulbar complexes are junctions found between Sertoli cells and spermatids which are about to be released at the apical border of the Sertoli cell (Russell and Clermont, 1976). Tubulobulbar complexes are thin cytoplasmic evaginations originating from the head region of mature spermatids terminating in bulbous dilations (Russell et al. 1990). Many complementary functions have been attributed to these complexes such as playing as anchoring devices between Sertoli cells and spermatids (Russell and Clermont, 1976), helping in the elimination of cytoplasm from spermatids (Russell, 1980) and eliminating junctional links between spermatid and Sertoli cell to permit disengagement (Russell et al., 1988). There is evidence to support tubulobulbar complexes for the second function. When these structures are prevented from forming, an abnormally swollen spermatid head is noted (Russell, 1980).

Thirdly, volume reduction of the sperm can be attributed to the separation of a cytoplasmic package (lobe) also known as the residual body which forms at sperm release (Fawcett and Philips, 1969; Russell, 1984). Except for the acrosome and the flagellum, the residual body contains virtually all organelles, packed RNA and remnants of the Golgi originating from the spermatid (Oko et al., 1993). The residual body permits a 25% reduction of the cytoplasm of its round spermatid predecessor (Sprando and Russell, 1987) and enables the spermatid to shed organelles and inclusions that were used earlier but that are no longer necessary for cell survival. These cytoplasmic fragments are then phagocytosed by the Sertoli cell and transported to the base of the tubule where they will be digested (Kerr and de Krester, 1974; Russell, 1993). After this cytoplasmic elimination, only a cytoplasmic droplet will remain around the neck of the spermatid. The cytoplasmic droplet will then transiently be retained through transit in caput epididymis and then detach from the spermatid and its components to be phagocytosed by epithelial clear cells in corpus and cauda epididymidis (Herms et al., 1988).

Sperm Flagellum

The sperm flagellum consists of a central axoneme with various specialized structures surrounding the axoneme.

Sperm flagellum formation commences after sperm head formation and lasts from the midpoint of the spermiogenic phase until the sperm are released. Once the round spermatid cell becomes polarized during sperm head shaping, the flagellum develops at the opposite pole of the nucleus where it harbors the centrosome. The flagellum develops from resident, paired centrioles containing a γ -tubulin foci (Manandhar et al., 1998). Migration of the paired centrioles to the cell surface forms an axoneme, a cytoskeletal structure which consists of nine peripheral microtubule doublets and two central singlets (Olson and Linck, 1977). The axoneme causes the spermatid plasma membrane to protrude from the cell with the extended axoneme reaching the tubular lumen. Then, the paired centrioles forming the flagellar axoneme will eventually move to the nuclear surface, placing the flagellum opposite the acrosome (Russell et al., 1990). Late in

spermiogenesis, accessory structures are added to the flagellum forming four distinct regions of the tail: the connecting piece, middle piece, principal piece and end piece (see fig. 2).

The axoneme runs the entire length of the flagellum and is responsible for generating motor force required for sperm motion and sperm form modulation. The inner and outer dynein arms of microtubule doublets' interaction of ATP with ATPase activity causes the sliding of adjacent outer microtubule pairs and caused the flagellum to bend (Gibbons, 1968).

The connecting piece is considered the neck region of the spermatozoon since it attaches the flagellum to the nuclear head (Fawcett, 1969). The midpiece is characterized by the presence of nine outer dense fibers (ODFs) which lie immediately peripheral to the microtubule doublets. The characteristic feature of the middle piece is the mitochondrial sheath, a helical pattern of mitochondria which surrounds the ODFs (Fawcett, 1975). The principal piece which makes up about three-fourth of the length of the flagellum has 7 ODFs, two ODFs extending from the middle piece being replaced by two longitudinal columns of the fibrous sheath (FS). The fibrous sheath is the unique cytoskeletal component of the principal piece, it underlies the plasma membrane and surrounds the ODFs and consists of two longitudinal columns connected by numerous semicircular ribs. The fibrous sheath imposes restraints to flagellar bending, helping generate a planar beat (Si and Okuno, 1993). Recently many proteins involved in energy production or motility and metabolism have been found in the FS suggesting that the FS doesn't merely serve as a cytoskeletal structure. For example, the AKAP (cAMP-dependent protein kinase anchoring proteins) proteins are implicated in the signaling pathway in spermatozoa (Miki and Eddy, 1998) while a family of glycolytic enzymes including HK1-S, a hexokinase type 1-s (Mori et al., 1998) is involved in motility. Thus the FS plays a role in regulating sperm motility by acting as a scaffold for glycolytic enzymes and proteins involved in signaling pathways (Eddy et al., 2003).

The end piece only consists of the axoneme and the overlying cytoplasm.

Structure of the Sperm Flagellum

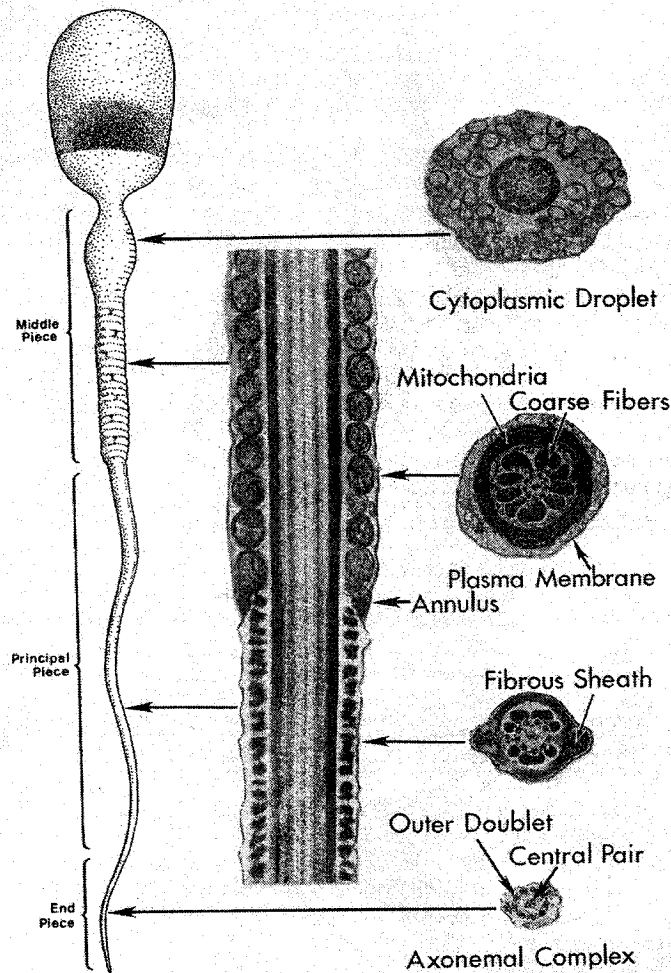


Fig 2. The sperm tail is divided into 4 pieces: connecting piece (not shown), middle piece, principal piece and end piece. Figure from Russell et al., 1990.

Completion of Spermiogenesis

Once spermiogenesis is complete, the late spermatids line up along the luminal border of the seminiferous tubules, in preparation for release by a process known as spermiation (Russell, 1993). The ectoplasmic specializations, the specialized junctions between the Sertoli cells and the germ cells dissipate and at the time of sperm release, the tubulobulbar complexes, the last of the junctional complexes, form between the mature spermatid and the Sertoli cell. As mentioned previously, the tubulobulbar complexes

along with the phagocytosis of residual bodies by Sertoli cells are a means by which cytoplasmic fluid and remnants are eliminated at sperm release (Russell, 1993).

Staging of Spermatogenesis

Cross-sections of seminiferous tubules contain several germ types since the maturing germ cells transcend towards the lumen. The vacated positions will simultaneously be filled by germ cells found at an earlier stage of development (Desjardins and Ewing, 1993). The study of these cross-sectioned tubules has revealed the grouping of germ cell types or cell associations leading to the division of the spermatogenic cycle into several discrete stages (Leblond and Clermont, 1952 a,b: see fig.3). This means that particular germ cells at a specific developmental stage will always be found together in a cross-sectioned tubule.

In the mouse, the spermatogenic cycle has been divided into twelve stages, designated by the roman numeral I-XII, with the entire spermatogenic process taking approximately 35 days (Oakberg, 1956 a,b). Spermatids are the cell type used to distinguish one stage from another, based on their morphological appearance (Russell et al., 1990). The development of round spermatids to elongating spermatids via the process of spermiogenesis has been divided into 16 steps. The first 12 steps are used to identify the stage of spermatogenesis since each of these steps is unique to each of the 12 stages of the cycle. The acrosomal system which increasingly spreads over the nucleus of the spermatids helps us locate step 1-7 spermatids. During step 7, the nucleus still remains centrally positioned within the cell and the acrosome continues to spread over the nucleus with the maximal spread approximating 150 degrees, thus covering almost half the surface of the nucleus (Russell et al., 1990). Nuclear shaping and increase in chromatin condensation helps us define the step 8-12 spermatids. At step 8, the acrosomal region of the nucleus finally makes contact with the cell surface and the nucleus assumes an eccentric position. By this step, the Golgi apparatus has also moved to the caudal end of the cell (Russell et al., 1990).

During step 13-16, final nuclear shaping results with the apex of the spermatid head forming a definite hook. Final stages of flagellum assembly such as mitochondrial alignment in the middle piece of the tail also take place around step 15. At stage VIII of the cycle, step 16 spermatids get released into the tubule lumen. The cytoplasmic lobe which forms a hood over the spermatid head and the tubulobulbar complexes formed at this step will be phagocytosed by the Sertoli cells right before sperm release (Russell et al., 1990).

In order for the germ cells of a specific type to undergo the same developmental changes at the same time and for cellular associations to be maintained within a particular segment of the seminiferous epithelium, developmental steps must be synchronized. In fact, the synchronization within a subset of germ cells is possible due to regions of communication between the cells known as intercellular bridges (ICBs) (Dym and Fawcett, 1971; Huckins, 1978; Weber and Russell, 1987). These intercellular bridges form when the germ cells divide and undergo incomplete cytokinesis, such that the daughter cells don't separate from one another but remain connected by these cytoplasmic constrictions (Dym and Fawcett, 1971). All 3 populations of germ cells (spermatogonia, spermatocytes and spermatids) are connected by these ICBs since new ICBs will form with each division, while the previously formed bridges will be maintained throughout the division process (Weber and Russell, 1987). Cytoskeletal components such as actin, keratin and microtubules are thought to maintain the integrity of these cytoplasmic bridges (Russell et al., 1987; Tres et al., 1996; Kierszenbaum 2002; Kato et al., 2004). The ICB's also allow the transport of organelles (Ventela, 2003) and substances such as mRNA (Braun et al., 1989) through them, such that members of a clonal population can express the same proteins.

Huntingtin- interacting protein 1

Huntingtin Interacting Protein 1 (HIP1) was first identified via its interaction with huntingtin (htt), a polyglutamine-containing protein associated with Huntington Disease (HD) (Kalchman et al., 1997; Wanker et al., 1997). Using the yeast two-hybrid system and the N-terminal huntingtin fragment as a “bait”, HIP1 was discovered as a novel protein of 120 kDa containing 1034 amino acids (Kalchman et al., 1997; Wanker et al., 1997). Fluorescent in situ hybridization (FISH) revealed that HIP1 maps to human chromosome 7q11.2 (Kalchman et al., 1997). This novel protein was shown to share similar homology with a hypothetical protein encoded by the gene ZK370.3 found in *C. elegans*. and sequence homology to the yeast protein Sla2p, the gene product of SLA2 (synthetic lethal with actin binding protein (ABP) in *S. cerevisiae* (Kalchman et al., 1997; Wanker et al., 1997). It has been suggested that HIP1 is the human homologue of SLA2 and ZK370.3. HIP1 also shares considerable homology with huntingtin- interacting protein1 related protein (HIP1r/HIP12), the only other member of the HIP1 family of cytoskeletal-associated proteins (Seki et al., 1998; Chopra et al., 2000). HIP1r, a 130 kDa protein containing 1068 amino acids, shows 47% identity and 64% amino acid conservation with HIP1 and also shows structural similarity to Sla2p and ZK370.3. HIP1r maps to a different chromosome (q24 region of chromosome 12) (Seki et al., 1998) and unlike HIP1, does not directly bind to huntingtin (htt) protein (Chopra et al, 2000).

Human htt is a large 350 kDa protein of 3144 amino acids encoded by IT15 gene found on chromosome 4 (Norremolle A et al., 1993; HDCRG et al., 1993). HD, an inherited progressive neurodegenerative disorder, is caused by an expansion of the polyglutamine (poly Q) tract (>37 glutamines) located at the N-terminus of the htt protein.

Interaction with huntingtin protein

The mutated htt confers new properties to the protein and alters its binding to other proteins. In order to gain insight into the underlying pathogenesis of HD, many researchers have focused on identified proteins that interact with htt. Four different categories of proteins have been identified that bind to htt: proteins involved in gene transcription, proteins involved in trafficking and endocytosis, proteins involved in signaling and proteins involved in metabolism (Li et al., 2004). HIP1 is placed under the category of proteins involved in trafficking and endocytosis.

In order for HIP1 to interact with Huntingtin (htt), a stretch of 588 amino acids from the N-terminal of htt is required. Using liquid β -galactosidase assays, it was found that the increased length of the huntingtin polyglutamine tract was associated with a decreased interaction with HIP1 (Kalchman et al., 1997). It was suggested at this time that an elongated polyglutamine sequence could lead to changes in protein interactions and biochemical events at the membrane and possibly lead to neurodegenerative changes. Co-immunoprecipitation of HIP1 using a huntingtin specific antibody from human control frontal cortex confirmed the interaction between HIP1 and htt (Kalchman et al., 1997).

Subcellular fractions of normal tissue from human and mouse brain were prepared by differential centrifugation to determine the subcellular localization of HIP-1 and htt. HIP1 was observed to co-localize with htt in all membrane fractions, including cell debris, nuclei, mitochondria, microsomes and the plasma membrane (Kalchman et al., 1997; Wanker et al., 1997).

Genome

HIP1 gene comprised 32 exons spanning approximately 215 kb of genomic sequence and gives rise to two alternate splice forms termed HIP1-1 and HIP1-2 which differ in their 5' sequences (Chopra et al., 2000). Translation initiation sites are present in

exon 1 and exon 3, alternative splicing occurs from either exons 2-4 or from exon 3-4 with exon 32 containing the stop codon.

Localization

Using Northern Blot analysis, HIP1 mRNA, with a size of 9kb, was shown to be ubiquitously expressed, with highest levels being found in brain tissue, most notably in the frontal cortex and the putamen (Wanker et al., 1997, Chopra et al., 2000). Using Western blot analysis to localize HIP1 protein in various human tissues, HIP-1 protein was found in lesser amounts in peripheral tissues such as the spleen, bone marrow, liver, kidney, testis and the heart, however high expression of HIP-1 was mostly found in brain extracts in all regions of the brain and in the gray matter of the spinal cord, indicating that HIP-1 is enriched in the central nervous system (Wanker et al., 1997, Chopra et al., 2000; Metzler et al., 2003). Within the brain, the highest levels of the protein were found in the frontal cortex, the hippocampus, the olfactory bulb and with slightly lower levels found in the cerebellum, the caudate and the putamen (Kalchman et al., 1997, Chopra et al., 2000; Metzler et al., 2003).

Clathrin- Mediated endocytosis

Clathrin-mediated endocytosis is used for the internalization of select molecules such as ligand-bearing cell receptors, neurotransmitter receptors and also used for synaptic vesicle recycling at the cell surface in neurons (Lafer, 2002). Clathrin-coated vesicles form at the plasma membrane with clathrin and the adaptor-binding protein 2 (AP-2) being the main components along with lipids and endocytic accessory proteins. Clathrin coated vesicles aren't only formed at the plasma membrane. Clathrin-coated endocytic vesicles also operate at the trans-Golgi network (TGN) whereby cargo proteins are sent from the TGN to endosomal/lysosomal compartments (Brodsky et al., 2001, Hinners and Tooze, 2003). Clathrin is composed of three heavy chains and three light chains. Clathrin has the property to self-assemble three-legged triskelia composed of

trimerized clathrin heavy chains each with a bound light chain subunit . The triskelia then oligomerize to form stable polyhedral lattices (Smith et al., 1999).

AP-2 is a member of the heterotetrameric family of clathrin adaptor proteins and is found exclusively at the plasma membrane (Hirst et al., 2000). AP-2 is a complex formed of 4 tightly bound subunits (adaptins): α -adaptin, β 2 adaptin, μ 2 adaptin and δ 2 adaptin. AP-2 binds clathrin via its β 2 subunit and interacts with the plasma membrane proteins and lipids through its core region (Slepnev et al., 2000).

Functional significance of HIP1 in Clathrin-mediated endocytosis

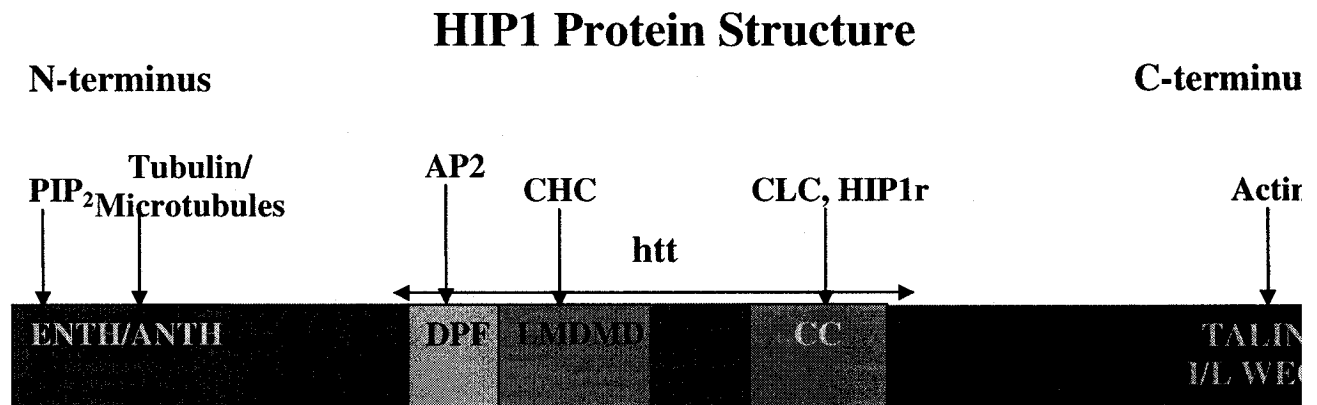


Figure 3. Schematic of HIP1 protein domains and sites of protein and phospholipids interaction. Adapted from (Metzler et al., 2003).

The HIP1 family contains 3 important domains: the AP180 N-terminal homology domain (ANTH), a central coiled-coil (CC) region and a C-terminal talin homology domain called the I/L WEQ domain (see fig.3).

Since the ANTH domain is similar to the Epsin N-terminal homology (ENTH) domain, HIP1 has been suggested to contain an ENTH domain. The ENTH/ANTH domain family includes many proteins including the epsins, enthoprintin, AP180, CALM (clathrin assembly lymphoid myeloid leukemia), HIP1 and HIP1r, all being implicated in the formation of Clathrin coated pits (CCP) and Clathrin coated vesicles (CCV) (Legendre-Guillemain et al., 2004). Recent data suggests that ENTH/ANTH domain

proteins play various roles: they can function as adaptor proteins by recruiting cargo to clathrin coated pits (Legendre-Guillemain et al. 2004). ENTH/ANTH domains can also bind tubulin and microtubules thus suggesting that proteins bearing ENTH/ANTH domains, including HIP1, can link clathrin-coated membranes to microtubules (Hussain et al. 2003).

ENTH/ANTH domains bind to inositol phospholipids, AP180 and epsin preferentially bind to phosphatidylinositol-4,5-bisphosphate [PtdIns (4,5) P₂], a predominantly plasma membrane inositol lipid (Lemmon MA, 2003; Itoh et al, 2001., Ford et al., 2001). It was recently discovered that unlike AP180 and epsin, HIP1 and HIP1r have different lipid specificities, they bind preferentially to 3-phosphate-containing inositol lipids, Ptd Ins (3,4) P₂ and Ptd Ins (3,5) P₂ (Hyun et al, 2004). These inositol lipids are found in intracellular membranes such as endosomes suggesting that HIP1 might participate in intracellular membrane trafficking (Hyun et al, 2004).

Downstream from the ANTH domain and just upstream from the coiled-coil domain lies the LMDMD amino sequence which represents the clathrin box which binds to the terminal domain of Clathrin Heavy Chain (CHC) (Metzler et al., 2001). Related sequences to LMDMD are found in other endocytic proteins such as amphiphysin and epsin1 that are also known to interact with clathrin. Right next to the LMDMD lies a DPF motif (amino acids 324-326) which binds to the ear domain of the α -adapin subunit of AP2 (Metzler et al., 2001; Waelter et al., 2001).

It has been shown that HIP1 is a component of clathrin coated vesicles (CCV), co-localizing with AP-2 and huntingtin in prepared human brain extracts and binding directly to clathrin heavy chain and AP-2 (Metzler et al., 2001;Waelter et al., 2001; Mishra et al., 2001). These studies demonstrate that HIP1 might play a role of an endocytic accessory protein in clathrin-mediated endocytosis (Metzler et al., 2001; Waelter et al., 2001, fig.4). HIP1 expression in mammalian cells also results in punctuate cytoplasmic immunostaining which is characteristic of CCV's (Waelter et al., 2001). It was also shown that when HIP1 is overexpressed in a truncated form (lacking the ANTH domain and talin-like domain), accumulation of large vesicle-like structures occurs in the perinuclear region (Waelter et al., 2001).

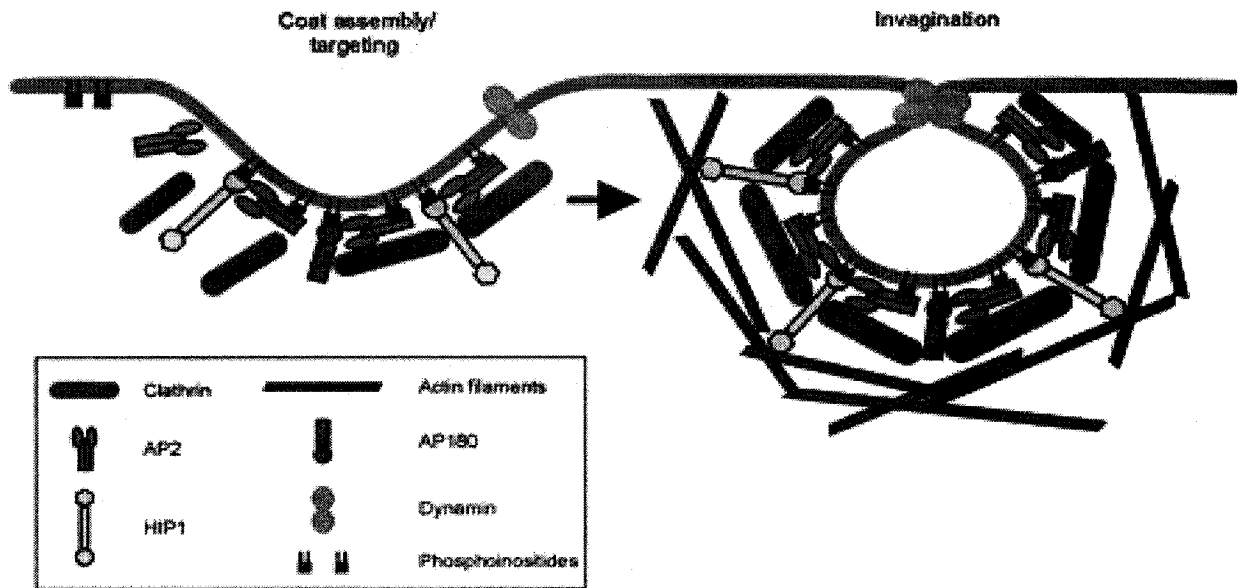


Figure 4: HIP1's role in clathrin mediated endocytosis. At the plasma membrane, the N-terminal ANTH domain of HIP1 most likely interacts with lipid phosphoinositide (s). HIP1 along with the adaptor proteins, AP-2 and AP180, then participates in assembling the clathrin lattice and promoting the invagination of clathrin-coated pits. In the mean time, actin filaments are recruited to the site to control the size of nascent clathrin-coated vesicles by the C-terminal talin-like domain of HIP1. Adapted from Waelter et al., 2001.

The central coiled domain of HIP1, which binds to huntingtin, HIP1r and to a conserved sequence of Clathrin Light Chain (CLC), promotes and regulates clathrin assembly in vitro and affects actin distribution in vivo (Legendre-Guillemain et al., 2002, Legendre-Guillemain et al., 2005; Chen et al., 2005). HIP1 homodimerization and its heterodimerization with HIP1r is also mediated by the central coil domain (Legendre-Guillemain et al., 2002). HIP1r just like HIP1 also promotes clathrin assembly in vitro by binding CLC through its own central domain (Legendre-Guillemain et al., 2002). Coiled coils are highly versatile α -helical motifs that mediate subunit oligomerization of many cytoskeletal proteins such as α -keratin, vimentin and motor proteins such as myosin and dynein (Burkhard P et al., 2001). The coiled-coil domain in yeast (Sla2p) plays an important role in actin polarization thus suggesting HIP1 might play the same role in mammalian cells (Yang et al. 1999). Sla2p has also been shown to play essential role in the assembly and function of the membrane cytoskeleton (Holtzman et al., 1993). It also

functions in vesicle transport from the Golgi apparatus to the plasma membrane (Mulholland et al., 1997, Blader et al., 1999).

The C-terminus of HIP1 contains a unique functional module named the talin-homology (I/L) WEQ domain which was shown initially to bind indirectly to the actin cytoskeleton via HIP1r (Chopra et al, 2000; Legendre-Guillemin et al, 2002). However recently, it has been shown that HIP1 does bind directly to F-actin via the I/L WEQ module (Senetar et al., 2004). The I/L WEQ module superfamily includes talin, HIP1, HIP1r and Sla2p, proteins all capable of binding actin (Senetar et al., 2004). It was recently shown that HIP1r plays a crucial role in mediating interactions between the actin cytoskeleton and clathrin at endocytic sites (Engqvist-Goldstein et al., 2004). In response to RNAi mediated silencing of HIP1r, unusual cortical tails accumulate near the cell cortex and an arrest of endocytosis implicating that HIP1r might play a role in regulating actin polymerization at clathrin coated pits (Engqvist-Goldstein et al., 2004). RNAi-mediated silencing of HIP1r also causes an accumulation of F-actin structures associated with CCVs on the TGN and disruption of the Golgi organization (Engqvist-Goldstein et al., 2004). HIP1r has also been shown to localize to the TGN (Carreno et al., 2004). This establishes a role for HIP1r in actin organization and endocytosis not only at the plasma membrane but also at the TGN. Since HIP1 has 47% sequence identity to HIP1r and the C-terminal (I/L) WEQ domain of HIP1 is 70% identical to HIP1r, it seems highly likely that HIP1 might also play a role in actin organization in the cell (Chopra et al., 2000; Mishra et al., 2001).

These data demonstrate that HIP1 by binding to inositol phosphates, Clathrin (CHC and CLC), HIP1r, AP2, huntingtin and actin plays a crucial role in clathrin-mediated endocytosis, vesicle trafficking, possibly acting as a linking protein between the endocytic machinery and the acting cytoskeleton at the plasma membrane and the TGN.

Function in apoptosis, tumorigenesis and regulation of receptors

The mutation of huntingtin, which is marked by an expansion of the glutamine repeats (>35) leads to a dramatically reduced binding of HIP1 to huntingtin (Kalchman et al., 1997). It has been suggested that the free HIP1 (which normally is bound to htt) may function as a pro-apoptotic protein by recruiting and activating caspase 8 activity via its interaction with Hippi (HIP1-protein interactor) (Hackam et al., 2000; Gervais et al., 2002). This protein interaction may initiate apoptosis and play a role in the neurodegenerative changes seen in Huntingtin's disease. In contrast to its role in apoptosis, HIP1 may also play a role in cellular survival and in the normal development of many cell types and tissues. It is suggested that the discrepancy in the reported pro- and anti-apoptotic effects of HIP1 can be explained by the HIP1 gene yielding two splice forms HIP1-1 and HIP1-2 (Hyun et al., 2004). HIP1 is highly expressed in many cancers and is overexpressed in prostate, breast and colon cancer (Rao et al., 2002). HIP1 plays an important role in tumorigenesis in mouse prostate and autoantibodies to HIP1 have developed in the sera of both humans and mice with prostate cancer (Bradley et al., 2005). Thus for the future, HIP1 might serve as a serum marker for prostate cancer. HIP1 might also play a role in tumorigenesis by altering receptor trafficking. In HIP1 transformed cells, HIP1-mediated upregulation of epidermal growth factor receptors (EGFR) occurs with associated increased EGF uptake (Rao et al., 2003). These changes result in altered EGF trafficking and altered intracellular signal transduction possibly leading to tumorigenesis.

HIP1 has also been shown to influence growth factor receptors. In cells overexpressing HIP1, there are increased levels of fibroblast growth factor (FGF) receptor and platelet derived growth factor (PDGF)- β receptors (Rao et al., 2003; Hyun TS et al., 2004). It has been shown by confocal microscopy that HIP1 colocalizes with AMPA (α -amino-3-hydroxy-5-methyl-4-isoxazolepropionic acid) type glutamate receptors (Metzler et al., 2003) and that clathrin-mediated internalization of these receptors is disrupted in HIP1^{-/-} mice.

Huntingtin protein

Human htt, when mutated, causes huntingtin's disease (HD), which is characterized by movement disorders, dementia and psychiatric abnormalities (Harpers, 1991). Symptoms of HD usually begin around the age of 40 and progressively worsen for the next 10-15 years until the patient dies. This autosomal dominant progressive neurodegenerative disorder is caused by an expansion of the polyglutamine (poly Q) tract (>37 glutamines) located at the N-terminus of the large 350 kDa htt protein (HDCRG, 1993). The htt protein, both in the normal and mutated form, have been shown to be expressed in the central nervous system and in peripheral tissues such as testis, heart, liver and lung (Trottier et al., 1995; Schilling et al., 1995) however most pathological findings are confined to the central nervous system. In HD, selective neuronal loss preferentially occurs in the caudate nucleus, the putamen as well as in the deeper layers of cerebral cortex (Vonsattel et al., 1985). Htt is primarily a cytoplasmic protein that has been shown to be associated with synaptic vesicles, microtubules, mitochondria, membranes of the trans-Golgi network and also with clathrin vesicles in the cytoplasm (Di Figlia et al., 1995; Sharp et al., 1995; Gutekunst et al., 1995; Velier et al., 1998). These observations suggest that htt might be involved in vesicle transport.

The true function of Htt is still not fully understood. Studies point at a multifunctional protein that can act both at the nucleus and the cytoplasm. Intranuclearly, toxic N-terminal mutant htt can accumulate and cause transcriptional dysfunction (Kegel et al., 2002; Dunah et al., 2002). Many researchers believe a toxic gain of function mechanism may be involved in the pathogenesis of HD due to the elongated polyglutamine sequence of the mutated htt conferring new properties to the protein and altering its binding to other proteins. Early degenerative changes in HD patient brains due to mutant htt affects proteins involved in synaptic function such as dynamins and cytoskeletal integrity such as the α -tubulins (Diprospero et al., 2004).

Role for Huntingtin in the testis

It has been shown that htt protein is highly expressed in neurons and in the testis of adults (Strong et al., 1993). Inactivation of the mouse homologue of the Huntington disease gene (Hdh) has adverse affects both in the brain and in testis leading to neuronal degeneration and defects in spermatogenesis (Dragatsis et al., 2000). In the seminiferous tubules, Hdh is highly expressed in primary and secondary spermatocytes (Dragatsis et al., 2000). Mutant seminiferous tubules are disorganized and show reduced sperm counts both in testis and in the lumen of epididymis. The important role of htt in male reproduction was further supported in another study. Loss of wild-type htt with the expression of mutant htt in the YAC128 mouse model also leads to testicular degeneration (Raamsdonk et al., 2005). Vacuolated seminiferous tubules were observed along with sloughing off of germ cells in the lumen of the tubules. Reduced sperm counts were found with some sperm cells having abnormal sperm heads (Raamsdonk et al., 2005). It is interesting to note that Sertoli cells are not affected confirming that htt protein is found in germ cells. These results show that htt protein's cytoskeletal functions might be critical for spermatogenesis.

HIP1^{-/-} Phenotype

It is surprising to note that HIP1^{-/-} young mice do not show abnormalities in brain morphology and neuronal densities when compared to wildtype mice (Metzler et al., 2003). However by 12 weeks of age, HIP1^{-/-} mice do develop a neurological phenotype with progressive marked and rigid thoracolumbar kyphosis, tremors and gait ataxia (Metzler et al., 2003). It was noted that these defects didn't result from a congenital skeletal abnormality, dysplasia, peripheral nerves or muscle function (Metzler et al., 2003). Also in HIP1^{-/-} mice, you have reduced membrane attachment of HIP1 interacting proteins such as HIP1r, AP2, htt and clathrin to liposomal membranes which might possibly lead to impaired CCV formation (Metzler et al., 2003).

Much emphasis has been placed on HIP1's role in the central nervous system, however HIP1's wide expression in peripheral tissues suggests that HIP1 might have other functions. For example, mutations of murine HIP1 leads to hematopoietic abnormalities and cataracts (Oravec-Wilson et al., 2004).

It has recently been shown that HIP1 can modulate the transcriptional activity of nuclear hormone receptors (Mills et al., 2005). HIP1 has been shown to associate with the androgen receptor and significantly repress transcription when knocked down (Mills et al., 2005). In the testis, HIP1^{-/-} mice causes defects in male reproduction, such as decreased testicular weights, degeneration of germ cells and decreased sperm counts (Rao et al., 2001). These changes appear to be intrinsic to the testis and not mediated by altered hormonal secretion by the pituitary gland. The increased apoptosis was limited to postmeiotic spermatids and spermatogenic stem cells, Leydig cells and Sertoli cells of the testes remained intact.

Objectives of the Current Study

In order to understand in greater detail the role that HIP1 plays in normal male reproduction, several parameters were examined in HIP1^{-/-} mice and compared to the wild-type littermates:

- A detailed light (LM) and electron (EM) microscopic analysis of structural abnormalities in the testis and the epididymis was performed of HIP1 knockout animals ranging from postnatal one week to 30 weeks of age.
- Immunocytochemical localization of HIP1 was performed in the testis to determine which cells expressed HIP1.
- The mean profile area of seminiferous tubules of HIP1^{-/-} mice at different ages was compared with +/+ mice using statistical analyses.
- The tubular profile areas of different epididymal regions of HIP1^{-/-} mice at 13 wks of age were compared with +/+ mice using statistical analyses.

- Sperm counts and sperm motility assays obtained from cauda epididymal sperm were analyzed on HIP1^{-/-} and ^{+/+} mice of 11 to 13 weeks of age.
- Morphological abnormalities of sperm of HIP1^{-/-} mice present in the epididymal lumen were compared with that of wild type mice.

It has been stated or evidence provided that HIP1 binds to inositol phosphates, clathrin heavy chain and clathrin light chain, HIP1r, AP2, huntingtin, tubulin/microtubules and actin and plays a crucial role in clathrin-mediated endocytosis and vesicle trafficking. It also has been suggested that HIP1 acts as a linking protein between the endocytic machinery and the acting cytoskeleton at the plasma membrane. In cells, clathrin mediated vesicles are formed both at the plasma membrane and the TGN (Wendland, 2002). Clathrin-coated pits have been found in germ cells mainly in pachytene spermatocytes and spermatids (Gerard et al., 1994) and it is well known that germ cells are capable of receptor-mediated endocytosis of certain molecules secreted by the Sertoli cells such as androgen binding protein, mannose 6-phosphate and testicular transferrin (Gerard , 1995; O'Brien et al., 1993; Petrie and Morales, 1992).

We speculate that HIP1's regulation of clathrin mediated endocytosis at the plasma membrane of these crucial molecules might prevent spermatocyte differentiation. A defect in this step of spermatogenesis thus can lead to loss of these cells with decreased late spermatids.

HIP1's involvement with cytoskeletal components, actin and microtubules, suggests that HIP1 can play a role in sperm tail proper alignment and orientation in the germ cells. Absence of a fully developed acrosome on the nuclear surface, but presence of many proacrosomic granules in some early spermatids suggests a role for HIP1 in proper acrosome formation and attachment to the nuclear envelope.

In Sertoli cells, HIP1 via its interaction with actin, can play a role at sites of ectoplasmic specializations and help in the anchoring of germ cells to the Sertoli cells preventing their premature release into the lumen of seminiferous tubules.

It seems as though HIP1 is a multifunctional protein that has the potential to act at multiple cellular sites where actin and microtubules are present: at the plasma membrane, the Golgi, the acrosome and the sperm tail in germ cells, and at ectoplasmic specializations in Sertoli cells.

REFERENCES

Bardin CW, Cheng CY, Musto NA, Gunsalus GL. 1998. The Sertoli Cell. *In* The Physiology of Reproduction, Vol 1 Knobil E and Neill JD, editors. Raven Press, New York, pp 933-974.

Benoff S. 1997. Carbohydrates and fertilization: an overview. *Mol Hum Reprod* 3:599-637.

Blader IJ, Cope MJTV, Jackson TR, Profit AA, Greenwood AF, Drubin DG, Prestwich GD, Theibert AB. 1999. GCS1, an arf guanosine triphosphate-activating protein in *Saccharomyces cerevisiae*, is required for normal actin cytoskeletal organization in vivo and stimulates actin polymerization. *Mol Biol Cell* 10: 581-596.

Bradley SV, Oravec-Wilson KI, Bougeard G, Mizukami I, Li L, Munaco AJ, Sreekumar A, Corradetti MN, Chinnaiyan AM, Sanda MG, Ross TS. 2005. Serum antibodies to huntingtin interacting protein-1: a new blood test for prostate cancer. *Cancer Res* 65: 4126-33.

Braun RE, Behringer RR, Peschon JJ, Brinster RL and Palmiter RD. 1989. Genetically haploid spermatids are phenotypically diploid. *Nature* 337:373-376.

Burkhard P, Strelkov SV, Stetefeld J. 2001. Coiled coils: a highly versatile protein folding motif. *Trends Cell Biol.*, 11, 82-88.

Brodsky FM, Chen CY, Knuehl C, Towler MC, Wakeham DE. 2001. Biological basket weaving: formation and function of clathrin-coated vesicles. *Annu Rev Cell Dev Biol* 17: 517-568.

Byers S, Pelletier RM, Suarez-Quian C. Sertoli cell junctions and the seminiferous epithelium barrier. *In the Sertoli Cell*. Russell LD and Griswold MD, editors. Cache River Press, Clearwater, Florida, pp 431-446.

Carreno S, Engqvist-Goldstein AE, Zhang CX, McDonald KL, Drubin DG. 2004. Actin dynamics coupled to clathrin-coated vesicle formation at the trans-Golgi network. *J Cell Biol*. Jun 21;165(6):781-8.

Chen C-Y, Brodsky FM. 2005. Huntingtin-interacting protein 1 (Hip1) and Hip1-related protein (Hip1R) bind the conserved sequence of clathrin light chains and thereby influence clathrin assembly *in vitro* and actin distribution *in vivo*. *J Biol Chem* 280: 6109-6117.

Chopra VS, Metzler M, Rasper DM, Engqvist-Goldstein AE, Singaraja R, Gan L, Fichter KM, McCutcheon K, Drubin D, Nicholson DW, Hayden MR. 2000. HIP12 is a non-proapoptotic member of a gene family including HIP1, an interacting protein with huntingtin. *Mammalian Genome* 11: 1006-1015.

Christensen AK. 1975. Leydig cells. *In Handbook of Physiology*, Vol. 5, Male Reproductive System. Hamilton DW and Greep RO, editors. Am Physiological Soc., Wash., DC., pp 57-94.

Clark RV. Three dimensional organization of testicular interstitial tissue of the mammalian testis. 1976. *Biol. Reprod.*, 9:500-512.

Clermont Y and Perey B. 1957. Quantitative study of the cell population of the seminiferous tubules in immature rats. *Am J Anat* 100: 241-267.

Clermont Y. 1958. Contractile elements in the limiting membrane of the seminiferous tubules of the rat. *Expt Cell Res* 15: 438-440.

Clermont Y and Huckins C. 1961. Microscopic anatomy of the sex cords and seminiferous tubules in growing and adult male albino rats. *Am J Anat* 108: 79-97.

Clermont Y, Tang XM. 1985. Glycoprotein synthesis in the Golgi apparatus of spermatids during spermiogenesis of the rat. *Anat Rec* 213: 33-43

Clermont Y, Oko R and Hermo L. 1993. Cell biology of mammalian spermiogenesis. *In* Cell and molecular biology of the testis. Desjardins V and Ewing L., editors. Oxford University Press, New York, pp 332-376.

Davis JR, Langford GA and Kirby PJ. 1970. The testicular capsule. *In* The Testis, Vol. I. Johnson AD, Gomes WR and VanDemark NL, editors. Academic Press, New York, pp 281-337.

De Duve C and Wattiaux R. 1966. Functions of lysosomes. *Annu Rev Physiol* 28:435-92.

De Krester DM and Kerr JB. 1988. The cytology of the testis. *In* the Physiology of Reproduction, Vol.1 Knobil E and Neill JD, editors. Raven Press, New York, pp 837-932.

Desjardins C and Ewing LL. 1993. Cell and Molecular Biology of the Testis. Oxford University Press, New York.

DiFiglia M, Sapp E, Chase K, Schwarz C, Meloni A, Young C, Martin E, Vonsattel JP, Carraway R, Reeves SA. 1995. Huntingtin is a cytoplasmic protein associated with vesicles in human and rat brain neurons. *Neuron* 14: 1075-1081.

Diprospero NA, Chen EY, Charles V, Plomann M, Kordower JH, Tagle DA. 2004. Early changes in Huntington's disease patient brains involve alterations in cytoskeletal and synaptic elements. *J Neurocytol.* 33: 517-33.

Dragatsis I, Levine MS, Zeitlin S. 2000. Inactivation of Hdh in the brain and testis results in progressive neurodegeneration and sterility in mice. *Nat Genet* 26: 300-306.

Dunah, AW, Jeong H, Griffin A, Kim YM, Standaert DG, Hersch SM, Mouradian MM, Young AB, Tanese N and Krainc D. 2002. Sp1 and TAFII130 transcriptional activity disrupted in early Huntington's disease. *Science* 296: 2238-2243.

Dym M and Fawcett DW. 1970. The blood-testis barrier in the rat and the physiological compartmentation of the seminiferous epithelium. *Biol Reprod* 3: 308-326.

Dym M and Fawcett DW. 1971. Further observations on the numbers of spermatogonia, spermatocytes and spermatids connected by intercellular bridges in the mammalian testis. *Biol Reprod* 4: 195-215.

Eddy EM, Toshimori K, O'Brien DA. 2003. Fibrous sheath of mammalian spermatozoa. *Microsc res Tech* 61: 103-15.

Engqvist-Goldstein AE, Kessels MM, Chopra VS, Hayden MR, Drubin DG. 1999. An actin-binding protein of the sla2/Huntingtin interacting protein 1 family is a novel component of clathrin-coated pits and vesicles. *J Cell Biol* 147: 1503-1518.

Engqvist-Goldstein AE, Zhang CX, Carreno S, Barroso C, Heuser JE, Drubin DG. 2004. RNAi-mediated Hip1R silencing results in stable association between the endocytic machinery and the actin assembly machinery. *Mol Biol Cell* 15: 1666-79.

Fawcett DW and Phillips DM. 1969. The fine structure and development of the neck region of the mammalian spermatozoa. *Anat Rec* 165: 153-184.

Fawcett DW, Anderson WA and Philips DM. 1971. Morphometric factors influencing the shape of the sperm head. *Dev Biol* 26: 220-251.

Fawcett DW and Philips DM. 1969. Observations on the release of spermatozoa and on changes in the head during passage through the epididymis. *J Reprod Fertil (Suppl.6)*: 405-418.

Fawcett DW. 1975. The mammalian spermatozoon. *Dev Biol* 44: 394-436.

Fawcett DW. 1975. Ultrastructure and function of the Sertoli cell. *In Handbook of Physiology, Section 7, Endocrinology, Vol. 5, Male Reproductive System.* Hamilton DW and Greep RO, editors. Williams and Wilkins, Baltimore, pp 21-55.

Ford MG, Pearse BM, Higgins MK, Vallis Y, Owen DJ, Gibson A, Hopkins CR, Evans PR, McMahon HT. 2001. Simultaneous binding of PtdIns_{4,5}P₂ and clathrin by AP180 in the nucleation of clathrin lattices on membranes. *Science* 291: 1051-1055.

Franke WW, Grund C, Schmid E. 1979. Intermediate-sized filaments present in Sertoli cells are of the vimentin type. *Eur J Cell Biol.* 19: 269-275.

French FS and Ritzen EM. 1973. A high-affinity androgen binding protein (ABP) in rat testis: evidence for secretion into efferent duct fluid and absorption by epididymis. *Endocrinology* 93:88-95.

Fritz IB, Kopec B, Lam K, Vernon RG. 1974. Effects of FSH on levels of androgen binding protein on the testis. *Curr Top Mol Endocrinol* 1:311-327.

Gartner LP, Hiatt JL. 1997. Male Reproductive System. *In Color Textbook of Histology.* Philadelphia, WB Saunders Company, pp 403-421.

Gerard H, Gerard A, En Nya A, Felden F, Gueant JL. 1994. Spermatogenic cells do internalize Sertoli androgen-binding protein: a transmission electron microscopy autoradiographic study in the rat. *Endocrinol* 134: 1515-27.

Gerard A. 1995. Endocytosis of androgen-binding protein (ABP) by spermatogenic cells. *J Steroid Biochem Mol Biol*: 53: 533-42.

Gervais FG, Singaraja R, Xanthoudakis S, Gutekuns C-A, Leavitt BR, Metzler M, Hackam AS, Tam J, Vaillancourt JP, Houtzager V, Rasper DM, Roy S, Hayden MR, Nicholson DW. 2002. Recruitment and activation of caspase-8 by the Huntingtin-interacting protein Hip-1 and a novel partner Hipp1. *Nat Cell Biol* 4: 95-105.

Gibbons IR. 1968. The biochemistry of motility. *Annu Rev Biochem* 37: 521-546.

Goodrowe KL, Heath E. 1984. Disposition of the manchette in the normal equine spermatid. *Anat Rec* 209:177-183.

Griffiths G, Warren G, Stuhlfauth I, Jockusch BM. 1981. The role of clathrin-coated vesicles in acrosome formation. *Eur J cell Biol* 26:52-60.

Griswold MD, Morales C and Sylvester SR. 1988. Molecular biology of the Sertoli cell. *Oxf Rev Reprod Biol* 10: 124-61.

Griswold MD. 1993. Protein secretion by Sertoli cells: general considerations. *In* The Sertoli Cell. Russell LD and Griswold MD, editors. Cache River Press, Clearwater, Florida, pp 195-200.

Griswold MD. 1995. Interactions between germ cells and Sertoli cells in the testis. *Biol Reprod* 52: 211-6.

Gutekunst CA, Levey AI, Heilman CJ, Whaley WL, Yi H, Nash NR, Rees HD, Madden JJ, Hersch SM. 1995. Identification and localization of huntingtin in brain and human lymphoblastoid cell lines with anti-fusion protein antibodies. *Proc Natl Acad Sci USA* 92: 8710-8714.

Hackam AS, Yassa AS, Singaraja R, Metzler M, Gutekunst CA, Gan L, Warby S, Wellington CL, Vaillancourt J, Chen N, Gervais FG, Raymond L, Nicholson DW, Hayden MR. 2000. Huntingtin interacting protein 1 induces apoptosis via a novel caspase-dependent death effector domain. *J Biol Chem* 275: 41299-41308.

Harper PS. 1991. Huntington's disease. W.B. Saunders Co, Ltd, London.

Hecht NB. 1998. Molecular mechanisms of male germ cell differentiation. *BioEssays* 20: 555-561.

Heid H, Figge U, Winter S, Kuhn C, Zimbelmann R, Franke W. 2002. Novel actin-related proteins Arp-T1 and Arp-T2 as components of the cytoskeletal calyx of the mammalian sperm head. *Exp Cell Res* 279: 177-87.

Hermo L, Dworkin J, Oko R. 1988. Role of epithelial clear cells of the rat epididymis in the disposal of the contents of cytoplasmic droplets detached from spermatozoa. *Am J Anat* 183: 107-24.

Hermo L and Lalli M. 1988. Binding and internalization in vivo of [¹²⁵I] hCG in Leydig cells of the rat. *J Androl* 9: 1-14.

Hermo L, Clermont Y and Lalli M. 1985. Intracellular pathways of endocytosed tracers in Leydig cells of the rat. *J Androl* 6:213-224.

Hermo L, Oko R, Morales CR. 1994. Secretion and endocytosis in the male reproductive tract: a role in sperm maturation. *Int Rev Cytol* 154: 105-189.

Hinners I and Tooze SA. 2003. Changing directions: clathrin-mediated transport between the Golgi and endosomes. *J Cell Sci* 116: 763-771.

Hinton BT and Setchell BP. 1993. Fluid secretion and movement, *In* The Sertoli Cell. Russell LD and Griswold MD, editors. Cache River Press, Clearwater, Florida, pp 249-267.

Hirst J, Robinson MS. Clathrin and adaptors. 1998. *Biochim Biophys Acta* 1404: 173-193.

Holtzman DA, Yang S, Drubin DG. Synthetic-lethal interactions identify two novel genes, SLA1 and SLA2, that control membrane cytoskeleton assembly in *Saccharomyces cerevisiae*. 1993. *J Cell Biol* 122: 635-644.

Huckins C. 1971. The spermatogonial stem cell population in adult rats, I. Their morphology, proliferation, and maturation. *Anat. Rec.* 169: 533-558.

Huckins C. 1978. The morphology and kinetics of spermatogonial degeneration in normal adult rats: An analysis using a simplified classification of the germinal epithelium. *Anat Rec* 190: 905-926.

The Huntington's Disease Collaborative Research Group. 1993. A novel gene containing a trinucleotide repeat that is expanded and unstable on Huntington's disease chromosomes. *Cell* 72: 971-983.

Hussain NK, Yanabhai M, Bhakar AL, Metzler M, Ferguson SSG, Hayden MR, McPherson PS, Kay BK. 2003. A role for epsin n-terminal homology/AP180 n-terminal homology (ENTH/ANTH) domains in tubulin binding. *J Biol Chem* 278: 28823-28830.

Hyun TS, Rao DS, Saint-Dic D, Michael LE, Kumar PD, Bradley SV, Mizukami IF, Oravec-Wilson KI, Ross TS. 2004. HIP1 and HIP1r stabilize receptor tyrosine kinases and bind 3-phosphoinositides via epsin N-terminal homology domains. *J Biol Chem* 279: 14294-14306.

Hyun TS, Ross TS. 2004. HIP1: trafficking roles and regulation of tumorigenesis. Trends in Mol Med 10: 194-199.

Itoh T, Koshiba S, Kigawa T, Kikuchi A, Yokoyama S, Takenawa T. 2001. Role of the ENTH domain in phosphatidylinositol-4,5-bisphosphate binding and endocytosis. Science 291: 1047-1051.

Jost A. 1973. A new look at the mechanism controlling sex differentiation in mammals. John's Hopkins Med. J. 130: 38-53.

Kalchman MA, Koide HB, McCutcheon K, Graham RK, Nichol K, Nishiyama K, Kazemi-Esfarjani P, Lynn FC, Wellington C, Metzler M, Goldberg YP, Kanazawa I, Gietz RD, Hayden M. HIP1, a human homologue of *S. cerevisiae* Sla2p, interacts with membrane-associated huntingtin in the brain. Nat Genet 16: 44-53.

Karnovsky MJ. 1971. Use of ferrocyanide-reduced osmium tetroxide in electron microscopy (Abstract). In: Proceedings of the 11th American Society of Cell Biology. New Orleans, Louisiana: November 17-20; 284:146.

Kang-Decker N, Mantchev GT, Juneja SC, McNiven MA, van Deursen JMA. 2001. Lack of acrosome formation in Hrb-deficient mice. Science 294: 1531-1533.

Kato A, Nagata Y, Todokoro K. 2004. Delta-tubulin is a component of intercellular bridges and both the early and mature perinuclear rings during spermatogenesis. Dev Biol 269: 196-205.

Kegel, KB., Meloni AR, Yi Y, Kim YJ, Doyle E, Cuiffo BG, Sapp, Wang Y, Qin ZH, Chen JD, Nevins JR, Aronin N, DiFiglia M. 2002. Huntingtin is present in the nucleus, interacts with the transcriptional corepressor C-terminal binding protein, and represses transcription. J Biol Chem 277: 7466-7476.

Kerr JB and de Krester DM. 1974. The role of the Sertoli cell in phagocytosis of residual bodies of spermatids. *J Reprod Fertil* 36: 439-440.

Kierszenbaum AL. 2002. Keratins: unraveling the coordinated construction of scaffolds in spermatogenic cells. *Mol Reprod Dev* 61:1-2.

Kierszenbaum AL, Rivkin E, Tres LL. 2003. Acroplaxome, an F-actin-Keratin-containing plate, anchors the acrosome to the nucleus during shaping of the spermatid head. *Mol Biol Cell* 14: 4628-4640.

Kierszenbaum AL and Tres LL. 2004. The acrosome-acroplaxome-manchette complex and the shaping of the spermatid head. *Arch Histol Cytol* 67: 271-284.

Kierszenbaum AL, Tres LL, Rivkin E, Kang-Decker N, van Deursen JMA. 2004. The Acroplaxome is the docking site of golgi-derived myosin Va/Rab27a/b-containing proacrosomal vesicles in wild-type and Hrb mutant mouse spermatids. *Biol Reprod* 70: 1400-1410.

Kim KS, Foster JA, Gerton GL. 2001. Differential release of guinea pig sperm acrosomal components during exocytosis. *Biol Reprod* 64:148-156.

Kluin PM, Kramer MF and de Rooij DG. 1984. Proliferation of spermatogonia and Sertoli cells in maturing mice. *Anat Embryol* 169: 73-78.

Korley R, Pouresmaeili F, Oko R. 1997. Analysis of the protein composition of the mouse sperm perinuclear theca and characterization of its major protein constituent. *Biol Reprod* 57: 1426-32.

Lafer EM. 2002. Clathrin-Protein Interactions. *Traffic* 3: 513-520.

Leblond CP, Clermont Y. 1952a. Definition of the stages of the cycle of the seminiferous epithelium in the rat. 1952a. *Ann NY Acad Sci* 55:548-573.

Leblond CP and Clermont Y. 1952b. Spermiogenesis of rat, mouse, hamster and guinea pig as revealed by the "periodic acid-fuschin sulphurous acid" technique, *Am J Anat* 90: 167-215.

Lecuyer C, Dacheux JL, Hermand E, Mazeman E, Rousseaux J, Rousseaux-Prevost R. 2000. Actin-binding properties and colocalization with actin during spermiogenesis of mammalian sperm calicin. *Biol Reprod* 63: 1801-10.

Leeson TS and Cookson FB. 1974. The mammalian testicular capsule and its muscular elements. *J Morph* 144: 237-354.

Legendre-Guillemain V, Metzler M, Charbonneau M, Gan L, Chopra V, Philie J, Hayden MR, McPherson PS. 2002. HIP1 and HIP12 display differential binding to F-actin, AP2, and clathrin. Identification of a novel interaction with clathrin light chain. *J. Biol. Chem.* 277: 19897-19904.

Legendre-Guillemain V, Wasiak S, Hussain NK, Angers A, McPherson PS. 2004. ENTH/ANTH proteins and clathrin-mediated membrane budding. *J. Cell Science* 117:9-18.

Legendre-Guillemain V, Metzler M, Lemaire JF, Philie J, Gan L, Hayden MR, and McPherson PS. 2005. Huntingtin interacting protein 1 (HIP1) regulates clathrin assembly through direct binding to the regulatory region of the clathrin light chain. *J Biol Chem* 280: 6101-6108.

Lemmon MA. 2003. Phosphoinositide recognition domains. *Traffic* 4: 201-213.

Li SH, Li XJ. 2004. Huntingtin-protein interactions and the pathogenesis of Huntington's disease. *Trends in Genetics* 20: 146-154.

Li SH, Li XJ. 2004. Huntingtin and its role in neuronal degeneration. *Neuroscientist* 10: 467-75.

Li SH, Hosseini SH, Gutenkust CA, Hersch SM, Ferrante RJ, Li XJ. 1998. A human HAP1 homologue. Cloning, expression, and interaction with huntingtin. *J Biol Chem* 273: 19220-19227.

Longo FJ, Krohne G, Franke WW. 1987. Basic proteins of the perinuclear theca of mammalian spermatozoa and spermatids: a novel class of cytoskeletal elements. *J Cell Biol* 105: 1105-20.

Louis BG, Fritz IB. 1977. Stimulation by androgens of the production of androgen binding protein by cultured Sertoli cells. *Mol Cell Endocrinol* 7: 9-16.

Man HY, Lin JW, Ju WH, Ahmadian G, Liu L, Becker LE, Shen M, Wang YT. 2000. Regulation of AMPA receptor-mediated synaptic transmission by clathrin-dependent receptor internalization. *Neuron* 25: 649-662.

Manandhar G, Sutovsky P, Joshi HC, Stearns T, Schatten G. 1998. Centrosome reduction during mouse spermiogenesis. *Dev Biol* 203: 424-434.

Mann T and Lutwak-Mann C. 1981. *Male Reproductive Function and Semen*. Springer-Verlag, New York.

Martin EJ, Kim M, Velier J, Sapp E, Lee HS, Laforet G, Won L, Chase K, Bhide PG, Heller A, Aronin N, DiFiglia M. 1999. Analysis of Huntingtin-associated protein 1 in mouse brain and immortalized striatal neurons. *J Comp Neurol* 403: 421-430.

Metzler M, Gertz A, Sarkar M, Schachter H, Schrader JW, Marth JD. 1994. Complex asparagines-linked oligosaccharides are required for morphogenic events during post-implantation development. *EMBO J* 13: 2056-2065.

Metzler M, Legendre-Guillemin V, Gan L, Chopra V, Kwok A, McPherson PS, Hayden MR. 2001. HIP1 functions in clathrin-mediated endocytosis through binding to clathrin and adaptor protein 2. *J Biol Chem* 276: 39721-39276.

Metzler M, Li B, Gan L, Georgiou J, Gutekunst CA, Wanf Y, Torre E, Devon RS, Oh R, Legendre-Guillemin V, Rich M, Alvarez C, Gertsenstein M, McPherson PS, Nagy A, Wang YT, Roder JC, Raymond LA, Hayden MR. 2003. Disruption of the endocytic protein HIP1 results in neurological deficits and decreased AMPA receptor trafficking. *EMBO J* 22: 3254-3266.

Millette CF and Bellvè AR. 1977. Temporal expression of membrane antigens during mouse spermatogenesis. *J Cell Biol* 74: 86-97.

Mills IG, Gaughan L, Robson C, Ross T, McCracken S, Kelly J, Neal DE. 2005. Huntingtin interacting protein 1 modulates the transcriptional activity of nuclear hormone receptors. *J Cell Biol* 18: 191-200.

Miki K, Eddy EM. 1998. Identification of tethering domains for protein kinase A type 1 alpha regulatory subunits on sperm fibrous sheath protein FSC1. *J Biol Chem* 273: 34384-34390.

Mishra SK, Agostinelli NR, Brett TJ, Mizukami I, Ross TS, Traub LM. 2001. Clathrin- and AP-2 binding sites in HIP1 uncover a general assembly role for endocytic accessory proteins. *J Biol Chem* 276: 46230-46236.

Morales C, Clermont Y and Hermo L. 1985. Nature and function of endocytosis in Sertoli cells of the rat. *Am J Anat* 173:203-217.

Morales CR and Clermont Y. 1993. Structural changes of the Sertoli cell during the cycle of the seminiferous epithelium. *In* the Sertoli Cell. Russell LD and Griswold MD, editors. Cache River Press, Clearwater, Florida, pp 305-330.

Morales CR, Zhao Q, El-Alfy M, Suzuki K. 2000. Targeted disruption of the mouse prosaposin gene affects the development of the prostate gland and other male reproductive organs. *J Androl* 21: 765-775.

Moreno RD and Schatten G. 2000. Microtubule configurations and post-translational α -tubulin modifications during mammalian spermatogenesis. *Cell Motil Cytoskeleton* 46:235-246.

Moreno RD, Ramalho-Santos J, Sutovsky P, Chan EKL, Wessel G, Schatten G. 2000. Vesicular traffic and golgi apparatus dynamics during mammalian spermatogenesis: implications for acrosome architecture. *Biol Reprod* 63:89-98.

Mori H and Christensen AK. 1980. Morphometric analysis of Leydig cells in the normal rat testes. *JCell Biol* 84: 340-354.

Mori C, Nakamura N, Welch JE, Gotoh H, Goulding EH, Fujioka M, Eddy EM. 1998. Mouse spermatogenic cell-specific type 1 hexokinase (mHk1-s) transcripts are expressed by alternative splicing from the mHK1 gene and the HK1-S protein is localized mainly in the sperm tail. *Mol Reprod Dev* 49: 374-385.

Mulholland J, Wesp A, Reizman H, Botstein D. 1997. Yeast actin cytoskeleton mutants accumulate new class of Golgi-derived secretory vesicle. *Mol Biol Cell* 8: 1481-1499.

Munell F, Suarez-Quian CA, Selva DM, Tirado OM, Reventos J. 2002. Androgen-binding protein and reproduction: where do we stand? *J Androl* 23: 598-609.

Nistal M, Santamaria L and Paniagua R. 1984. Mast cells in the human testis and epididymis from birth to adulthood. *Acta Anat* 119: 155-160.

Norremolle A, Riess O, Epplen JT, Fenger K, Hasholt L, Sorensen SA. 1993. Trinucleotide repeat elongation in the Huntingtin gene in Huntington disease patients from 71 Danish families. *Hum Mol Genet* 2: 1475-6.

Oakberg EF. 1956a. A description of spermiogenesis in the mouse and its use in analysis of the cycle of the seminiferous epithelium and germ renewal. *Am J Anat* 99:391-413.

Oakberg EF. 1956b. Duration of spermatogenesis in the mouse and timing of stages of the cycle of the seminiferous epithelium. *Am J Anat* 99: 507-516.

O'Brien DA, Gabel CA, Eddy EM. 1993. Mouse Sertoli cells secrete mannose 6-phosphate containing glycoproteins that are endocytosed by spermatogenic cells. *Biol Reprod* 49:1055-65.

Olson GE and Linck RW. 1977. Observations of the structural components of flagellar axonemes and central pair microtubules from rat sperm, *J Ultrastruc Res* 61:21-43.

Oko R, Hermo L, Chan PT, Fazel A, Bergeron JJ. 1993. The cytoplasmic droplet of rat epididymal spermatozoa contains saccular elements with Golgi characteristics. *J Cell Biol* 123: 809-21.

Oko R, Hermo L and Hecht NB. 1991. Distribution of actin isoforms within cells of the seminiferous epithelium of the rat testis: evidence for a muscle form of actin in spermatids. *Anat Rec* 231: 63-81.

Oko R, Clermont Y. 1988. Isolation, structure and protein composition of the perforatorium of rat spermatozoa. *Biol Reprod* 39: 673-87.

Oko R, Jando V, Wagner CL, Kistler WS and Hermo LS. 1996. Chromatin reorganization in rat spermatids during the disappearance of testos-specific histone, H1t, and the appearance of transition proteins TP1 and TP2. *Biol Reprod* 54: 1141-1157.

Oravez-Wilson KI, Kiel MJ, Li L, Rao DS, Saint-Dic D, Kumar PD, Provot MM, Hankenson KD, Reddy VN, Lieberman AP, Morrison SJ, Ross TS. 2004. Huntingtin interacting protein 1 mutations lead to abnormal hematopoiesis, spinal defects and cataracts. *Hum Mol Genet* 13: 851-867.

Petrie RG Jr, Morales CR. 1992. Receptor-mediated endocytosis of testicular transferrin by germinal cells of the rat testis. *Cell Tissue Res* 267: 45-55.

Price D and William-Ashman HG. 1961. The accessory reproductive glands of mammals. *In Sex and Internal Secretions*, Vol. 1, 3rd ed. Young WC, editor. Williams and Wilkins, Baltimore, pp 366-448.

Raamsdonk JMV, Pearson J, Rogers DA, Bissada N, Vogl AW, Hayden MR, Leavitt BR. 2005. Loss of wild-type huntingtin influences motor dysfunction and survival in the YAC128 mouse model of Huntington disease. *Hum Mol Genet* 14: 1379-1392.

Rao DS, Chang JC, Kumar PD, Ikuko M, Smithson GM, Bradley SV, Parlow AF, Ross TS. 2001. Huntingtin interacting protein 1 is a clathrin coat binding protein required for differentiation of late spermatogenic progenitors. *Mol Cell Biol* 21:7796-7806.

Rao DS, Hyun TS, Kumar PD, Ikuko MF, Rubin MA, Lucas PC, Sanda MG, Ross TS. 2002. Huntingtin-interacting protein 1 is overexpressed in prostate and colon cancer and is critical for cellular survival. *J. Clin Invest.* 110: 351-360.

Rao DS, Bradley SV, Kumar PD, Hyun TS, Saint-Dic D, Oravez-Wilson K, Kleer CG, Ross TS. 2003. Altered receptor trafficking in Huntingtin Interacting Protein 1-transformed cells. *Cancer Cell* 3: 471-482.

Robaire B and Hermo L. 1988. Efferent ducts, epididymis, and vas deferens: structure, functions, and their regulation. *In the Physiology of Reproduction*, Vol. 1. Knobil and Neill JD, editors. Raven Press, New York, pp 999-1080.

Rosenthal JA, Chen H, Slepnev VI, Pellegrini L, Salcini AE, Di Fiore PP, De Camili P. 1999. The epsins define a family of proteins that interact with components of the clathrin coat and contain a new protein module. *J Biol Chem* 274: 33959-33965.

Russell LD, Saxena NK, Turner TT. 1989. Cytoskeletal involvement in spermiation and sperm transport. *Tissue and Cell* 21: 361-379.

Russell L, Clermont Y. 1976. Anchoring device between Sertoli cells and late spermatids in rat seminiferous tubules. *Anat Rec* 185:259-278.

Russell LD. Observation on rat Sertoli ectoplasmic ('junctional') specializations in their association with germ cells of the rat testis. 1977. *Tissue and Cell* 9: 475-498.

Russell LD and Clermont Y. 1977. Degeneration of germ cells in normal, hypophysectomized and hormone-treated hypophysectomized rats. *Anat Rec* 187: 347-366.

Russell LD. 1980. Deformities in head region of late spermatids of hypophysectomized-hormone treated rats. *Anat Rec* 197: 21-31.

Russell LD and Frank B. 1978. Characterization of rat spermatocytes after plastic embedding. *Arch Androl* 1: 5-18.

Russell LD, Lee IP, Ettlin R, Peterson RN. 1983. Development of the acrosome and alignment, elongation and entrenchment of spermatids in procarbazine-treated rat. *Tissue and Cell* 15: 615-626.

Russell LD. Spermiation-the sperm release process: Ultrastructural observations and unresolved problems 1984. *In* Van Blerkom J, Motta PM (ed.), *Ultrastructure of Reproduction*. Boston: Martinus Nijhoff Publishers, pp 46-66.

Russell LD, Weber JE and Vogl AW. 1986. Characterization of filaments within the subacrosomal space of rat spermatids during spermiogenesis. *Tissue and Cell* 8: 887-898.

Russell LD, Vogl AW, Weber JE. 1987. Actin localization in male germ cell intercellular bridges in the rat and ground squirrel and disruption of bridges by cytochalasin. *Am J Anat* 180:25-40.

Russell LD, Goh JC, Rashed RM, Vogl AW. 1988. The consequences of actin disruption at Sertoli ectoplasmic specialization sites facing spermatids after in vivo exposure of rat testis to cytochalasin. *D Biol Reprod* 39:105-118.

Russell LD, Ettlín RA, SinhaHikim AP and Clegg ED. 1990. Histological and histopathological evaluation of the testis. Cache River Press. Clearwater, Florida, pp 1-40, 119-161.

Russell LD, Russell JA, MacGregor GR, Meistrich ML. 1991. Linkage of manchette microtubules to the nuclear envelope and observations of the role of the manchette in nuclear shaping during spermiogenesis in rodents. *Am J Anat* 192: 97-120.

Russell LD. 1993. Role in spermiation. *In* *The Sertoli Cell*. Russell LD and Griswold MD, editors. Cache River Press, Clearwater, Florida, pp 269-304.

Setchell BP. 1982. Spermatogenesis and spermatozoa. *In* *Reproduction in Mammals, Book I: Germ Cells and Fertilization*, 2nd ed. Austin CR and Short RV, editors. Cambridge University Press, Cambridge, U.K., pp 63-101.

Sanborn BM, Steinberger A, Tcholakian RK and Steinberger E. 1977. Direct measurement of androgen receptors in cultured Sertoli cells. *Steroids* 29: 493-502.

Sar M, Hall SH, Wilson EM, French FS. 1993. Androgen Regulation of Sertoli Cells. Russell LD. 1993. *In The Sertoli Cell*. Russell LD and Griswold MD, editors. Cache River Press, Clearwater, Florida, pp 509-516.

Schilling G, Sharp AH, Loev SJ, Wagster MV, Li S-H, Stine OC, Ross CA. 1995. Expression of the Huntington's disease (IT-15) protein product in HD patients. *Hum Mol Genet* 4: 1365-1371.

Seki N, Muramatsu M, Sugano S, Suzuki Y, Nakagawara A, Ohhira M, Hayashi A, Hori T, Saito T. 1998. Cloning, expression analysis, and chromosomal localization of HIP1R, an isolog of huntingtin interacting protein 1 (HIP1). *J Hum Genet* 43: 268-71.

Senetar MA, Foster SJ, McCanna RO. 2004. Intrasteric inhibition mediates the interaction of the I/LWEQ module proteins talin 1, talin 2, hip1, and hip12 with actin. *Biochemistry* 43: 15418-15428.

Setchell BP. The secretion of fluid by the testes of rats, rams, and goats with some observations on the effect of age, cryptorchidism and hyphophysectomy. 1970. *J Reprod Fert* 23: 79-85.

Sharp AH, Love SJ, Schilling G, Li S-H, Li X-J, Bao J., Wagster MV, Kotzuk JA, Steiner JP. 1995. Widespread expression of Huntington's disease gene (IT15) protein product. *Neuron* 14: 1065-1074.

Si Y, Okuno M. 1993. The sliding of the fibrous sheath through the axoneme proximally together with microtubule extrusion. *Exp Cell Res* 208:17-174.

Skinner MK and Griswold MD. Sertoli cells synthesize and secrete transferrin-like protein. 1980. *J Biol Chem* 255: 9523-9525.

Slepnev VI, Camilli DP. 2000. Accessory Factors in Clathrin-Dependent Synaptic Vesicle Endocytosis. *Nature Reviews* 1: 161-172.

Smith CJ, Pearse BM. 1999. Clathrin: anatomy of a coat protein. *Trends Cell Biol.* 9:335-338.

Sprando RL, Russell LD. 1987. Comparative study of cytoplasmic elimination in spermatids of selected mammalian species. *Am J Anat* 178: 72-80.

Steger K, Failing K, Klonisch T, Behre HM, Manning M, Weidner W, Hertle L. 2001. Round spermatids from infertile men exhibit decreased protamine-1 and -2 Mrna. *Hum Reprod* 16: 709-716.

Steinberger A. Inhibin production by Sertoli cells in culture. 1979. *J. Reprod Fertil Suppl* 1979: 31-45.

Strong TV, Tagle DA, Valdes JM, Elmer LW, Boehm K, Swaroop M, Kaatz KW, Collins FS, Albin RL. 1993. Widespread expression of the human and rat Huntington's disease gene in brain and nonneuronal tissues. *Nature Genet* 5: 259-265.

Syntin P, Robaire B. 2001. Sperm structural and motility changes during aging in the brown norway rat. *J Androl* 22: 235-244.

Tang XM, Clermont Y and Hermo L. 1988. Origin and fate of autophagosomes in Leydig cells of normal adult rats. *J Androl* 9: 284-293.

Thorne-Tjomsland G, Clermont Y and Hermo L. 1988. Contribution of the Golgi apparatus components to the formation of the acrosomic system and chromatoid body in rat spermatids. *Anat Rec* 221:591-598.

Tindall DJ, Miller DA and Means AR. 1977. Characterization of androgen receptors in Sertoli cell enriched testis. *Endocrin* 101: 13-23.

Toshimori K and Ito C. 2003. Formation and organization of the mammalian sperm head. *Arch Histol Cytol* 66: 383-396.

Tres LL, Rivkin E, Kierszenbaum AL. 1996. Sak 57, an intermediate filament keratin present in intercellular bridges of rat primary spermatocytes. *Mol Reprod Dev* 45:93-105.

Trottier Y, Devys D, Imbert G, Saudou F, An L, Lutz Y, Weber C., Agid Y., Hirsch EC, Mandel J-L. 1995. Cellular localization of the Huntington's disease protein and discrimination of the normal and mutated form. *Nature Genet.* 10: 104-110.

Tulsiani DR, Abou-Haila A, Loeser CR and Pereira BM. 1998. The biological and functional significance of the sperm acrosome and acrosomal enzymes in mammalian fertilization. *Exp Cell Res* 240: 151-164.

Velier J, Kim M, Schwarz C, Kim TW, Sapp E, Chase K, Aronin N, DiFiglia M. 1998. Wild-type and mutant huntingtin's function in vesicle trafficking in the secretory and endocytic pathways. *Exp Neurol* 152: 34-40.

Ventela S, Toppari J, Parvinen M. 2003. Intercellular organelle traffic through cytoplasmic bridges in early spermatids of the rat: mechanisms of haploid gene product sharing. *Mol Biol Cell* 14: 2768-80.

Vogl AW. 1989. Distribution and function of organized concentrations of actin filaments in mammalian spermatogenic cells and Sertoli cells. *Int Rev Cytol* 119: 1-56.

Vogl AW, Pfeiffer DC, Redenbach DM and Grove BD. 1993. Sertoli cell cytoskeleton. *In* The Sertoli Cell. Russell LD and Griswold MD, editors. Cache River Press, Clearwater, Florida, pp 39-86.

Vonsattel JP, Myers RH, Stevens TJ, Ferrante RJ, Bird ED, Richardson EP Jr. 1985. Neuropathological classification of Huntington's disease. *J Neuropathol Exp Neurol* 44: 559-577.

Wanker EE, Rovira C, Scherzinger E, Hasenbank R, Walter S, Tait D, Colicelli J, Lehrach H. 1997. HIP-1: a huntingtin interacting protein isolated by the yeast two-hybrid system. *Hum Mol Genet* 6: 487-495.

Weber JE and Russell LD. 1987. A study of intercellular bridges during spermatogenesis in the rat. *Am J Anat* 180: 1-24.

Wendland B. 2002. Epsins: adaptors in endocytosis? *Nat Rev Mol Cell Biol* 3: 971-977.

Wilson JD, George FW and Griffin JE. 1981. The hormonal control of sexual development. *Science* 211: 1278-1284.

William-Ashman HG. 1983. Regulatory features of seminal vesicle development and function. *Curr Top Cell Regul* 22: 202-273.

Wing TY, Ewing LL and Zirkin BR. 1984. Effects of luteinizing hormone withdrawal on Leydig cell smooth endoplasmic reticulum and steroidogenic reactions which convert pregnenolone to testosterone. *Endocrin* 115: 2290-2296.

Wing TY, Ewing LL, Zegeye B and Zirking BR. 1985. Restoration effects of exogenous luteinizing hormone on the testicular steroidogenesis and Leydig cell ultrastructure. *Endocrin* 117: 1179-1787.

Wong V and Russell LD. 1983. Three-dimensional reconstruction of a rat stage V Sertoli cell: I. Methods, basic configuration and dimensions. *Am J Anat* 167: 143-161.

Wu JY, Ribar TJ, Cummings DE, Burton KA, McKnight GS, Means AR. 2000. Spermiogenesis and exchange of basic nuclear proteins are impaired in male germ cells lacking Camk4. *Nat Genet* 25: 448-452.

Yang S, Cape MJ, Drubin DG. 1999. Sla2p is associated with the yeast cortical actin cytoskeleton via redundant localization signals. *Mol Biol Cell* 10: 2265-83.

Yao R, Ito C, Natsume Y, Sugitani Y, Yamanaka H, Kuretake S, Yanagida K, Sato A, Toshimori K, Noda T. 2002. Lack of acrosome formation in mice lacking a Golgi protein, GOPC. *Proc Natl Acad Sci USA* 99:11211-11216.

Yoshinaga K and Toshimori K. 2003. Organization and modifications of sperm acrosomal molecules during spermatogenesis and epididymal maturation. *Mic Res Tech* 61: 39-45.

Zirking BR, Ewing LL, Kromann N and Cochran RC. 1980. Testosterone secretion by rat, rabbit, guinea pig, dog and hamster testes perfused in vitro: correlation with Leydig cell ultrastructure. *Endocrin* 107:1867-1874.

Zirkin BR. 1995. What is the relationship between the various endocrine components of the male reproductive system? *In Handbook of Andrology*. Lawrence, Allen Press, pp 5-7.

Chapter II

Abnormalities in the Testis, Reduced Sperm Counts,
and Altered Sperm Motility Measures Are All Detected
in HIP1-Deficient Mice

Abnormalities in the Testis, Reduced Sperm Counts, and Altered Sperm Motility Measures Are All Detected in HIP1-Deficient Mice

Karine Khatchadourian,¹ Charles E. Smith,² Mary Gregory,³
Daniel G.Cyr,³ Martina Metzler,⁴ Michael R. Hayden⁴ and Louis Hermo¹

¹ Department of Anatomy and Cell Biology, McGill University, Montreal, Canada

² Département de Stomatologie, Université de Montréal, Montreal, Canada

³ INRS-Institut Armand Frappier, Université du Québec, Pointe-Claire, Canada

⁴ Centre for Molecular Medicine and Therapeutics, Department of Medical Genetics, University of British Columbia, Vancouver, Canada

Running Title: Abnormalities of sperm in HIP1^{-/-} mice

Key Words: gene knockout; HIP1 ^{-/-} mice; seminiferous tubules; epididymis; spermatids; immunocytochemistry; electron microscopy; sperm counts and motility

Supported by grants from the Canadian Institutes of Health Research (LH, MRH), Dan Cyr (NSERC/CIHR) and the National Institutes of Health (CES; DE013237)

Send reprint requests to:
Dr. Michael R. Hayden
Centre for Molecular Medicine and Therapeutics
980 West 28th Avenue
Vancouver, BC, Canada
V5Z 4H4

e-mail : mrh@cmmt.ubc.ca

ABSTRACT

Huntingtin -interacting protein 1 (HIP1), a component of the endocytic machinery, associates with clathrin on coated vesicles and binds directly to actin and microtubules. In the present study, the testes of mice deficient in HIP1 were examined from 7–30 wks of age and compared to their wild type littermates. In the testis of wild type mice, high levels of HIP1 protein were detected by western blotting that was seen by LM immunocytochemistry to result from prominent reactions over Sertoli cells, the Golgi of germ cells, and the cytoplasm of late elongating spermatids (steps 9-16) all of which weren't seen in HIP1 $-/-$ mice. The knock out mice showed moderate to severe abnormalities to some but not all seminiferous tubules (STs). Adversely affected STs had fewer germ cells, including pachytene spermatocytes and/or postmeiotic spermatids, and the epithelium appeared vacuolated. Quantitative measurements confirmed that mean profile areas of seminiferous, but not epididymal, tubules were significantly decreased in HIP1 $-/-$ mice compared to wild-type littermates. In the EM, major structural abnormalities were noted with respect to the association of elongating spermatids with ectoplasmic specializations of Sertoli cells, which were absent or altered in appearance in HIP1 $-/-$ mice. Postmeiotic spermatids also showed a varying degrees of alterations. While some of these cells appeared normal, others had structural deformations of their heads, bent flagella, the complete or partial absence of an acrosome or its detachment from the nucleus, and retention of the cytoplasm enveloping the spermatid head. In the epididymal lumen of HIP1 $-/-$ mice, the presence of structurally abnormal sperm, as well as numerous spherical germ cells supported the testicular finding of abnormal development of spermatids and the sloughing and loss of germ cells due to Sertoli cell alterations. Sperm counts from the cauda epididymidis were significantly reduced in HIP1 $-/-$ mice (7.14 M/ml) compared to their wild-type littermates (19.13 M/ml) at 12 wks of age ($p < 0.05$). In addition, computer assisted sperm analyses indicated that velocities, amplitude of lateral head displacements, and numbers and percentages of sperm in the motile, rapid, and progressive categories were all much lower in HIP1 $-/-$ mice. The numbers and percentages of sperm in the static category, however, were greatly increased in HIP1 $-/-$ mice.

These data suggest that HIP1 plays a role in germ cells at the time of acrosome formation and its tethering to the nuclear surface, proper orientation of the flagellum, displacement of the nucleus in relation to the cytoplasm, as well as shaping of the sperm head. HIP1 also affects Sertoli cell ectoplasmic specializations and their role in binding spermatids in the epithelium. These interactions highlight a role for HIP1 in relation to actin and microtubules which have been implicated in these different cellular processes in germ and Sertoli cells.

INTRODUCTION

Huntingtin-interacting protein 1 (HIP1) was first identified via its interaction with huntingtin (htt), a polyglutamine-containing protein associated with Huntington Disease (HD) (Kalchman et al., 1997; Wanker et al., 1997). HIP1 is a 116-kDa cytosolic protein ubiquitously expressed and highly enriched in human and mouse brain tissue (Kalchman et al., 1997; Wanker et al., 1997). HIP1, an ortholog of the yeast protein Sla2p, acts as an endocytic protein at the plasma membrane, and is a component of clathrin coated vesicles co-localizing with adaptor protein 2 and clathrin in various cells and tissues (Metzler et al., 2001; Waelter et al., 2001; Mishra et al., 2001). At its N-terminus, HIP1 contains an AP180 N-Terminal Homology domain (ANTH), a domain which is very similar in structure to the Epsin N-terminal Homology (ENTH) domain (Ford et al., 2002). ENTH domains are evolutionarily conserved modules found in various proteins such as the epsins (Chen et al., 1998). Both ANTH and ENTH domain-bearing proteins bind to phosphatidylinositol-4, 5-bisphosphate (PIP), at the plasma membrane (Ford et al., 2001) and play a crucial role in the formation of clathrin coated pits and clathrin-coated vesicles (Rosenthal et al., 1999; Itoh et al., 2001; Legendre-Guillemain et al., 2004). It has been shown that ENTH/ANTH domains, including that of HIP1, also bind to tubulin heterodimers and to assembled microtubules (Hussain et al., 2003). In addition to its interaction with tubulin/microtubules, HIP1 also directly interacts with actin via an I/L WEQ module (talin homology domain) located at its C-terminus (Senetar et al., 2004;

Legendre-Guillemain et al., 2005). Since HIP1 binds both to actin and microtubules, HIP1 might also play a role in cytoskeletal-based vesicular trafficking and/or act as a linking protein between actin and microtubule networks.

During the process of spermatogenesis in seminiferous tubules of the testis, a series of dramatic chronological events leads to the production and final outcome of sperm released into the lumen and destined for maturation in the epididymis. Spermatogonia divide to give rise to spermatocytes that undergo meiosis resulting in the haploid spermatids (Leblond and Clermont, 1952; Clermont, 1972; Russell et al., 1990). These spermatids produce a modified lysosome called the acrosome (Eddy and O'Brien DA, 1993; Abou-Haila and Tulsiani, 2000), undergo remodeling of their nuclear shape including chromatin condensation, develop a flagellum with its characteristic structural components and maintain close associations with Sertoli cells via ectoplasmic specializations (Russell, 1977; Clermont et al., 1993; Meistrich, 1993; Vogl et al, 1993; Oko and Clermont, 1991; Oko, 1998). In many of these dynamic processes, cytoskeletal elements of spermatids, such as microtubules of the manchette and actin filaments of the acroplaxome are involved (Clermont et al., 1993; Russell et al., 1991; Meistrich, 1993; Kierszenbaum et al., 2003). Closely monitoring germ cell development and differentiation, protection and release from the epithelium are the supportive nondividing Sertoli cells. Sertoli cells produce glycoproteins, hormones, androgen binding proteins and growth factors that may influence the developing germ cells (O'Brien et al., 1993; Griswold, 1993). In addition, Sertoli cells bind germ cells in the seminiferous epithelium via actin filaments of their ectoplasmic specializations (Russell, 1993; Vogl et al., 1993). Sertoli cells are also highly endocytic in nature and contain numerous lysosomes at specific stages of the seminiferous cycle (Morales et al., 1985). They possess coated pits both apically and basally and thus take up substances from the interstitial space as well as from the lumen (Morales and Clermont, 1993). All germ cells to a degree possess endocytic organelles and have coated pits (Segretain et al., 1992; Gerard et al., 1991, 1994). They are involved in the endocytosis of substances such as androgen binding protein (ABP), transferrin and mannose 6 phosphate containing glycoproteins, derived from Sertoli cells (Sylvester and Griswold, 1984; O'Brien et al., 1989, 1993;

Gerard et al., 1991, 1994; Petrie and Morales, 1992). Thus both germ and Sertoli cells are equipped with organelles that may be altered in the absence of HIP1.

In the testis, a role for HIP1 has been implicated by the generation of mice that have a targeted deletion of exons 2 to 7 of the mHIP1 gene. Male HIP1-deficient mice revealed testicular degeneration associated with the presence of multinucleated giant cells in seminiferous tubules of the testis, decreased testicular weights, apoptosis of postmeiotic germ cells (Rao et al., 2001). Leydig cells and Sertoli cells of the testes were stated to remain intact. Although sperm counts were affected in the young mice (at 6 wks), older mice (20 wks) had comparable numbers of sperm in HIP1+/+ mice (Rao et al., 2001). These changes appeared to be intrinsic to the testis and not mediated by altered hormonal secretion by the pituitary gland or altered levels of testosterone.

In order to gain a better understanding of the role of HIP1 in normal male reproduction, we examined the structural abnormalities of the testis and epididymis of HIP1-/- mice. This included profile area measurements of seminiferous and epididymal tubules, electron microscopic (EM) analyses of Sertoli and germ cells of the testis and sperm in the epididymal lumen, as well as sperm counts, motility characteristics and fertility. Our data indicate that both germ and Sertoli cells expressed HIP1 and in its absence causes major structural alterations to both of these cell types. The HIP1 deficient animals also show reduced sperm counts, altered sperm motility features and lowered fertility levels.

MATERIALS AND METHODS

Animals

This investigation was approved by the Animal Care committee of McGill University and was conducted according to accepted standards of animal experimentation. Mouse models of HIP1-/- were developed through targeted disruption of the HIP1 gene as described by Martina et al. (1994). Correctly targeted ES cell clones were microinjected into C57/B16 blastocysts and implanted into pseudopregnant females

to produce chimeras. Chimeras were bred with C57/B16 females and F1 heterozygous mice were intercrossed to generate the F2 generation. The characterization of HIP1^{-/-} mice was performed on a mixed background of 129/SvJ x C57/B16 with mice from line 3 and 4.

Routine Light and Electron Microscopic Preparations of Testicular and Epididymal Tissues of HIP1^{-/-} and wild type mice

10 Wild-type and 10 HIP1^{-/-} mice at ages 9-11 months, comprising a total of 20 animals were used for testicular weight measurements. Statistical analysis was done by two-tailed t-tests using Graph Pad Prism Software; p values <0.05 were considered significant.

Wild-type and HIP1^{-/-} mice at ages 7-11, 15-19 and 24-30 wks, comprising a total of 18 animals with n= 3 per age group were used for quantitative analyses of testicular profile areas and for ultrastructural light microscopic and electron microscopic analyses of their epithelium and sperm. A total of 6 mice at 13 wks of age (wild type, n=3; HIP1^{-/-}, n=3) were used for quantitative analyses of epididymal profile areas. The mice were anaesthetized by intraperitoneal injection of sodium pentobarbital (Somnitol, MTC Pharmaceuticals, Hamilton, ON). Prior to vascular perfusion, a hemostat was clamped over the left testicular vessels entering the testis of each animal; the testis and the epididymides of this side were removed and immersed immediately in Bouin's fixative for 72 hours, after which they were dehydrated in alcohol, embedded in paraffin and sectioned at 5 μ m.

The testis and epididymis of the right side of each animal were fixed by cardiac perfusion with 5% glutaraldehyde buffered in sodium cacodylate (0.1 M) containing 0.05% calcium chloride (pH 7.4). After 10 min of perfusion, the testis and epididymis were removed and cut into 1 mm³ pieces and placed in the same fixative for an additional 2 hr at 4°C. The tissue samples were subsequently rinsed three times in 0.1 M sodium cacodylate buffer containing 0.2 M sucrose and then left in this buffer overnight. The following day, the samples were postfixated in ferrocyanide-reduced osmium tetroxide for 1 hour at 4°C, dehydrated in a graded series of ethanol and propylene oxide, and

embedded in Epon. Semi-thin sections (0.5 μ m) were cut with glass knives and stained with toluidine blue and observed by light microscopy. Thin sections of selected regions of each block were cut with a diamond knife, placed on copper grids, and counterstained with uranyl acetate (5 min) and lead citrate (2 min). These sections were examined and photographed with a Philips 401 electron microscope.

Light Microscopic Immunocytochemical procedures

The following antibodies (polyclonal and monoclonal) were used at various dilutions for routine peroxidase immunostaining: (1) an affinity purified polyclonal anti-prosaposin antibody (1:200 dilution) provided by Dr. C.R. Morales (McGill University, Montreal, QC), and purified and characterized as described previously (Morales et al., 2000); and, (2) mouse monoclonal and rabbit polyclonal anti-HIP1 antibodies generated, purified and characterized as described previously (Chopra et al., 2000; Metzler et al., 2001). The monoclonal and polyclonal anti-HIP1 antibodies were tried at different dilutions (1:50-1:200) in Tris-buffered saline (TBS), pH 7.4. Optimal reactions for the type of fixation and immunostaining methods used were obtained at 1:50 dilution for the monoclonal HIP1 antibody.

For the anti-prosaposin antibody, paraffin sections were processed for immunostaining using the Vectastain Elite ABC kit, Vector K-6101 (Vector Laboratories, Burlingame, CA). Paraffin sections, 5 μ m thick, of Bouin's-fixed testis were deparaffinized in Histoclear (Diamed Lab Supplies Inc., Mississauga, ON) and hydrated through a series of graded ethanol solutions. During hydration, residual picric acid was neutralized in 70% ethanol containing 1% lithium carbonate, and endogenous peroxidase activity was abolished by treating the sections with 70% ethanol containing 1% (v/v) H₂O₂. Once hydrated, the tissue sections were washed in distilled water containing glycine to block free aldehyde groups. After rinsing with tap water and phosphate buffered saline (PBS), sections were incubated in normal blocking serum (ABC kit) for 30 min and then with the primary antibody diluted 1:200 with PBS. The sections were then washed three times with PBS and incubated with biotinylated secondary antibody (ABC kit) for 30 min at room temperature. The sections were washed again in PBS and

incubated with the ABC reagent for 30 min and washed subsequently with PBS. Reactions were visualized with diaminobenzidine tetrahydrochloride (DAB) (BioFX Laboratories Inc., Owings Mills, MD). Sections were counterstained with methylene blue, dehydrated in ethanol and HistoClear and mounted with cover slips using Permount (Fisher Scientific, Montreal, QC). PBS substitution for primary antibody was used as a negative control for these studies.

For the monoclonal anti-HIP1 antibody, sections were deparaffinized, hydrated and washed as described above. Non-specific binding sites were blocked using 10% goat serum for 30 min. The sections were then incubated overnight at 4°C with primary antibody diluted 1:50 with Tris-buffered saline (TBS). Following washes in 0.1% Tween20 in TBS, the slides were incubated with horseradish peroxidase-conjugated secondary antibody (1:250) for 30 min at 37°C in a humidified chamber. Sections were then processed as described above. Normal blocking serum substitution for primary antibody was used as a negative control for these localizations while murine brain tissue was used as a positive control.

Western blot

Testis tissue was obtained from adult mice (4 month old) and kept frozen at -80°C until use. Frozen tissue was homogenized using a Polytron homogenizer in buffer containing 20 mM Tris-Cl pH 7.5, 0.25 M sucrose, 500 mM EDTA, 1 mM MgCl₂ supplemented with a protease inhibitor cocktail (Roche). The homogenate was sonicated and centrifuged at 4000 rpm for 10 min at 4°C to remove cellular debris. After loading 50 µg of protein per lane, proteins were separated by 7.5% SDS-PAGE and transferred to an Immobilon-P membrane (Millipore, Boston, MA) according to standard protocols. Western blot analyses were performed with a mouse monoclonal antibody recognizing HIP1 (mAb HIP1-9; Metzler et al., 2001) at a dilution of 1:1000 followed by incubation with a horseradish-peroxidase-labelled secondary sheep anti-mouse antibody at a dilution of 1:2000. Expression of actin was determined with the mouse mAb AC-40 (Sigma) at a dilution of 1:800.

Quantitative Histological Analyses

Animals of closely related ages were grouped together due to insufficient numbers at identical ages. Scaled digital images of 5- μ m-thick paraffin sections of Bouin's-fixed seminiferous tubules in cross sectional orientation from testes of wild type and HIP1^{-/-} mice at 7-11, 15-19 and 24-30 wks of age, and the initial segment and caput/corpus regions of epididymal tubules of mice at 13 weeks of age, were captured on a Zeiss Axioskop 2 equipped with an AxiocamMR camera (Carl Zeiss Canada Ltd., Montreal, QC). The peripheral outlines of the transversely sectioned seminiferous or epididymal tubules, and the luminal regions, were traced with a mouse cursor and profile areas were calculated via measurement tools available in Version 3.1 of the AxioVision Imaging Software (Carl Zeiss Canada Ltd.). In the testis, values obtained for profile areas were an overall mean for normal looking as well as mild-to severely affected tubules. In the epididymis, the area of epithelium forming the walls of the tubules in each tubule was computed as the difference between the outer peripheral and inner luminal area measurements in each field. Statistical analyzes including power tests of sample sizes for comparing two means of independent samples, distribution test, and nonparametric tests (Mann-Whitney U-test) were done using Version 7.0 of the Statistica Data Miner for Windows (Statsoft Inc., Tulsa, OK); p values < 0.05 were considered significant.

Sperm Collection for Motility Analyses

Nine wild type mice and 5 HIP1^{-/-} mice at 11-13 weeks of age were used for this part of the study. The mice were weighed and then anesthetized with isofluorane. The cauda region of the right epididymidis of each mouse was dissected and placed in a freezer at -20°C for subsequent sperm count analyses. The left cauda epididymidis of each animal was clamped both proximally and distally, then cut out and rinsed in a 35 mm plastic Petri dish containing pre-warmed Hank's medium M199 (Invitrogen Canada Inc., Burlington, ON) supplemented with 0.5% bovine serum albumin at 37°C. It was then transferred to a fresh Petrie dish, unclamped and using a surgical blade (Number 11;

Fisher Scientific, Nepean, ON), the cauda was pierced allowing sperm to disperse into the medium. The cauda tissue was removed and the Petri dish was placed in an incubator at 37°C in 5% CO₂ atmosphere for 5 min. Subsequently, an aliquot of the sperm suspension was placed into an 80 µm glass chamber and analyzed using a Hamilton Thorne IVOS automated semen analyzer (Hamilton-Thorne Biosciences, Beverly, MA). Analyses were carried out for 30 image frames at a frequency of 60 frames/sec. Fourteen of 15 measurement parameters (variables) available through software were analyzed (see Table 3).

Correlation and statistical analyses of data and power tests of motility data were done using Version 7.0 of the Statistica Data Miner for Windows (Statsoft Inc., Tulsa, OK). Initial analyses indicated that raw values for some parameters did not follow normal distributions and these were obtained by doing log₁₀ transformations on continuous variables (e.g., VAP) or arcsine of the square root transformations for ratio or percentage variables (e.g., LIN) as required. In subsequent Univariate Factorial ANOVA test and Post-hoc unequal N HSD *t*-tests (continuous variables) and Fisher's exact tests (variables as proportions) *p* values < 0.05 were considered significant.

Sperm Counts (Indicated as Experiment 1 in Table 3)

The frozen right cauda epididymidis of each animal was placed in a 50 ml conical tube to thaw then homogenized in 1 ml of distilled water on ice for 1-2 min with a Polytron. A 100 µl aliquot of the resulting homogenate was placed in a 1.5 ml microcentrifuge tube coated with "IDENT fluorescent dye" (Hamilton-Thorne Biosciences) and incubated at room temperature for 5-10 min. The solution was mixed and a 5 µl aliquot was placed on a 20 µm sperm analysis chamber (2X Cel; Hamilton-Thorne Biosciences) and quantified with the IVOS semen analyzer under ultraviolet light using the IDENT option/static sperm. As with motility data, sperm counts in wild type and the HIP1^{-/-} mice did not follow normal distributions and log₁₀ transformations of raw values were done prior to carrying out *t*-tests assuming unequal variances; *p* values < 0.05 were considered significant.

Assessment of Sperm Morphology

Spermatozoa obtained from cauda epididymidis of HIP1^{-/-} and wild type mice at 11-13 weeks of age were used for electron microscopy analyses. A 500 µl aliquot of sperm suspended in Hanks' media M199 (Invitrogen Canada Inc., Burlington, ON) supplemented with 0.5% bovine serum albumin from the sperm motility tests was placed in an Eppendorf tube with 500 µl of a solution containing 5% glutaraldehyde in 0.1 M sodium cacodylate buffer and 0.05% calcium chloride at pH 7.4. The sperm were then postfixed in ferrocyanide-reduced osmium tetroxide and embedded in epoxy resin. Ultra thin sections were cut on an ultramicrotome, counterstained with uranyl acetate and lead citrate, and examined with a Philips 400 electron microscope (Philips, Eindhoven, The Netherlands).

Fertility tests

The average number of newborn mice derived from homozygous matings of HIP1^{-/-} mice at 9-11 months of age were obtained over a 3 month time period. Subsequently, male HIP1^{-/-} mice were tested over the same time period in matings with wild-type partners and compared to heterozygous matings (n=8 mating pairs for each genotype combination). Statistical analysis was done by two-tailed t-tests using GraphPad Prism software; p values <0.05 was considered significant.

RESULTS

Light Microscopic Appearance of the Testis of HIP1^{-/-} mice at different ages

Gross examination of the testes of HIP1^{-/-} mice at 9-11 months of age revealed that they were considerably reduced in size. The average testicular weight of HIP1^{-/-}

mice was $73.6 \text{ g} \pm 15.49$, while that of wild type mice was 123.8 ± 22.98 , with the values being significant at the level of $p < 0.05$. In the LM, the testes of HIP1^{-/-} mice ranging from 7 to 30 weeks of age had obvious morphological abnormalities associated with germ cells of seminiferous tubules, and while this effect was evident as early as 7 weeks of age, the severity increased, to include more seminiferous tubules with advancing age. Essentially, the HIP1^{-/-} phenotype resulted in a mosaic appearance to the seminiferous tubules. At low magnification, the normal appearance of different generations of germ cells tightly packed and arranged in concentric layers from the base of the tubule to the lumen, as noted in wild type mice (Fig. 1a), appeared morphologically to be preserved in some seminiferous tubules of HIP1^{-/-} mice while others showed varying phenotypes (Figs. 1b-f). Some tubules had fewer germ cells, with mainly the late elongating spermatids being affected (Fig. 1b), to tubules showing a severe loss of pachytene spermatocytes as well as the early round and late elongating spermatids (Fig. 1d). Tubules showing a range of differences between these two extremes were also observed. Some affected tubules showed a partial loss of round and elongating spermatids such that quadrants of the epithelium were often devoid of these cells, leaving only a single layer of cells at the base of the epithelium consisting of spermatogonia, early spermatocytes and the supporting Sertoli cells (Figs. 1c-f). Due to the loss of germ cells, the more severely affected tubules often contained large vacuoles in the epithelium (Figs. 1d, e). The heads of elongating spermatids in HIP1^{-/-} mice were sometimes abnormal in shape and surrounded by a mass of cytoplasm (Fig. 1e).

The seminiferous tubules of HIP1^{-/-} mice in some cases had a near spherical outline and did not appear to be reduced in size, while other tubules were so depleted of germ cells that they were dramatically reduced in size and highly irregular in outline (Figs. 1c-e). The lumen of such tubules was indistinct and often difficult to discern. Morphometric measurements indicated that the profile areas of seminiferous tubules of HIP1^{-/-} mice were reduced in size by 18-28% depending on the age of the animals (Table 1). All differences in profile areas between HIP1^{-/-} and wild type mice in each age group were significant (Table 1).

Germ cells, such as spermatogonia and early spermatocytes, residing at the base of the epithelium of severely affected tubules appeared to be intact (Fig. 1f). Noticeable,

however, was the absence of the normal layering and full complement of pachytene spermatocytes and early and late spermatids. While some early spermatids were still evident, they appeared to be displaced from the epithelium, floating freely in the tubular lumen (Fig. 1f). The latter was highly irregular in appearance due to the severe loss of germ cells, however, a few elongating spermatids were still noted showing their deeply stained heads and moderately stained flagella (Fig. 1f). In the epithelium of highly distorted tubules, membranous profiles of unknown origin were at times present (Fig. 1f).

In HIP1^{-/-} mice at various ages, LM observations did not reveal major changes to the shape or topographical distribution of Sertoli cells, with their pale stained nuclei and prominent nucleoli (Figs. 1b-f), as found in wild type mice (Fig. 1a). While their numbers were not counted, these cells continued to be distributed around the circumference of the tubule in a manner characteristic of wild type mice. No signs of nuclear degeneration were ever observed, even within the most severely affected tubules (Figs. 1d-f). Immunostaining with an anti-prosaposin antibody, which selectively stains the cytoplasm of Sertoli cells, revealed a spoke like distribution of these cells around the circumference of the tubule in wild type mice (Fig. 2a). Even, in severely affected tubules of HIP1^{-/-} mice, while the integrity of the epithelium was disrupted due to the dramatic loss of generations of germ cells, Sertoli cells were still reactive and distributed radially around the tubule, with their reactive apical processes bordering the edge of the lumen in the absence of the heads and flagella of elongating spermatids (Fig. 2b).

Western blots of testicular extracts from wild type mice confirmed the presence of a 120 kDa band corresponding to HIP1 (Fig. 3). Sections incubated with anti-HIP1 showed an intense reaction over the generation of germ cells bordering the lumen of seminiferous tubules (Fig. 2c). The highly reactive cells corresponded to the late elongating spermatids, beginning at step 9 of spermiogenesis and extending till step 16. The reaction was seen over the cytoplasm of these cells, including their flagella (Fig. 2d). However, an intense reaction was also noted over the Golgi apparatus of these cells as well as all other generations of germ cells (Fig. 2d). A reaction also appeared over the cytoplasm of Sertoli cells at different stages of the cycle (Fig. 2d) and in the cytoplasm of round spermatids (not shown). Sections in which the primary antibody was omitted from the immunocytochemical procedure were unreactive (not shown).

Electron microscopic appearance of cells in the testis of HIP1^{-/-} mice at different ages

The supporting Sertoli cells of the testis showed an intact Sertoli-Sertoli blood testis barrier in HIP1^{-/-} mice. Organelles such as the Golgi apparatus, widely dispersed endoplasmic reticulum (ER), lysosomes, and mitochondria showed no apparent differences in size, appearance or topographical distribution. The nuclei of Sertoli cells and nucleolus with its accessory satellite bodies were also normal in appearance. However, noticeable in HIP1^{-/-} mice, were alterations of the ectoplasmic specializations of Sertoli cells, formed of filaments and overlying ER, and normally associated with step 9-16 spermatids. In HIP1^{-/-} mice, some of these spermatids showed no association with ectoplasmic specializations, while in others, the ER was greatly distended with few or no filaments being present (Figs. 4a, b, 5a, 6a).

Late elongating spermatids from steps 10-16 showed marked abnormalities in HIP1^{-/-} mice. However, these cells showed a variable phenotype even in the most severely affected tubules. While the heads of some elongating spermatids were smooth and tubular in profile, with their nucleus showing a condensed chromatin pattern and an acrosomal cap (Figs. 5a, b, 6a), as found in wild type mice, others presented slightly bent (Fig. 5a), enlarged (Fig. 6a), scalloped (Fig. 6a) or deeply indented heads (Figs. 4b, 5b, 6a, 6b). In addition, the nuclear chromatin of some elongating spermatids was loosely granulated, uncondensed and separated from the nuclear envelope leaving a distinct space, unlike that of adjacent elongating spermatids which showed a tight condensed chromatin pattern (Fig. 5a). The nuclear envelope of such spermatids was also highly irregular and formed extensions without chromatin content. Such cells also revealed the absence of an acrosomal cap to their nucleus (Figs. 5a, 6b), unlike that of adjacent spermatids (Figs. 5a, 6b). In some spermatids, the axoplaxome, seen as a dense filamentous band on one pole of the nuclear envelope, was present, but with only a partial acrosome associated with it (Fig. 7a).

In wild type mice, the spherical nucleus of step 7 spermatids located centrally in the cytoplasm displaces itself and moves to one pole of the cytoplasm by step 8, such that the acrosome makes contact with its plasma membrane. In this eccentric position, as the

spermatid head, composed of the nucleus and acrosome, begins to elongate, the cytoplasm is displaced caudally leaving the region of the spermatid head surrounded by a thin scanty rim of cytoplasm from steps 9-16 of spermatid development. In tubules of HIP1^{-/-} mice, some elongating spermatids maintained this feature (Figs. 5a, b, 6a), however in other cases, the nucleus failed to migrate caudally and remained completely surrounded by cytoplasm. In the expanse of caudal cytoplasm, the components of the flagellum develop and assemble to form its definitive shape, in a direction extending away from and in an orientation along the long axis of the spermatid's head. In those spermatids where the nucleus failed to displace itself, a flagellum was at times seen developing adjacent to and parallel to its head (Fig. 6b), in an orientation never seen in wild type mice. Such images suggested a severe bending of the flagellum during its development leading to its aberrant orientation. This was substantiated by the presence of more than one cross sectional flagellar profile sharing a common cytoplasm in round and elongating spermatids (Figs. 6a, 7a). Although the flagellum was abnormally oriented and bent in some spermatids, its structural components, i.e. axoneme, outer dense fibers, fibrous sheath and mitochondrial sheath, were not altered either in their shape, number or alignment. In spermatids retaining their cytoplasm around their heads, ectoplasmic specializations were noticeably absent (Figs. 5a, 6b).

Light microscopic appearance of sperm in the epididymal lumen of wild type and HIP1^{-/-} mice

In the epididymis of wild type mice, the lumen was filled with the heads of sperm, seen as deeply stained tubular profiles in longitudinal section and circular profiles in cross section, along with their moderately stained flagella cut in cross, oblique or longitudinal sections (Fig. 8a). In HIP1^{-/-} mice, there was both a noticeable reduction of sperm and the presence of numerous spherical cells, some with a prominent spherical or lobulated nucleus (Figs. 8b, 8c). While some of the sperm heads had a normal tubular profile, others were irregular in shape. In addition, some of the sperm heads were enveloped by a mass of cytoplasm (Fig. 8b, 8c), which was not a common feature of wild type mice (Fig. 8a). The epithelium of HIP1^{-/-} tubules appeared comparable to that of

wild type mice. This was substantiated by quantitative analysis that revealed no major significant difference in the outer profile areas, luminal areas, or epithelial areas of epididymal tubules of HIP1^{-/-} and wild type mice (Table 2).

Electron microscopic analyses of sperm in the epididymal lumen and of isolated sperm in wild type and HIP1^{-/-} mice

In the lumen of the epididymis of wild type mice, the heads of sperm were tubular in profile showing a densely stained compacted nucleus capped by a moderately stained acrosome. The flagella were seen in cross sectional or longitudinal profiles, with each being enveloped by its own membrane and surrounding cytoplasm. In appropriate planes of section, the flagellum was oriented away from and parallel to the long axis of the sperm head (Fig. 9a). In HIP1^{-/-} mice, many abnormalities were noted with respect to the contents of the epididymal lumen. Most noticeable were spherical cells some of which represented early spermatids with round or lobulated nuclei and irregularly shaped acrosome capping their nuclei. Their cytoplasm contained mitochondria and numerous vesicular profiles, and an additional acrosome far removed from their nuclear surface was also observed (Fig. 9b). In the cytoplasm of some spherical cells, many small proacrosomic granules were present, while in other cells, such granules were larger in appearance but still plentiful (Figs. 7b-d). In both cases such granules were not associated with a nucleus. In addition to spherical cells, the heads of sperm with a tubular appearance and showing a densely stained compacted nucleus were also noted. However, some of these heads were devoid of a conspicuous acrosome and were enveloped by a mass of densely stained cytoplasm (Fig. 9c), uncharacteristic of wild type sperm.

Sperm isolated from the cauda epididymidis of HIP1^{-/-} mice revealed many differing abnormalities. While the heads of some sperm did not show an acrosome, others revealed only a residual acrosome or an acrosome that appeared to be peeled away from the surface of the nucleus or be enlarged and folded upon itself (Figs. 10a, c, d). Some sperm heads were abnormally elongated and at times showed a constriction along their length (Figs. 10a, d). Some flagellar profiles were seen oriented perpendicular to the sperm head, or parallel to and alongside the sperm head, where they were enveloped by a

mass of cytoplasm (Figs. 10a, b, c). Such images suggested an abnormal development and orientation of the flagellum in relation to the sperm head. In addition, the cytoplasm encompassing the flagella of some sperm revealed two or more flagellar cross sectional profiles sharing a common cytoplasm, with cross sectional profiles of the mid and principal pieces lying side by side (Figs. 10a, d, e).

Sperm Counts and Motility Analyses

Sperm counts in HIP1^{-/-} mice were greatly altered and about 50% less compared to wild type controls (Table 3). This included dramatic reductions in numbers of motile, rapid, or progressive sperm and numbers of sperm moving at a medium speed. The numbers of static sperm in the HIP1^{-/-} mice in contrast were greatly increased in the HIP1^{-/-} mice (Table 3). Parameters related to sperm velocity (VAP, VSL, VCL) were also reduced by 25% and the amplitude of lateral head displacement (ALH) of sperm was 48% less in the HIP1^{-/-} mice (Table 3). No significant changes were detected in beat cross frequency (BCF), head shape (Elong) or path (LIN and STR) of sperm in HIP1^{-/-} mice as compared to controls (Table 3). There were also no significant differences in the numbers of slow moving sperm or in the percentages of medium or slow moving sperm in HIP1^{-/-} mice (Table 3).

Fertility data

The average number of newborn pups derived from homozygous matings over a 3 month time period revealed a reduction by more than 75% in HIP1^{-/-} mice (Fig. 11). In contrast, heterozygous littermates exhibited normal reproduction (Fig. 11 and data not shown). The average number of progeny of HIP1^{-/-} mice revealed a value of 3.2 ± 7.146 , while that of wild type mice was 34.38 ± 7.6333 . In fact, for the HIP1^{-/-} mice matings, newborns were observed in only 2 out of the 8 mating pairs. These observations demonstrate a profound reproductive defect in HIP1^{-/-} mice compared to wild-type littermates.

DISCUSSION

Structural abnormalities of germ cells in the testis as seen by LM

In the present study, the absence of HIP1 appeared to have a major effect on germ cells of some but not all seminiferous tubules. For those tubules that were adversely affected, the phenotype revealed varying degrees of abnormalities, ranging from a dramatic loss of both pachytene spermatocytes and spermatids to a loss of round and/or elongating spermatids. These data are in variance with those of Rao et al. (2001), who reported that only postmeiotic spermatids degenerated. However, even in the most severely affected tubules, a few round and elongating spermatids remained intact, suggesting that the absence of HIP1 affected some but not all germ cells of a given generation in any given tubule. This phenotype was also not restricted to a particular stage of the cycle. A rough estimate of the percentage of affected tubules in HIP1^{-/-} mice indicated that about 25% of all tubules in a given cross section through the entire testis showed moderate to severe structural abnormalities at early ages to about 35% at later ages. However, despite the low percentages noted visually of HIP1^{-/-} affected tubules, quantitative analyses of profile areas of tubules at different ages indicated that there was a significant decrease (50%) in tubular size in HIP1^{-/-} mice that was substantiated by reduced testicular weights and epididymal sperm counts as compared to wild type mice. Thus germ cells of the testis are compromised in HIP1^{-/-} mice, although this is not readily visually in all seminiferous tubules.

The presence of HIP1 in the testis was confirmed by western blotting which showed a band at the correct molecular weight of 120 kDa. LM immunocytochemistry revealed that HIP1 was expressed at high levels as a diffuse cytoplasmic reaction in elongating spermatids from steps 9 to 16, with the reaction being evident in all cells of a given tubule. However, the finding that in some HIP1^{-/-} tubules, these cells appear to be maintained at seemingly normal numbers and morphology, while in others they are not, is perplexing. In addition, in some tubules not only were elongating spermatids affected, but round spermatids and/or pachytene spermatocytes as well, and this was more prominent

in older mice. This finding suggests that an entire clone of different generations of germ cells may degenerate, beginning with the elongated spermatids, but extending with time to early spermatids and spermatocytes, as intercellular bridges have been shown to join together germ cells of different generations amounting to over 100 cells (Weber and Russell, 1987). This would account for the loss of germ cells and the presence of large vacuoles in the epithelium noted in the present study. However, our data also reveal that a reduction in tubular size appears to be the result of sloughing of germ cells from the seminiferous epithelium into the tubular lumen, as spherical cells, some identified as round spermatids by the presence of an acrosome, were noted in the epididymal lumen. Our findings are at variance with that of Rao et al. (2001), who reported that the reduction in size of seminiferous tubules was due solely to degeneration of postmeiotic germ cells. However, as also indicated by Rao et al. (2001), we did not observe any apparent effect on the spermatogonial population. Unlike the observations of Rao et al. (2001), giant, multinucleated cells, arising from disruptions of the intercellular bridges between germ cells, were not seen in the testis of our HIP1^{-/-} mice. Such a phenomenon was a feature of hormone sensitive lipase knockout mice, which appeared to be a consequence of the cholesterol integrity of the membranes of these structures (Chung et al., 2001).

The presence of both affected and normal looking tubules has been reported for other knockout mice that exhibit testicular abnormalities (Lufkin et al., 1993; Zhao et al., 1998; Grover et al., 2004). It is still unclear why a knockout of a given gene produces variable effects on spermatogenesis. Some genes seem to be essential for normal male fertility, while others have minor roles (Eddy, 1998, 1999). Most probable is the fact that partial compensatory mechanisms exist to sustain fertility in some gene knockouts. In fact, huntingtin protein also localizes to pachytene spermatocytes and to round spermatids (Syed et al., 1999), and inactivation of the huntingtin gene leads to disorganized seminiferous tubules and decreased sperm counts (Dragatsis et al., 2000). Expression of mutant huntingtin in mice leads to vacuolated seminiferous tubules, sloughing off of germ cells in the lumen of the tubules and reduced sperm counts with some sperm cells having abnormal heads (Raamsdonk et al., 2005). HIP1-related protein is also expressed in the testis and performs similar functions to HIP1 (Chopra et al., 2000; Engqvist-

Goldstein et al., 1999, 2001; Chen and Brodsky, 2005; Legendre-Guillemain et al., 2005). However, unlike HIP1 knockouts, HIP1-related knock out mice are totally fertile (Hyun et al., 2004). Since HIP1 interacts with huntingtin and HIP1-related protein, our present findings suggest that these two proteins may play a compensatory role in some germ cells of the testis in the absence of HIP1.

While degeneration of spermatids can be associated with abnormal pituitary hormone levels (Russell and Clermont, 1977), the testis of HIP1^{-/-} mice did not appear to be affected by reduction or absence of hormones. Indeed, there were no differences in morphology of Sertoli cells, unlike that seen in the FSH knockout mouse model (Grover et al., 2004), and previous reports of hormones in HIP1^{-/-} mice revealed normal levels (Rao et al., 2001). As also reported by Rao et al. (2001), the present study demonstrated no differences in the size of seminal vesicles of HIP1^{-/-} mice. In addition, Leydig cells were similar in appearance, size and distribution to that seen in wild type mice at different ages, suggesting that LH and testosterone levels are all normal.

Structural abnormalities of germ cells in the testis as seen by EM

In the EM, major structural abnormalities were noted for germ cells and especially for the late elongating spermatids. However, as stated above, even in those tubules revealing extensive alterations to the epithelial cells, both normal looking and abnormal morphologies were noted for the elongating spermatids. For the abnormal elongating spermatids, several different phenotypes were noted. In some cases, the heads of elongating spermatids presented a compact nuclear chromatin with an overlying acrosome, but they were highly irregular in appearance with a bent or highly twisted shape. During spermiogenesis, the nucleus of step 8 spermatids, spherical and centrally located in the cytoplasm, relocates itself to one pole of the cytoplasm, leaving the cytoplasm to trail behind as the cytoplasmic lobe by step 9 and all subsequent steps of spermatid development (Clermont et al., 1993). In HIP1^{-/-} mice, the nucleus of some elongating spermatids were seen centrally in their cytoplasm indicating that the nucleus failed to migrate to one pole of its cytoplasm. Migration of the nucleus to one pole may involve microtubules and/or actin, and as HIP1 plays a role in relation to these

cytoskeletal elements, it is suggested that deletion of HIP1 alters the normal functioning of these elements. Once the spherical nucleus of step 8 spermatids take on an eccentric position, the nucleus begins to elongate to take on its characteristic shape, and this appears to be under the guidance of the manchette, a transient microtubular/actin-containing structure (Clermont et al., 1993; Meistrich, 1993). Proteins such as Hook 1 have been shown to act as linking proteins between the membranes of vesicles and microtubules. Absence of Hook 1 results in spermatids and sperm with coiled tails and abnormal sperm heads (Mendoza-Lujambio et al., 2002). Since HIP1 is known to physically interact with F-actin and with assembled microtubules (Hussain et al., 2003; Senetar et al., 2004), it seems likely that the absence of HIP1 alters normal manchette functioning leading to disruption of the shape of spermatid heads. It should be pointed out that the manchette was normal in appearance in abnormal spermatids of HIP1^{-/-} mice, but the present data suggest that it may not be functioning properly.

In addition, the shape and chromatin condensation of the spermatid head has been shown to be a function of a cytoskeletal scaffold, referred to as the acroplaxome, containing F-actin and keratin filaments (Kierszenbaum et al., 2003; Kierszenbaum and Tres, 2004). In the present study, some elongating spermatids of HIP1^{-/-} mice showed an irregular superfluous nuclear membrane encasing an uncondensed state of their chromatin. These data suggest a role for HIP1 in relation to the acrosome-acroplaxome-manchette complex in the dynamics of spermatid head development.

In the present study, HIP1 expression in wild type mice was also seen as a small spherical ball of reaction in the cytoplasm of all germ cells, similar to that noted for a reaction of the Golgi apparatus of these cells (Igdoura et al., 1999) and suggesting a role for HIP1 and Golgi components. During early spermiogenesis (steps 1-2), the Golgi apparatus is involved in formation of the proacrosomic granules. These granules subsequently fuse with each other and then migrate and grow on one pole of the nuclear surface to form the acrosome from steps 3-7 (Clermont et al., 1993; Abou-Haila and Tulsiani, 2000). Notable for some spermatids in the testis, from steps 4 to 7, was the presence of an incomplete acrosome capping the nuclear surface or complete absence of one that was also seen in elongating spermatids and sperm in the epididymal lumen. These observations along with the presence of spherical germ cells in the epididymal

lumen, which showed numerous proacrosomic granules floating in their cytoplasm, suggested that in some early spermatids of HIP1^{-/-} mice, proacrosomic granules were forming, but that they were unable to fuse with each other and migrate to the nuclear surface or do so only partially. Another role for the acroplaxome is to anchor the developing acrosome to the nuclear envelope (Kierszenbaum et al., 2003). In the absence of a noticeable acrosome on the nuclear surface of some spermatids, it is suggested HIP1 interacts with the actin filaments of the acroplaxome. Indeed, at its C-terminus, HIP1 was shown to bind indirectly to the actin cytoskeleton via HIP12/HIP1R, (Chopra et al, 2000; Legendre-Guillemain et al., 2002), and directly with F-actin via its talin homology domain (Senetar et al., 2004). In the present study some elongating spermatids showed an acrosome on their nuclear surface, but one that was detached and peeling away from it. As actin is present in the subacrosomal space and acroplaxome (Vogl, 1989; Oko and Clermont, 1991; Prigent and Dadoune, 1993), a role for HIP1 and its interaction with actin in stabilizing the acrosome to the nucleus is also suggested from the present data.

In the Golgi apparatus of early spermatids, coated pits are present in the trans Golgi network (TGN) (Susi et al., 1971; Hermo et al., 1980; Griffiths et al., 1981; Thorne-Tjmosland et al., 1988; Moreno et al., 2000) and are involved in forming the acrosome. While HIP1 interacts with clathrin, no accumulation of coated pits was observed in the TGN of HIP1^{-/-} spermatids. Rather they appeared to fuse together and form the larger proacrosomic granules, which subsequently form an incomplete or partial association with the nuclear surface. A similar phenotype, albeit more pronounced, is also noted for other knock out mice in relation to GOPC and Hrb proteins localized to the Golgi apparatus (Yao et al., 2002; Kang-Decker et al., 2001). GOPC-deficient mice and Hrb-deficient mice show globozoospermia (round-headed spermatozoa), numerous proacrosomic vesicles that fail to fuse with each other and an arrest in acrosome vesicle formation.

In the EM, the secretory organelles of Sertoli cells of HIP1^{-/-} mice at the different stages of the cycle did not appear to be affected, as did the Sertoli-Sertoli blood testis barrier. Sertoli cells are well defined endocytic cells involved in endocytosis both apically and basally, and at the latter domain, coated pits are prominent (Morales et al., 1985; Petrie and Morales, 1992). In HIP1^{-/-} mice, the endocytic organelles appeared

comparable to that of wild type mice. As HIP1 plays an important role with clathrin of coated pits, these data suggest that despite the absence of HIP1, Sertoli cells are still capable of performing endocytosis and are involved in the production of lysosomes as noted in wild type mice of this and other studies (Chung et al., 2001; Grover et al., 2004). A notable alteration however occurred with respect to the ectoplasmic specializations of these cells. In wild type mice, the ectoplasmic specialization, a layer of filaments and ER cisternae of the Sertoli cytoplasm is closely juxtaposed to the plasma membrane of spermatids in the area of their acrosome, and this occurs from step 9-16 of spermiogenesis (Vogl et al., 1986; Russell et al., 1988, 1993). In HIP1^{-/-} mice, some of these spermatids maintained this association; however, others showed no such association or an alteration of the components of this specialization. As these specializations serve to bind the elongating spermatids to Sertoli cells, the findings of spermatids (steps 12-15) released into the tubular lumen prior to their due departure time at step 16 suggests that these specializations are altered in HIP1^{-/-} mice. As HIP1 plays an important role in relation to the F-actin and as the latter is a component of ectoplasmic specializations, it is suggested that the absence of HIP1 affects the integrity of these specializations and their role in holding spermatids to the epithelium. Our findings that ectoplasmic specializations were missing for those elongating spermatids whose heads failed to migrate to one pole of their cytoplasm, and hence be enveloped by a mass of cytoplasm, suggest that spermatid head displacement is a prerequisite for Sertoli cell ectoplasmic specialization formation.

Structural abnormalities of cells in the epididymal lumen as seen with EM

In the epididymal lumen, many sperm showed abnormal and variable phenotypes, such as the presence of irregularly shaped heads or heads surrounded by a mass of cytoplasm, sperm lacking or showing a partial or aberrant acrosome, or an acrosome that appeared to be detached from the nuclear surface. All of these images complemented those seen for developing cells in the seminiferous epithelium and suggested their abnormal development occurred within the testis. Also of particular interest was the finding of two or more flagellar cross sections enveloped by a common cytoplasm. While

this could be attributed to the development of more than one flagellum per spermatid, the finding of instances where the flagellum was oriented alongside the sperm head instead of away from it suggested a 180 degree bending of the flagellum in relation to the head. This appeared to occur at the level of the connecting piece of the tail. In addition, in other cases, cross sectional profiles of the mid piece were found alongside the principal piece sharing a common cytoplasm. Such images suggested that the flagella were unstable and prone to abnormal bending and twisting. In some cases, as many as 3-5 flagellar cross sections shared a common cytoplasm indicating the highly flexible nature of the flagellum in HIP1^{-/-} mice. The mitochondria also fail to condense and aren't helically wound around the axoneme (Fig. 6a). In all cases, there were no conspicuous alterations in the number of structural components of the entire flagellum as they appeared comparable to wild type mice (Toshimori, 2003). Interestingly, actin has been localized to the mid and principal pieces of the flagellum, as well as to the connecting piece (Paranko et al., 1994; Fouquet and Kann, 1992). In this regard, HIP1 may play an important role with actin in flagellar stability. Indeed, HIP1 and HIP1-related proteins have been shown to stabilize F-actin polymers against depolymerization (Senetar et al., 2004). Alternately, HIP1 may affect microtubular stability in the flagellum. Microtubules are a component of the axoneme of the flagellum (Clermont et al., 1993) and while normal in appearance in HIP1^{-/-} mice, it is suggested that in the absence of HIP1, the interaction between HIP1 and microtubules is altered in some way leading to abnormal flagellar instability of the microtubules. The phenotype of abnormal flagellar bending was also noted for elongating spermatids in the seminiferous epithelium of the testis, and thus does not represent an abnormality occurring during epididymal transit and as a consequence of altered epididymal functions associated with sperm maturation. In fact our data on epididymal epithelial profile areas revealed no gross changes to the epididymis in HIP1^{-/-} mice. Our observations on flagellar instability and the proposed role of HIP1 and actin suggest that the outer dense fibers and fibrous sheath both normal in appearance in HIP1^{-/-} mice do not play a role in flagellar stability.

Of particular significance in the present study are the findings in relation to the acrosome formation, sperm head shape, retaining of cytoplasm around the sperm head and flagellar bending. All of these attributes in HIP1^{-/-} mice suggest a role for HIP1 with

respect to actin and/or microtubules. Rao et al. (2001) suggested that the abnormalities seen in postmeiotic germ cells of HIP1^{-/-} mice were related to a regulation of endocytosis due to the association of HIP1 with plasma membrane associated clathrin coated pits. However, while coated pits have been described in germ cells and been shown to be involved in the uptake of ABP and transferrin, the phenotypes noted in spermatids do not appear to be the consequence of an alteration of endocytic activity. Indeed, abnormalities of elongating spermatids occur after the synthesis of mRNA is terminated or limited which occurs by step 7 spermatids (Monesi, 1965; Hecht, 1998). Furthermore the abnormalities in HIP1^{-/-} mice are not related to the lack of organelle formation, as proacrosomic granules still form and actin and microtubules are present and comparable to that seen in wild type mice. It is more likely that the abnormalities seen in germ cells are the result of an alteration of HIP1 in relation to the cytoskeleton involving actin and/or microtubules and their functions in germ cell developmental dynamics.

The structural abnormalities of sperm noted in HIP1^{-/-} mice are corroborated by our data on sperm motility. One of the most profound alterations occurs in relation to the total number of sperm, which are reduced by 50% in HIP1^{-/-} mice. This reduction results in significantly fewer total numbers of sperm cells being detected in all motility categories (summarized in Fig. 13A). Their distributions in terms of percentages are also significantly different compared to controls except for 2 parameters (% Medium and % Slow) (summarized in Fig. 13B). The most noticeable change is observed in the % Static sperm, which are increased by 143% in HIP1^{-/-} mice (Table 2, Fig. 13B). HIP1^{-/-} mice revealed significant reductions in most sperm motility parameters, such as numbers of motile sperm and rapid, medium and progressive moving sperm, and this coincided with the greatly increased numbers of static sperm in the HIP1^{-/-} mice. Parameters related to sperm velocity (VAP, VSL, VCL) were also reduced by 25% and the amplitude of lateral head displacement (ALH) of sperm was 48% less in the HIP1^{-/-} mice (Table 3; Fig. 12). Structural alterations to the flagellum of sperm appeared to be substantiated by increased numbers of static sperm and by decreased degree of motility and velocity in moving sperm. Clearly sperm of HIP1^{-/-} mice are less motile than wild type mice. It is interesting to note that altered sperm motility analyses from different knockout mouse models such as FORKO and α ERKO, revealed major differences in sperm motility parameters

between each other (Grover et al., 2005; Ruz et al., 2005, manuscript in review) and both differed from that of HIP1 in the present study, suggesting that sperm alterations to their motility is a complex phenomenon regulated by a multitude of different factors stemming from their development and formation in the testis and to their eventual maturation as they traverse the epididymis. In the case of HIP1^{-/-} mice altered sperm motility appear to be caused solely by defects of their structure arising during development in the testis, as the epididymal epithelium was normal in appearance and size. Sperm of α ERKO mice were affected by changes occurring to the efferent ducts, while sperm of FORKO mice were affected by testicular and epididymal changes (Grover et al., 2005; Ruz et al., 2005, manuscript in review).

In HIP1-deficient mice, the abnormalities in germ cells development and their outcome on sperm structure leads to severely impaired sperm motility. This in turn accounts for the low fertility noted in HIP1^{-/-} mice, as demonstrated by their poor mating ability with a significant reduction in number of progeny as compared to wild-type mice over a 3-month time course.

ACKNOWLEDGEMENTS

We are grateful to Jeannie Mui for the technical assistance dealing with electron microscopy and to Haitham Badran who kindly provided the schematic drawing for figure 12 and to Dr. C.R. Morales for the prosaposin antibody.

Figure 1a: Light micrograph of a cross section of a seminiferous tubule from the testis of a wild type mouse at 19 weeks of age. The tubule reveals a seminiferous epithelium (SE) at stage IX of the cycle and consists of several superimposed generations of germ cells, i.e. spermatogonia, early and late spermatocytes, and step 9 spermatids (thin arrows), along with the non dividing supportive Sertoli cells (thick arrows). The latter present large pale nuclei with a prominent nucleoli. The germ cells are tightly packed together and organized in a concentric manner from the base of the tubule to the lumen (Lu). The tubule, more or less circular in appearance, is smooth in contour and has a diameter of large size. IS, interstitial space. x275.

Figure 1b: Light micrograph of a cross section of a seminiferous tubule of the testis of a HIP1^{-/-} mouse at 11 weeks of age. The tubule, at stage II-III of the cycle, is mildly affected and reveals an irregular outline and smaller diameter compared to wild type mice. Spermatogonia, spermatocytes and round step 2-3 spermatids (thin arrows) are present, but the deeply stained heads of elongating step 14 spermatids (arrowheads) appear reduced in number (arrowheads). Sertoli cell nuclei (thick arrows) bordering the periphery of the tubule are abundant. Lu, lumen. x275.

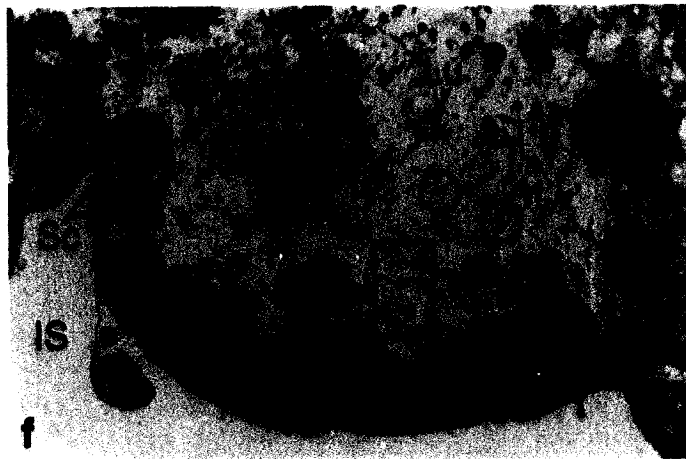
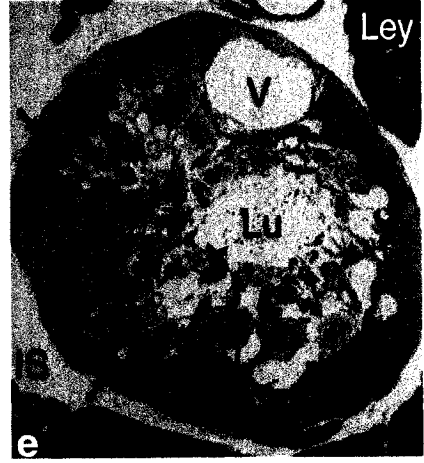
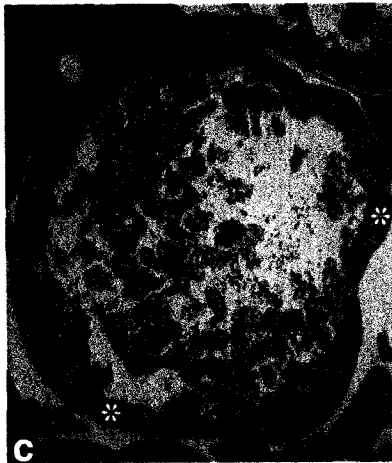
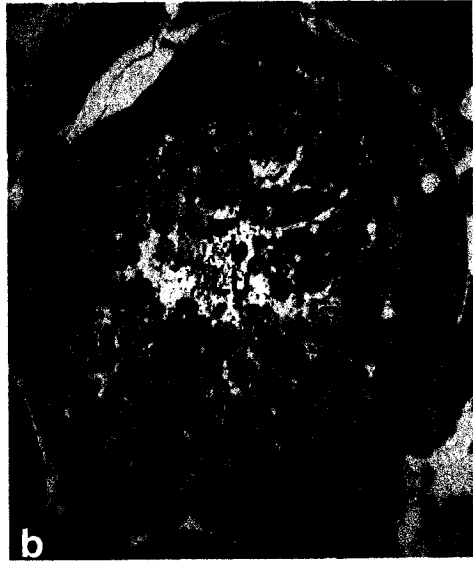
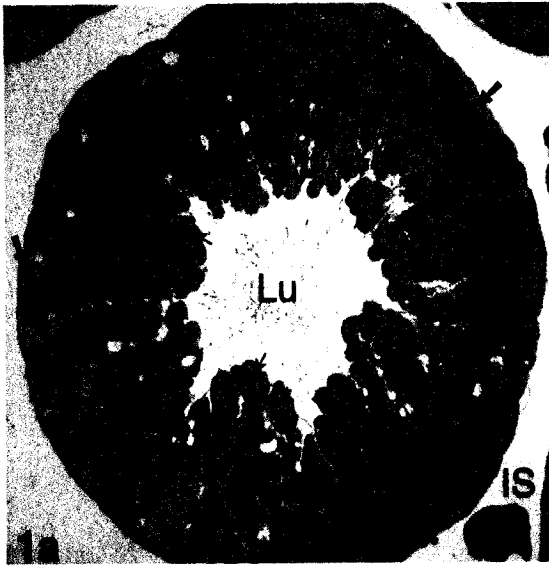
Figure 1c: Light micrograph of a cross section of a seminiferous tubule of the testis from a HIP1^{-/-} mouse at 11 weeks of age. The tubule, at stage V-VI of the cycle, shows a disruption of the seminiferous epithelium. Noticeable is the virtual absence of elongating spermatids (arrowheads). On the left and right sides of the tubule, step 5-6 round spermatids (thin arrows) are displaced from the base of the epithelium creating areas of the epithelium which are limited to a single layer of cells (asterisks). The lumen is not well defined in this tubule. Sertoli cell nuclei (thick arrows) are prominent and border the periphery of the tubule. x275.

Figure 1d: Light micrograph of a cross section of a seminiferous tubule of the testis from a HIP1^{-/-} mouse at 11 weeks of age. The tubule is severely affected revealing an irregular outline and small diameter. Elongating spermatids are completely absent from

the epithelium and only a few round spermatids (thin arrows) and spermatocytes are evident creating large vacuoles (V) in the epithelium. Sertoli cell nuclei (thick arrows) border the tubular periphery. Lu, lumen; IS, interstitial space; Ley, Leydig cells. x275.

Figure 1e: Light micrograph of a cross section of a seminiferous tubule of the testis from a HIP1^{-/-} mouse at 11 weeks of age. The epithelium is disrupted revealing few round spermatids (thin arrows), pachytene spermatocytes (Sc) and elongating spermatids. The latter are enveloped by cytoplasm (arrowheads), uncharacteristic of what is seen in wild type mice. Germ cells are drastically reduced in number, leaving the epithelium in some areas thinned down (asterisk) and creating large vacuolations (V) in other areas. Ley, Leydig cells; IS, interstitial space; thick arrows, Sertoli cell nuclei. x275.

Figure 1f: High power light micrograph of a portion of a seminiferous tubule of the testis from a HIP1^{-/-} mouse at 15 weeks of age. The epithelium, at stage VI of the cycle, appears empty and lacks the uniform concentric layering of the different generations of germ cells, characteristic of what is seen in wild type mice. Only a few round step 6 spermatids (thin arrows) are evident and they appear to be detached from the epithelium. Early spermatocytes (Sc) reside at the base of the epithelium along with Sertoli cell nuclei (thick arrow). A few heads of elongating spermatids (arrowheads) and their flagella (circles) are noted in longitudinal and cross sectional profiles in an area of the epithelium where pachytene spermatocytes and step 6 spermatids normally reside. Large empty irregularly shaped membranous profiles (box) are also present. IS, interstitial space. x600.



Figures 2a, b: Light micrographs of cross sections of seminiferous tubules of the testis from (a) wild type mouse and (b) HIP1^{-/-} mice at 15 weeks of age, immunostained with anti-prosaposin antibody. In (a), the tubule, at stage VII of the cycle, shows an immunoperoxidase reaction (curved arrows) over Sertoli cells and radiates from the base of the epithelium to the lumen at regular intervals around the circumference of the tubule in a spoke wheel-like fashion. The tubular diameter is large in size and contains unreactive germ cells uniformly and concentrically layered as distinct generations from the base to the lumen (Lu), which contains the unreactive flagella of the elongating spermatids. Pale large Sertoli cell nuclei (arrows) abound at the base of the epithelium. In (b), the tubular diameter is smaller in size and round and elongating spermatids are conspicuously absent. Reactive Sertoli cells (curved arrows) radiate around the circumference of the tubule, with their apices bordering the lumen (Lu) of the tubule, which shows an absence of flagella of elongating spermatids. Sertoli cell nuclei (arrows) are evident at the base of the epithelium. Ley, Leydig cells; IS, interstitial space. x400.

Figure 2c, d : Low (a) and high (b) power light micrographs of the testis of a 23 week old wild type mouse immunostained with a monoclonal anti-HIP1 antibody. In (a), the many cross sectional profiles of seminiferous tubules reveal an intense immunoperoxidase reaction over the cytoplasm (curved arrows) and flagella (diamonds) of elongating spermatids bordering the lumen (Lu) of each tubule. In (b), cross sectional profiles of three adjacent seminiferous tubules, at stages XII, I and VII of the cycle, reveal an intense reaction over the cytoplasm of elongating spermatids (curved arrows) and their flagella (diamond) in the lumen (Lu). Weak staining is seen over the cytoplasm of round spermatids and the other germ cells. However, an intense reaction appears over the spherical Golgi apparatus of all generations of germ cells (circles). Sertoli cells also show a cytoplasmic reaction (white arrows). IS, interstitial space. (a) x100; (b) x400.

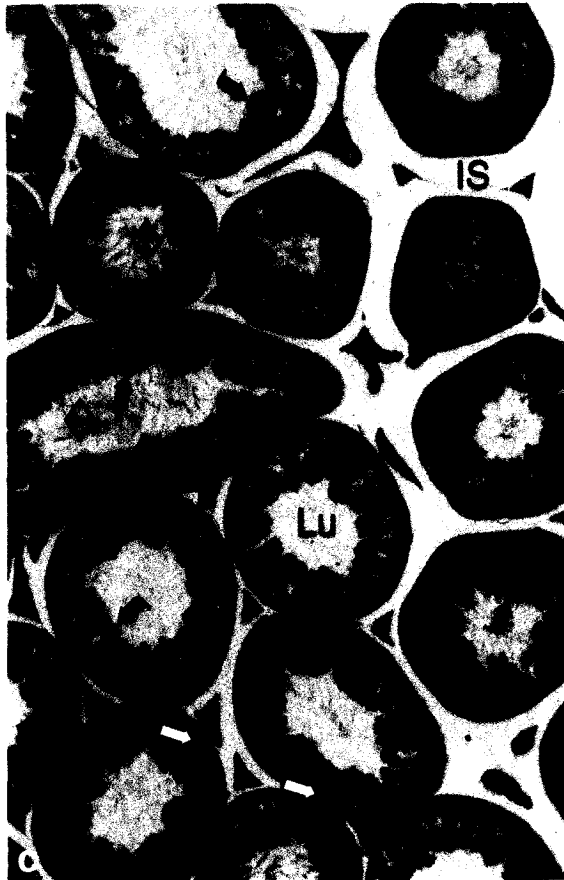


Figure 3. HIP1 expression in testis. The expression of HIP1 was analyzed by Western blot in testis of wild-type mice and compared to the expression of actin. A distinct immunoreactive band at 120 kDa corresponds to HIP1.

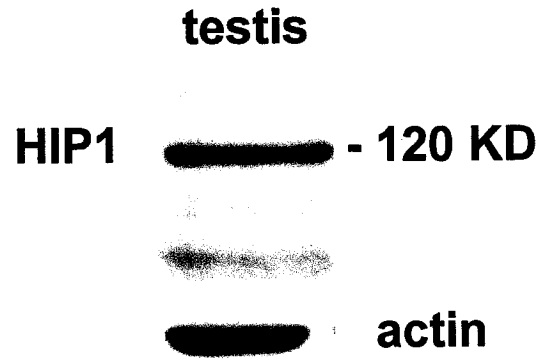
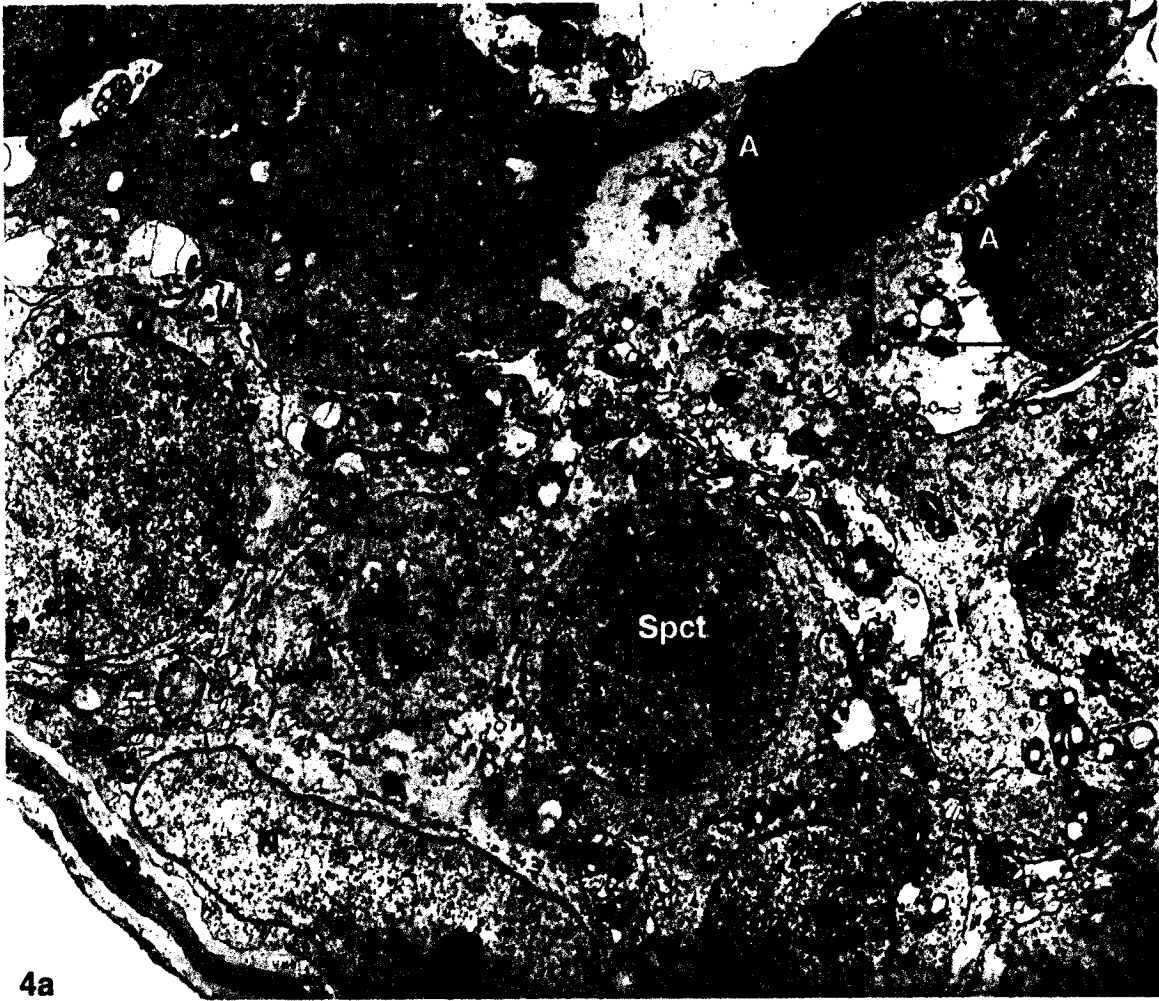


Fig.3

Figures 4a and b: Electron micrographs of the seminiferous epithelium at low (a) and higher (b) magnification from HIP1^{-/-} mice at 15 weeks of age. In (a), a Sertoli cell shows an intact Sertoli-Sertoli blood testis barrier (arrowheads) and its usual organelles as seen in wild type cells. However, 2 elongating spermatids at step 10 (Sp), while showing a normal nuclear shape (N) capped by an acrosome (A) do not reveal any association (arrows) with ectoplasmic specializations, formed by ER and filaments, in the cytoplasm of adjacent Sertoli cells. In (b), the step 13 spermatid heads show abnormal shaped nuclei (N) and acrosomes (A) with the ER of the ectoplasmic specializations of Sertoli cells (Ser) being greatly enlarged; filaments are not prominent in relation to the ectoplasmic specializations of these spermatid heads. M, manchette; N, nucleus of Sertoli cell; Spct, spermatocyte. (a) x4,400; (b) x7,000.



4a

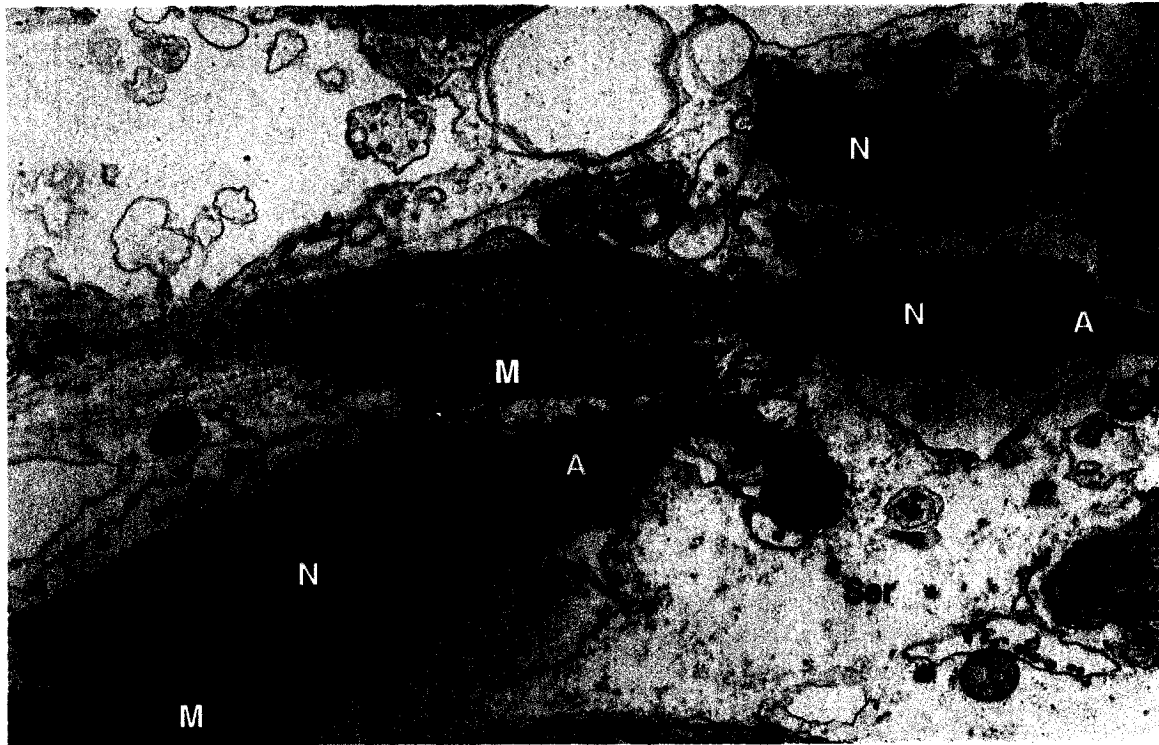


Figure 5a: Electron micrograph of the seminiferous epithelium of the testis at stage XI-XII of the cycle from a 30 week old HIP1^{-/-} mouse revealing numerous abnormalities to the heads of the elongating steps 11-12 spermatids. Some spermatid heads appear structurally normal (Sp1). They have a smooth tubular profile, sparse cytoplasm over their heads and an acrosome (A) encompassing their nucleus (N) which shows a condensing chromatin pattern. Other spermatids (Sp2) show similar features, but have a severely bent or notched head. In other cases, elongating spermatids (Sp3) are highly abnormal with their nuclei (N) presenting a less condensed chromatin pattern, an irregular, superfluous nuclear membrane (arrows) and artificial space between the chromatin and nuclear membrane. Such cells also reveal no acrosome and are enveloped by a large expanse of cytoplasm, completely atypical of wild type spermatids. Sp4 appears to be free in the lumen (Lu) of the tubule, uncharacteristic for step 11-12 spermatids. F, flagella of spermatids. x4,300.

Figure 5b: Electron micrograph of the seminiferous epithelium of the testis from a 15 week old HIP-1^{-/-} mouse at stage II-III of the cycle. Of the three step 14 elongating spermatid heads, two appear normal (Sp1), showing a tubular profile and a nucleus (N) with condensed chromatin capped by an acrosome (A). The developing flagellum (F) along with a delayed descent of the microtubule containing manchette (M) are shown in one spermatid head. An adjacent spermatid head (Sp2), while presenting similar features, shows a deep indentation of its head, uncharacteristic of wild type spermatids. The filaments and endoplasmic reticulum of the ectoplasmic specializations (ES) of the apical Sertoli cell processes (Ser) are present in relation to all spermatid heads, as seen in wild type spermatids. m, mitochondrion of Sertoli cell. x11,700.

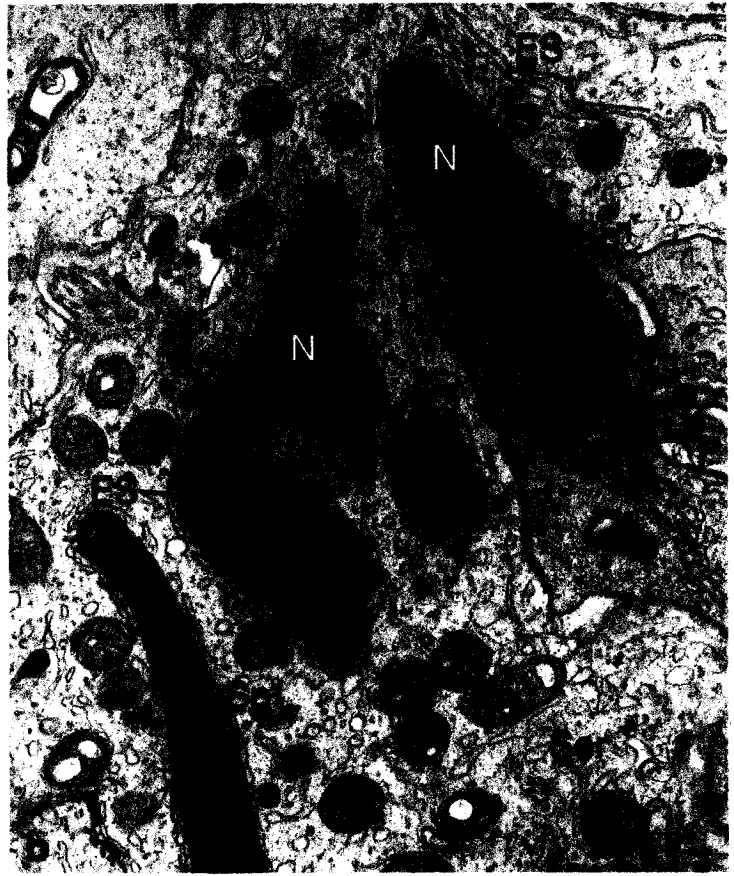
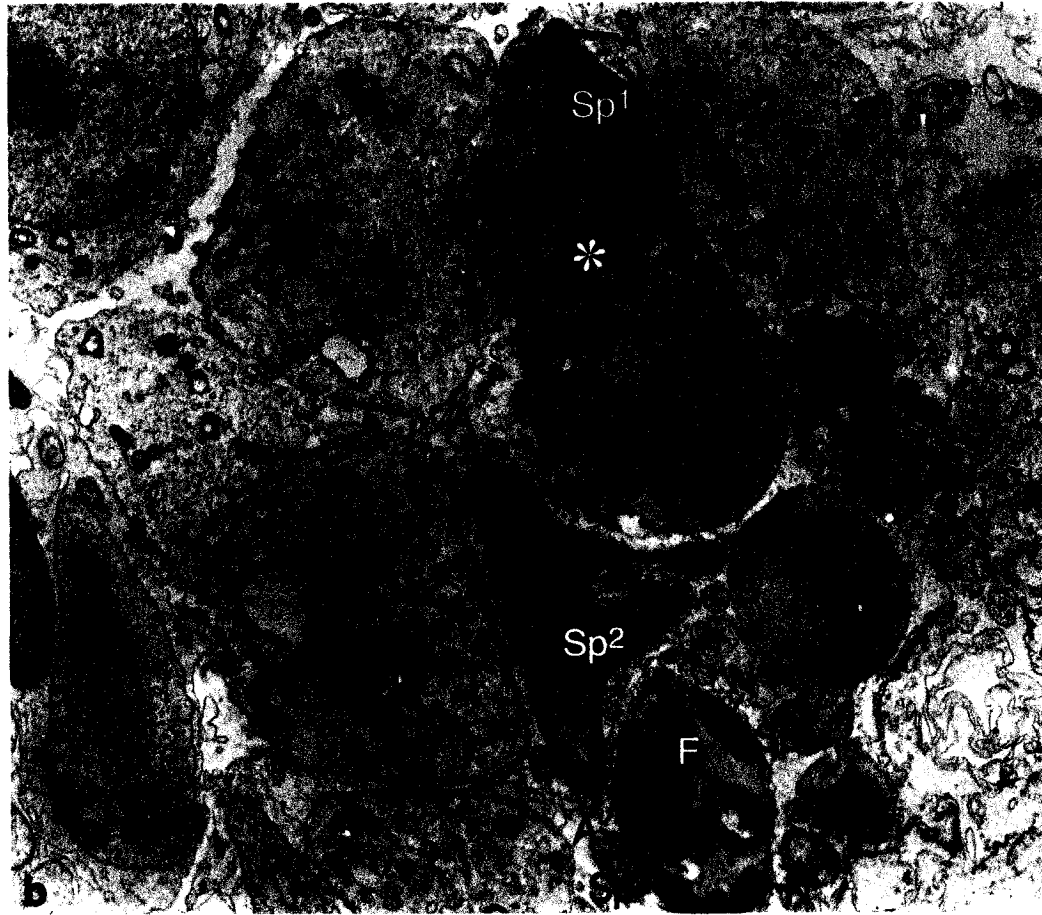
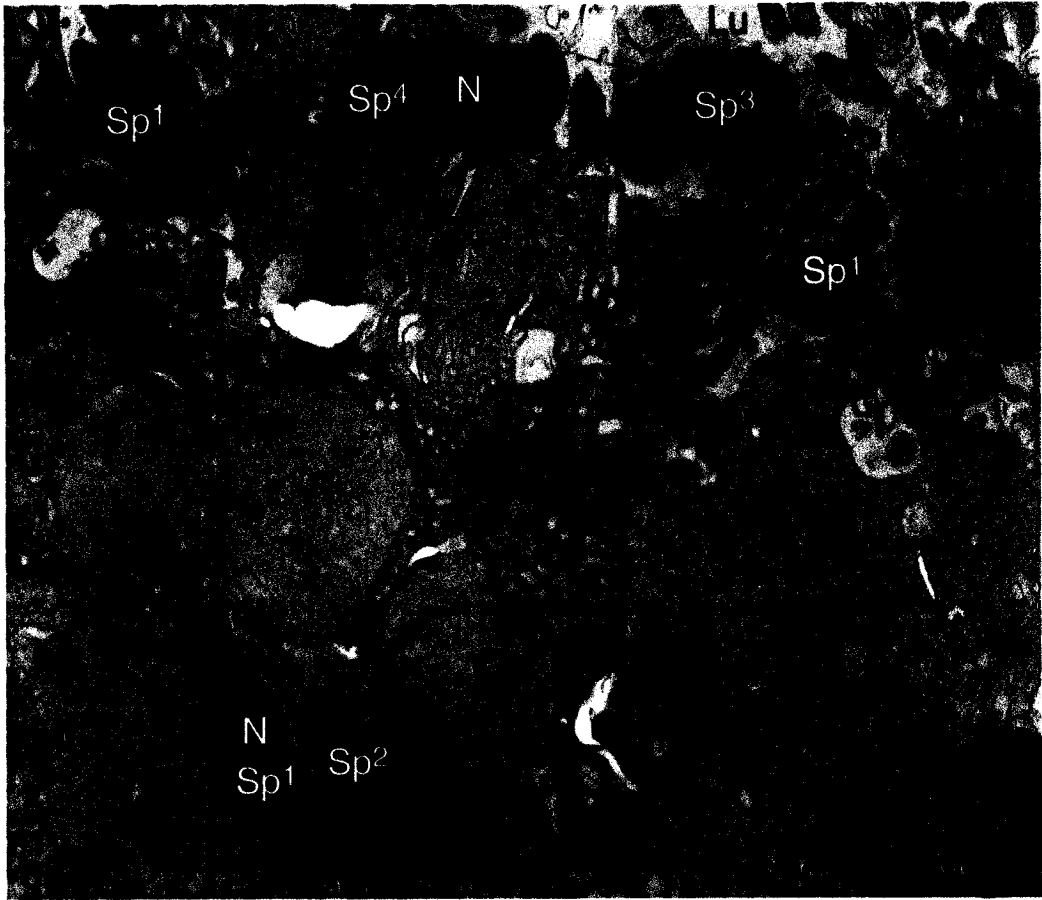
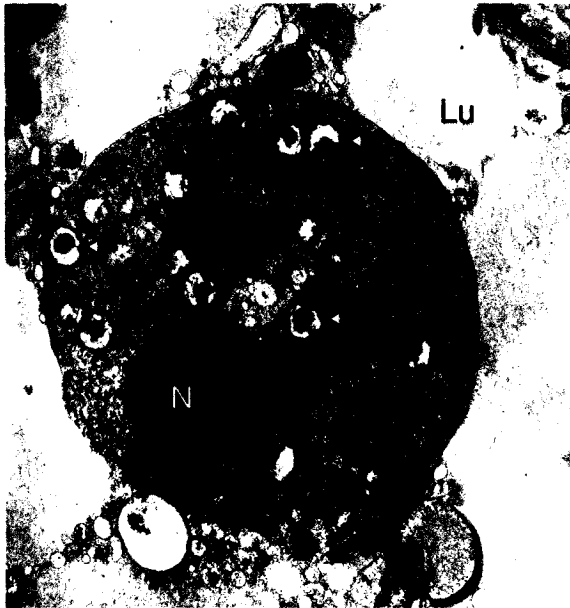
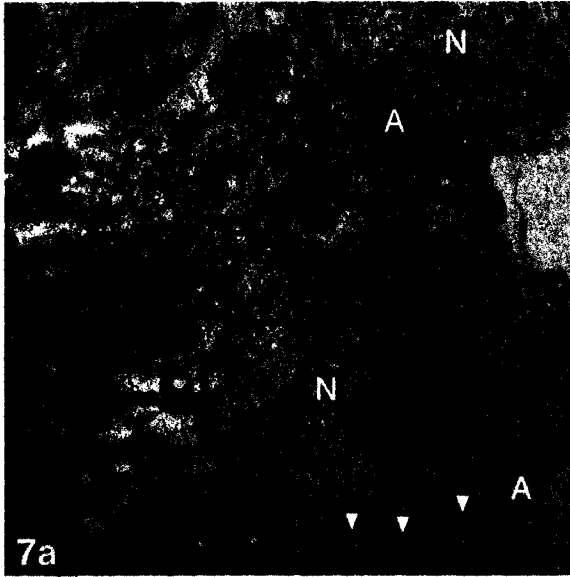


Figure 6a: Electron micrograph of the seminiferous epithelium of the testis at stage IV-V of the cycle from a 21 week old HIP1^{-/-} mouse revealing numerous abnormalities in relation to the heads of step 15 elongating spermatids. Several spermatid heads appear normal (Sp1), showing a smooth tubular profile, condensed nucleus (N) and overlying acrosome (A) and Sertoli cell-associated ectoplasmic specialization (ES). Sp2 shows a forked head and is so twisted upon itself that it envelops a portion of Sertoli cell cytoplasm containing a mitochondrion (m). Sp3 shows a deeply scalloped nuclear profile, while Sp4 has an enlarged, slightly irregular nucleus. While both Sp3 and Sp4 contain an acrosome, they are not associated with an ectoplasmic specialization, unlike the heads of Sp1 and Sp2. Two cross sectional profiles of a developing flagellum (F) share a common cytoplasm. Mitochondrial sheath formation is also delayed with mitochondria not fully condensed and not helically wound. x5,500.

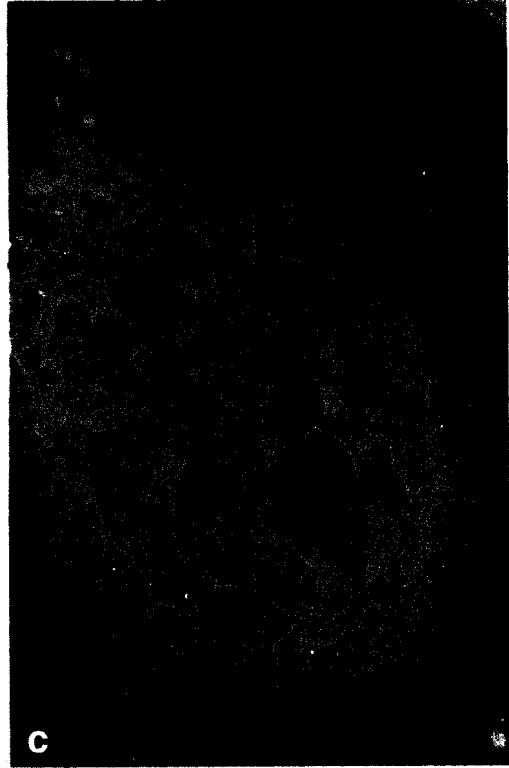
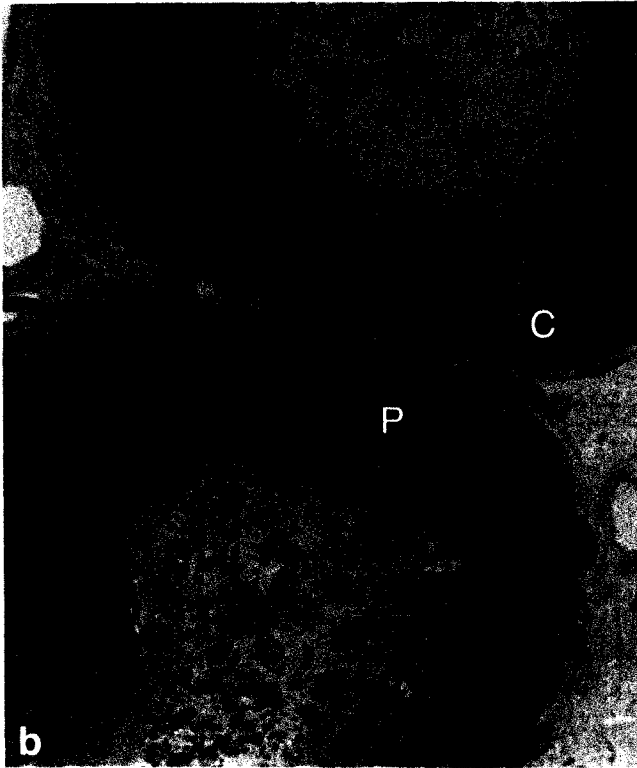
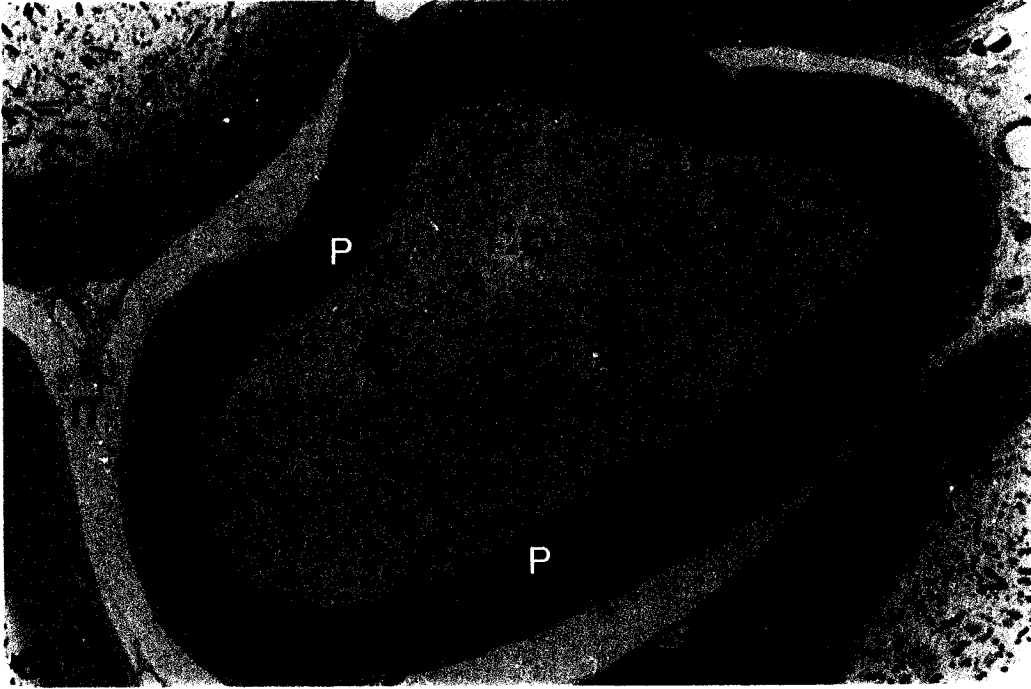
Figure 6b: Electron micrograph of the seminiferous epithelium of the testis at stage XI-XII of the cycle from a 30 week old HIP1^{-/-} mouse revealing numerous abnormalities in relation to the heads of step 11-12 elongating spermatids. Sp1 shows a condensed chromatin pattern of its nucleus and is closely enveloped by an acrosome (A), however, this spermatid is associated with a vast amount of cytoplasm (asterisk). Sp2 shows a highly indented nucleus (N) with a knob-like extension, and while it is capped by an acrosome (A), it does not show a condensed chromatin pattern. Sp3 possesses a bent head, but has an acrosome, while Sp4 lacks an acrosome. Both Sp3 and Sp4 have a condensed chromatin and appear to be enveloped by a common cytoplasm that contains a flagellum (F) showing an abnormal orientation to the spermatid heads. Sp4 is surrounded by a large amount of cytoplasm and has an uncondensed nucleus with a superfluous nuclear membrane (arrow) and complete absence of an acrosome. Only Sp2 is associated with an ectoplasmic specialization (ES). x4,300.



Figures 7a-d: Electron micrographs of spermatids at stage VII of the cycle of the testis from HIP1^{-/-} mice at 28 weeks of age (a), and of spherical germ cells in the epididymal lumen (Lu) at 21 weeks (b-c) and at 30 wks of age (d). In (a), an early spermatid (top) shows a proper developing acrosome on its nuclear surface. Another spermatid (below) shows a well defined thickened acroplaxome applied to its nuclear surface (arrowheads), but with only a partial acrosome (A) being applied to it, suggesting incomplete acrosome biogenesis in this cell. The cytoplasm of this cell shows several cross sectional flagellar profiles (F). In (b and c), spherical cells show numerous proacrosomic granules (arrows) in their cytoplasm that appear to have failed to fuse with each other. In (d), a spherical cell shows several larger acrosomic vesicles (A) that are not fused or associated with a nucleus. Note sperm head associated with a flagellum bounded by a common cytoplasm (curved arrow) and two flagella enveloped by a common cytoplasm (thick arrow). (a) x8,200; (b) x9,030; (c) x14,700; (d) x8,250.



Figures 8a-c: Light micrographs of cross sections of tubules of the epididymis from (a) wild type mice at 23 weeks and (b, c) HIP1^{-/-} mice at 11 weeks of age. The epithelium in (a) consists of numerous principal cells (P) with prominent microvilli and a few clear cells (C). Various sectional profiles of sperm heads, seen as dense tubular elements (arrowheads), and their flagella, seen as paler structures (circles), fill the lumen (Lu). In (b) and (c), the epithelial principal (P) and clear (C) cells are unchanged in appearance, but the lumen contains cells with a spherical appearance (solid arrows), some revealing a round nucleus with prominent nucleolus. While some sperm heads appear normal (arrowhead), others are enveloped by a mass of cytoplasm (open arrows). Circle, flagella of sperm. (a) x450; (b) x550; (c) x750.



Figures 9a-c: Electron micrographs of the lumen of the cauda epididymidis from (a) wild type mice at 12 weeks and (b, c) HIP1^{-/-} mice at 30 (b) and 21 (c) weeks of age. In (a), the lumen is filled with the heads of sperm consisting of their nucleus (N) and overlying acrosome (A). The heads of the sperm show a tubular appearance when cut within their long axes, and their nuclei are densely stained. There is no visible area of cytoplasm associated with the sperm heads of wild type mice. Their flagella (arrowheads), when cut in cross section, reveal that each is enveloped by its own plasma membrane, and only one flagellum is present within a given area of cytoplasm. In (b), spherical cells in the lumen present nuclei (N) with a granulated chromatin pattern capped by an irregularly shaped pale stained acrosome (A). These cells contain mitochondria (m) and small vesicular membranous profiles dispersed throughout their cytoplasm. The larger spherical cell shows 2 nuclei and an acrosome separated from the nucleus. In (c), several sperm heads present a residual acrosome (A) capping their nucleus or none at all. The sperm heads are enveloped by a dense mass of cytoplasm (stars), uncharacteristic of sperm in wild type mice. E, epithelium. (a) x1,700; (b) x6,000; (c) x8,580.

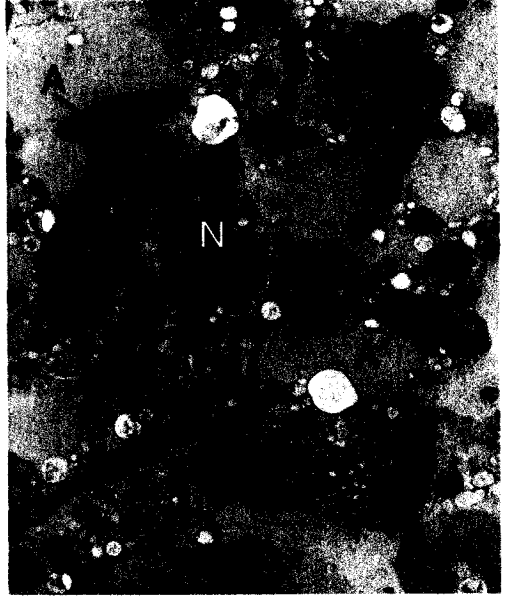
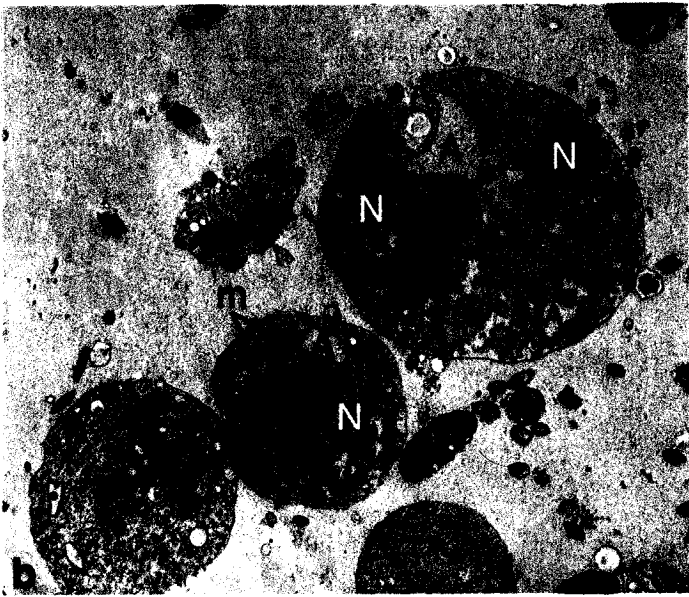
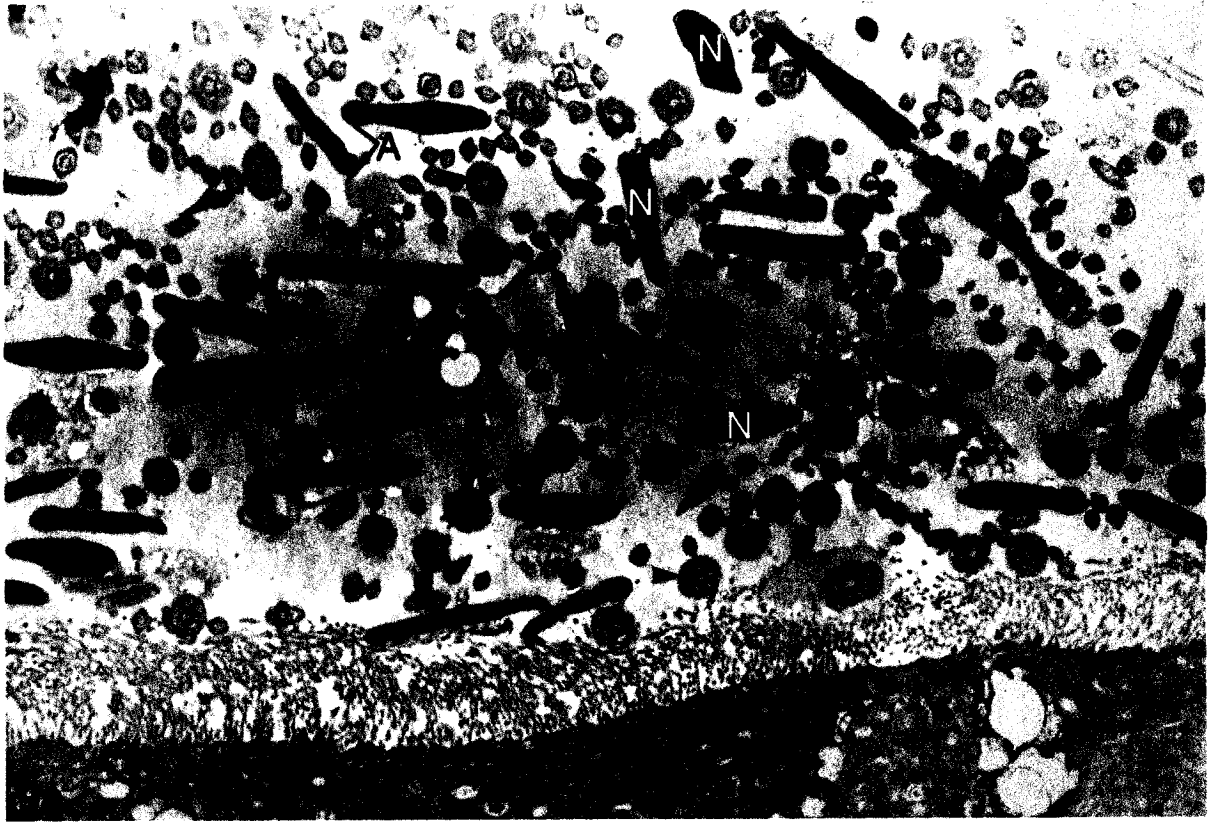


Figure 10a-e: Electron micrographs of isolated sperm obtained from the cauda epididymidis of HIP1^{-/-} mice at 12 weeks of age (a, c, d) and sperm present within the lumen of the cauda epididymidis of HIP1 knockout mice at 15 weeks of age (b, e). In (a), the heads of sperm present densely stained nuclei (N) that are more or less tubular in profile, with one showing a constriction along its length (arrow). The acrosome (A) caps the sperm nucleus, but is often detached from it and is at times highly irregular in appearance and folded upon itself. Several sperm heads are enveloped by a mass of cytoplasm containing a cross sectional profile of a flagellum (curved arrows). One sperm head is enveloped by a mass of cytoplasm with a bent flagellum (F) oriented perpendicular to its long axis. In some cases, an area of cytoplasm bordered by a single delimiting membrane contains more than one flagellar cross sectional profile (thick arrows). In (b), the flagellum (F) is closely juxtaposed and oriented parallel to the sperm head, a position never seen in wild type mice. In (c), the acrosome (A) overlying the sperm nucleus (N) is greatly displaced, and the sperm head is enveloped by a mass of cytoplasm containing a cross sectional profile of the flagellum (curved arrow). In (d), the sperm head has a constriction in its nucleus, a loosely applied acrosome (A), and several flagellar sectional profiles (thick arrows) in the cytoplasm extending away from the sperm head. In (e), two cross sectional flagellar profiles (thick arrows) share a common cytoplasm. (a, b, c,) x10,320; (d) x13,200; (e) x18,200.

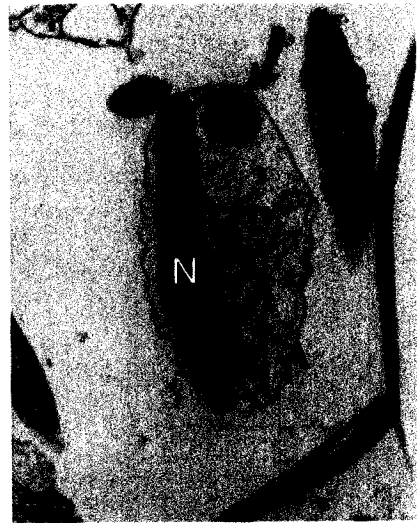


Figure 11. HIP1^{-/-} mice exhibit major problems reproducing. The average number of progeny that are obtained over a 3 month period is significantly reduced in homozygous matings of HIP1^{-/-} mice. Even fewer progeny are produced in male HIP1^{-/-} mice matings with wild-type partners (n = 8 mating pairs for each genotype combination; mean ± SEM, *** p < 0.0001).

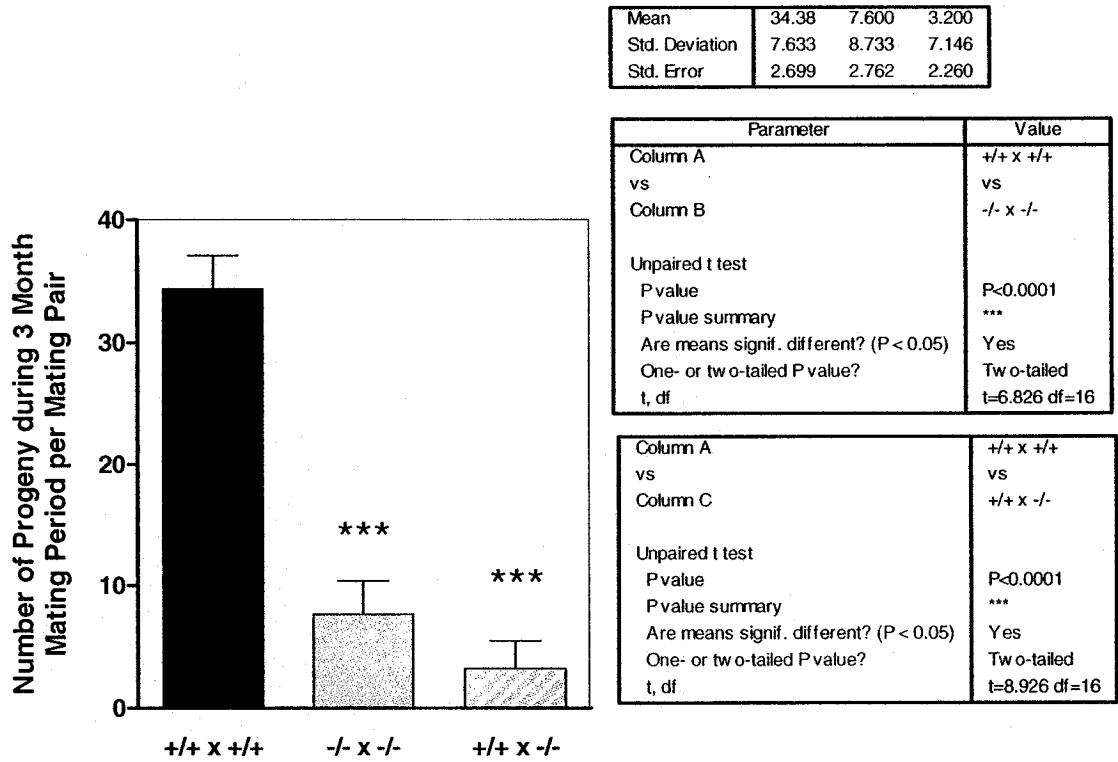


Fig. 11

Figure 12: Schematic drawings of the correct orientation and positioning of the flagellum of sperm in the epididymal lumen of wild type mice (a) as compared to its abnormal orientation in HIP1^{-/-} mice (b). In (a), the flagellum is oriented away from the long axis of the sperm head. Cross sections of the head (a1) reveal a nucleus capped by a tightly associated acrosome, with both being surrounded closely by a plasma membrane. In (a2 and a3), cross sections of the flagellum at its mid (MP) and principal piece (PP), show only one flagellum surrounded by a single membrane and scanty cytoplasm. In (b), the sperm head and flagellum are surrounded by a mass of cytoplasm, with the flagellum abnormally bent. In (b1), the sperm head is closely associated with flagellar cross sectional profiles that lie parallel to it. The acrosome is detached from the nuclear surface. In (b2), the cytoplasm of the flagellum contains 3 flagellar cross sectional profiles all bounded by a single plasma membrane. Such images suggest the instability of the flagellum in HIP1^{-/-} sperm possibly due to the absence of HIP1 and its role in actin and microtubule dynamics.

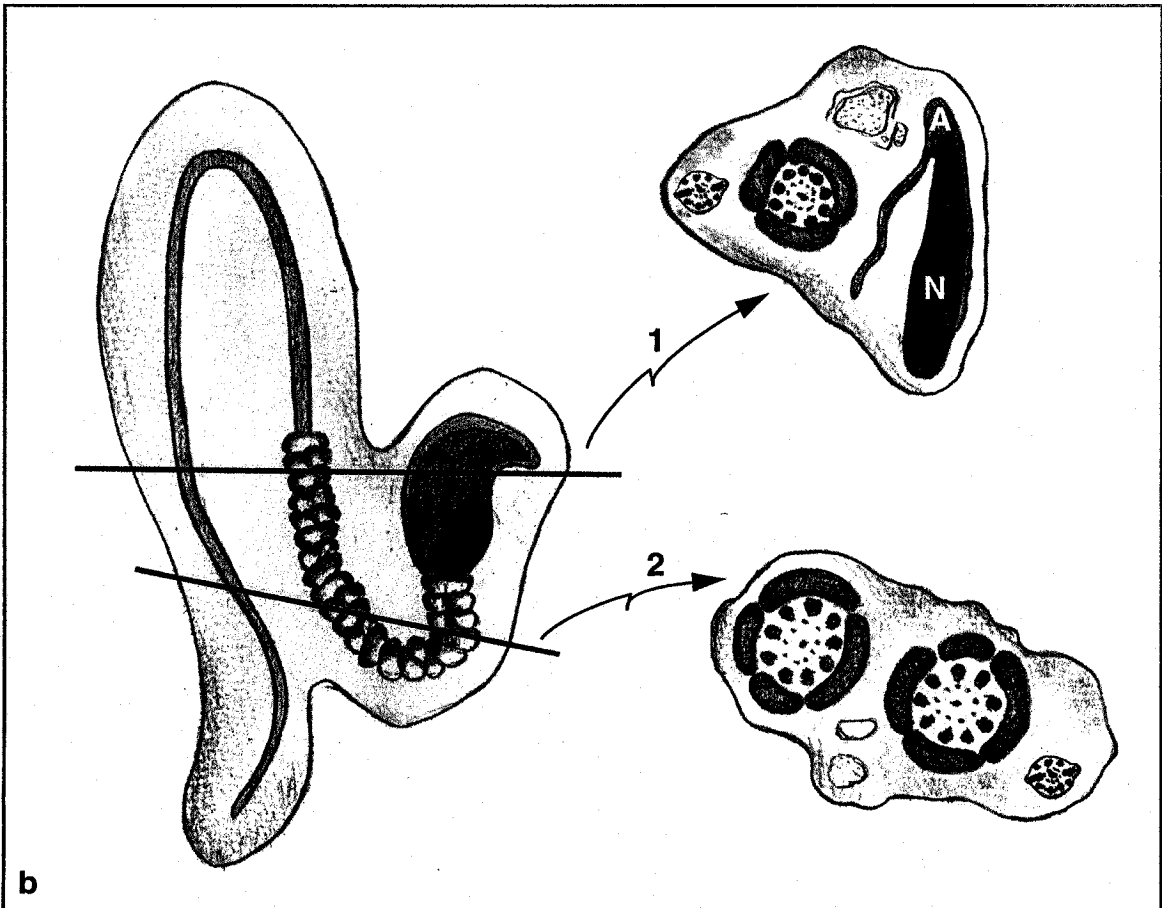
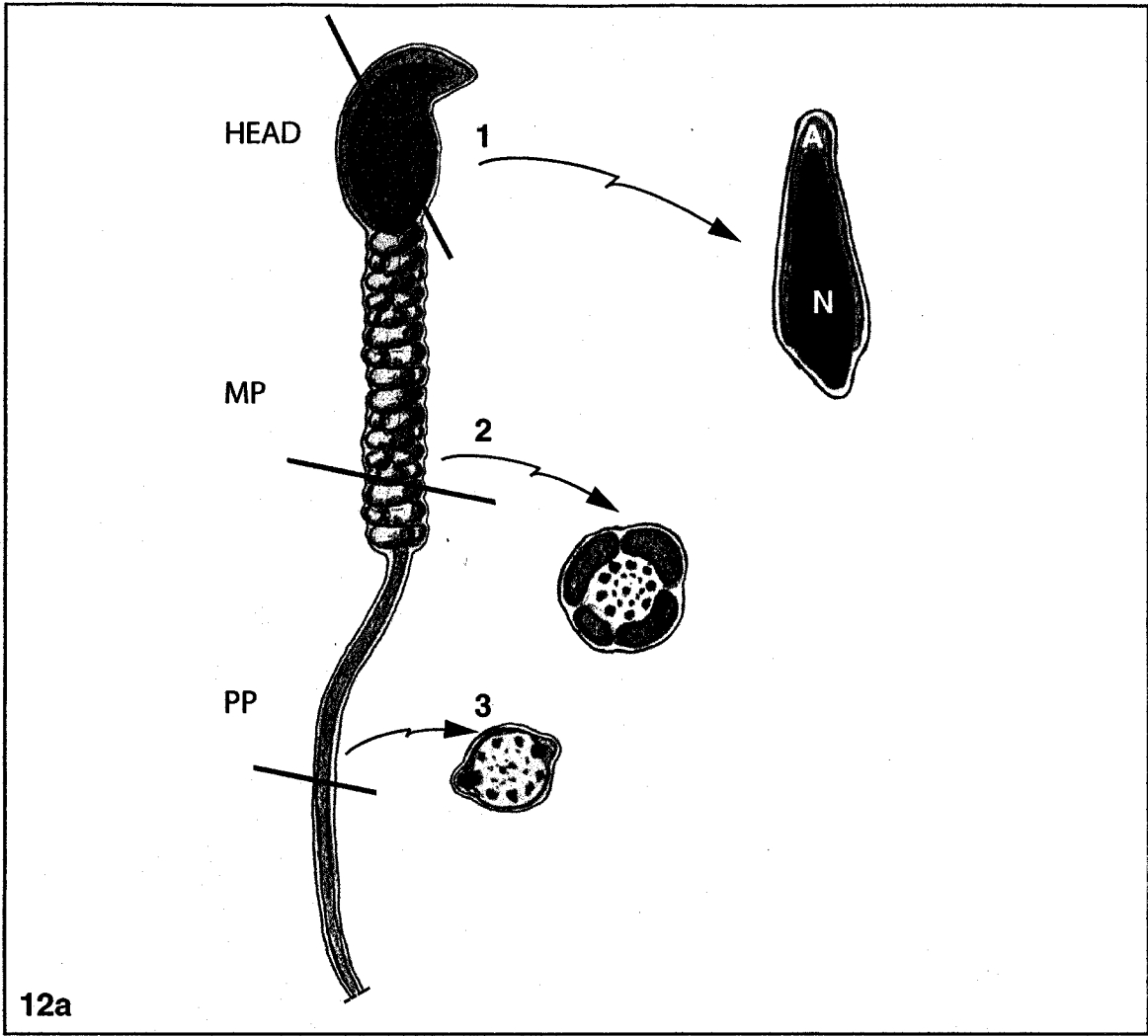


Figure 13: Scatter plots summarizing changes in the motility behavior of sperm from HIP1-/- mice compared to wild type controls. In Panels A and B, differences in means determined for each of the 14 motility parameters analyzed by CASA are plotted as percentages along the abscissa (from column 4 of Table 3; $\text{Mean}_{\text{HIP1-/-}} - \text{Mean}_{\text{WILD TYPE}} / \text{Mean}_{\text{WILD TYPE}} \times 100\%$), and differences between the sums of correlation coefficients computed for each parameter are plotted along the ordinate ($\sum \text{Pearson } r$ for Parameter_A across Parameters_{A-N} in HIP1-/- mice – $\sum \text{Pearson } r$ for Parameter_A across Parameters_{A-N} in wild type mice). Panel A shows results for correlation coefficients computed from raw sperm cell counts (Table 3, top) whereas Panel B shows results for correlation coefficients computed from motility data expressed as percentages of total sperm cell counts (Table 3, bottom). If there were no differences in the motility behavior of sperm from HIP1-/- mice and wild type mice then all points should plot near the “0” x-axis and “0” y-axis position (which they do not). **PANEL A:** motility parameters based on raw counts appear grouped into four clusters, one representing a sperm feature descriptor (Elong) and the directional descriptors (LIN, STR) (no significant changes in means and correlations slightly more negative overall in HIP1-/- mice), a second cluster representing the three velocity descriptors (VAP, VSL, VCL) (means less and correlations much more negative overall in HIP1-/- mice), a third cluster representing motility descriptors (Rapid, Prog, Medium, Motile) (means much less and correlations much more negative overall in HIP1-/- mice), and a fourth cluster containing one sperm (ALH) and one motility (Slow) descriptor (means less and correlations much more negative overall in HIP1-/- mice). Of the remaining two parameters, BCF shows no significant change in mean and slightly more positive correlations while Static increases dramatically in mean value and shows more negative correlations overall in HIP1-/- mice. **PANEL B:** correlations are shifted more positively and relationships between parameters are distributed somewhat differently when analyses are based on relative percentages rather than raw counts for motility parameters. Three groupings of the parameters are evident. One group contains %Rapid, %Prog, %Motile and BCF (decrease in means and mildly positive or negative correlations overall in HIP1-/- mice). A second group contains LIN and STR (no change of means and correlations more negative overall in HIP1-/- mice). The third group

contains VSL, VAP, VCL and ALH (decrease in means and correlations more negative overall in HIP1-/- mice). Three parameters - %Medium, %Slow, and Elong – have no significant change in mean value but show widely differing correlations in HIP1-/- mice. The percentage of sperm that are static (%Static) is markedly increased in the HIP1-/- mice. Taken together these graphs provide a visual “fingerprint” of changes in sperm numbers and behavior that characterize the HIP1-/-condition.

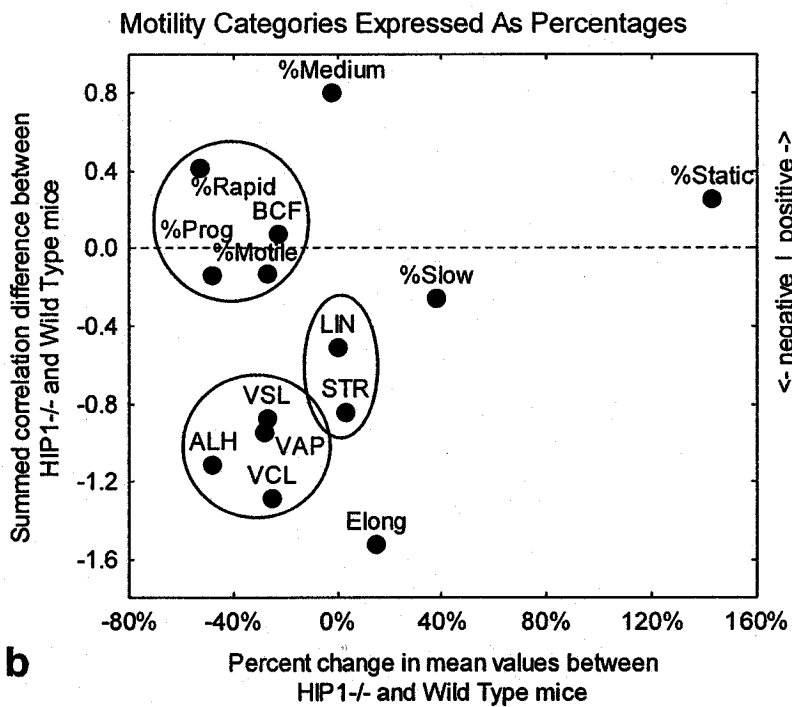
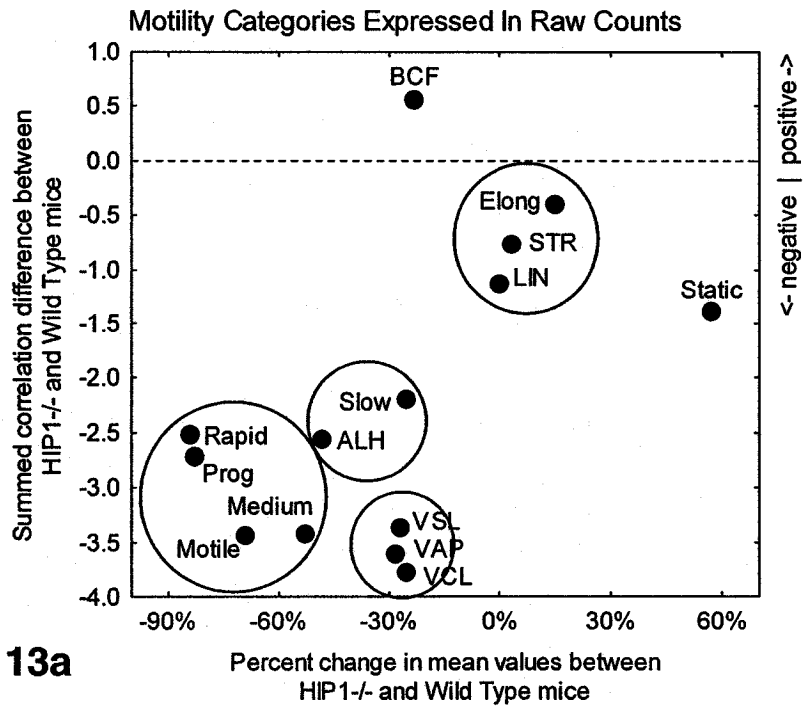


TABLE 1. Summary Statistics for Profile Area Measurements of Seminiferous Tubules in Testis

<u>Age</u>	<u>Wild Type Mice</u> Mean \pm SD (num. obs.) ¹	<u>HIP1-/- Mice</u> Mean \pm SD (num. obs.) ¹	<u>Change</u> ²	<u>p Values</u> ³	<u>Power</u> ⁴
7-11 wks	33302 \pm 7992 (289)	27225 \pm 6472 (282)	-18%	0.0000	1.0000
15-19 wks	32445 \pm 7234 (299)	23228 \pm 5967 (208)	-28%	0.0000	1.0000
24-30 wks	37816 \pm 7836 (198)	27829 \pm 7114 (216)	-26%	0.0000	1.0000

¹Number of observations= number of tubular profiles measured in sections from 3 mice per age per group

²For HIP1-/- mice compared to wild type mice

³Mann-Whitney U Test for Wild Type vs HIP1-/- by age; p values < 0.05 are considered significantly different

⁴This is the power associated with rejecting the null hypothesis the two means are equal

TABLE 2. Summary Statistics for Profile Area Measurements in Epididymis¹

	<u>Wild Type Mice</u>	<u>HIP1-/- Mice</u>	<u>Change</u> ³	<u>p Values</u> ⁴
	Mean ± SD (N= 202) ²	Mean ± SD (N=188) ²		
Outer	14170 ± 7247	13392 ± 6529	-5%	0.9169 NS
Lumen	3015 ± 1292	3203 ± 1502	6%	0.1863 NS
Epithelium	11131 ± 6308	10205 ± 5467	-8%	0.6589 NS

¹In animals at 13 weeks of age; pooled results from measurements taken from initial segment and caput/corpus regions

²Number of observations= number of tubular profiles measured in sections from 3 mice per age per group

³For HIP1-/- mice compared to wild type mice

⁴Mann-Whitney U Test for Wild Type vs HIP1-/-; p values < 0.05 are considered significantly different (NS, not significant)

Table 3. Sperm Counts & Motility Changes Comparing HIP1^{-/-} to Wild Type Mice

Parameter ¹	Wild Type Mice	HIP1 ^{-/-} Mice	Change ³	p values ⁴	Power ⁵
	Mean ± SD (Num Obs) ²	Mean ± SD (Num Obs) ²			
Sperm Counts					
Expt 1	19.1 ± 5.8 (180)	7.1 ± 2.9 (144)	-63%	0.0000	1.0000
Expt 2 ⁶	45.6 ± 31.1 (185)	22.9 ± 21.4 (159)	-50%	0.0000	1.0000
Raw Values:					
	(185)	(159)			
VAP	59.2 ± 11.9	42.6 ± 12.7	-28%	0.0000	1.0000
VSL	47.1 ± 10.4	34.4 ± 11.3	-27%	0.0000	1.0000
VCL	89.4 ± 16.6	67.0 ± 18.7	-25%	0.0000	1.0000
ALH	2.9 ± 1.0	1.8 ± 1.4	-48%	0.0000	1.0000
BCF	1.7 ± 2.0	1.3 ± 2.7	-23%	0.1955	NS 0.2527
Motile	37.5 ± 27.6	11.8 ± 9.5	-69%	0.0000	1.0000
Prog(ressive)	11.5 ± 9.4	2.0 ± 1.8	-83%	0.0000	1.0000
Rapid	18.8 ± 14.4	3.1 ± 2.5	-84%	0.0000	1.0000
Medium	18.7 ± 14.4	8.7 ± 8.5	-53%	0.0000	1.0000
Slow	2.0 ± 2.5	1.5 ± 2.4	-25%	0.1020	NS 0.3712
Static	6.1 ± 4.6	9.6 ± 15.1	57%	0.0030	0.8393
Ratios:					
	(185)	(159)			
STR	78.7 ± 4.8	80.7 ± 7.8	3%	0.6464	NS 0.0747
LIN	54.3 ± 5.9	54.0 ± 11.0	0%	0.9556	NS 0.0500
Elong(ation)	46.1 ± 4.1	52.8 ± 8.6	15%	0.2161	NS 0.2345
Percentages:					
	(185)	(159)			
%Motile	81.4 ± 9.1	59.1 ± 22.4	-27%	0.0000	0.9959
%Prog(ressive)	25.0 ± 8.9	13.0 ± 13.2	-48%	0.0053	0.8072
%Rapid	40.9 ± 10.8	19.3 ± 16.3	-53%	0.0000	0.9935
%Medium	40.6 ± 9.9	39.8 ± 18.9	-2%	0.8802	NS 0.0523
%Slow	3.9 ± 4.0	5.4 ± 7.3	38%	0.5080	NS 0.0999
%Static	14.6 ± 8.9	35.5 ± 23.1	143%	0.0000	0.9950

¹Explanation of parameters

Sperm Counts (millions/ml)

VAP: Smoothed Path Velocity (µm/sec)

VCL: Track Velocity (µm/sec)

VSL: Straight Line Velocity (µm/sec)

ALH: Amplitude of Lateral Head Displacement (µm)

BCF: Beat Cross Frequency (hertz)

Number (in millions) or Percent of:

Motile, Progressively Motile (Prog), Rapid, Medium, Slow and Static Cells

STR: Straightness (ratio of VSL/VAP)

LIN: Linearity (ratio of VSL/VCL)

Elongation: head shape (ratio of minor to major axis of sperm head)

²Total number of observations (measurements) made from a pool of 9 wild type and 5 HIP1^{-/-} mice

³For HIP1^{-/-} mice compared to wild type mice

⁴p values < 0.05 are considered significantly different (NS, Not Significant). A Fisher's Exact Test was used to compare differences between means for "Ratios" and "Percentages"

⁵This is the power associated with rejecting the null hypothesis the two means are equal. The Z-test for comparing two proportions was used in power calculations for variables listed under "Ratios" and "Percentages"

⁶This experiment at roughly 2.5 times higher sperm concentrations was used to obtain all data listed below under "Raw Counts", "Ratios", and "Percentages"

REFERENCES

- Abou-Haila A, Tulsiani DR. 2000. Mammalian sperm acrosome: formation, contents, and function. *Arch Biochem Biophys* 379:173-82.
- Chen H, Fre S, Slepnev VI, Capua MR, Takei K, Butler MH, Di Fiore PP, and De Camili P. 1998. Epsin is an EH-domain-binding protein implicated in clathrin-mediated endocytosis. *Nature* 394: 793-797.
- Chen C-Y, Brodsky FM. 2005. Huntingtin-interacting protein 1 (Hip1) and Hip1-related protein (Hip1R) bind the conserved sequence of clathrin light chains and thereby influence clathrin assembly *in vitro* and actin distribution *in Vivo*. *J Biol Chem* 280: 6109-6117.
- Chopra VS, Metzler M, Rasper DM, Engqvist-Goldstein AE, Singaraja R, Gan L, Fichter KM, McCutcheon K, Drubin D, Nicholson DW, Hayden MR. 2000. HIP12 is a non-proapoptotic member of a gene family including HIP1, an interacting protein with huntingtin. *Mammalian Genome* 11: 1006-1015.
- Chung S, Wang SP, Pan L, Mitchell G, Trasler J, Hermo L. 2001. Infertility and testicular defects in hormone-sensitive lipase-deficient mice. *Endocrinol* 142:4272-81.
- Clermont Y. Kinetics of spermatogenesis in mammals: seminiferous epithelium cycle and spermatogonial renewal. 1972. *Physiol Rev* 52:198-236.
- Clermont Y, Oko R and Hermo L. 1993. Cell biology of mammalian spermiogenesis. *In* Cell and molecular biology of the testis. Desjardings V and Ewing L., editors. Oxford University Press, New York, pp 332-376.

Dragatsis I, Levine MS, Zeitlin S. 2000. Inactivation of Hdh in the brain and testis results in progressive neurodegeneration and sterility in mice. *Nat. Genet*, 26: 300-306.

Eddy EM. 1998. Regulation of gene expression during spermatogenesis. *Semin Cell Dev Biol* 9:451-457.

Eddy EM. 1999. The effects of gene knockouts on spermatogenesis. *In The Male Gamete: applications*. C. Gagnon, editor. Cache River Press, Vienna, Ill, pp 23-26.

Eddy EM, O'Brien DA. 1993. The spermatozoon. *In The Physiology of Reproduction*. Knobil E, Neill JD, editors. New York, Raven Press, pp 29-77.

Engqvist-Goldstein AE, Kessels MM, Chopra VS, Hayden MR, Drubin DG. 1999. An actin-binding protein of the sla2/Huntingtin interacting protein 1 family is a novel component of clathrin-coated pits and vesicles. *J Cell Biol* 147:1503-1518.

Engqvist-Goldstein AE, Warren RA, Kessels MM, Keen JH, Heuser J, Drubin DG. 2001. The actin-binding protein Hip1R associates with clathrin during early stages of endocytosis and promotes clathrin assembly in vitro. *J Cell Biol* 154:1209-23.

Engqvist-Goldstein AE, Zhang CX, Carreno S, Barroso C, Heuser JE, Drubin DG. 2004. RNAi-mediated Hip1R silencing results in stable association between the endocytic machinery and the actin assembly machinery. *Mol Biol Cell* 15:1666-79.

Ford MG, Pearse BM, Higgins MK, Vallis Y, Owen DJ, Gibson A, Hopkins CR, Evans PR, McMahon HT. 2001. Simultaneous binding of PtdIns_{4,5}P₂ and clathrin by AP180 in the nucleation of clathrin lattices on membranes. *Science* 291: 1051-1055.

Ford MG, Mills IG, Peters BJ, Vallis Y, Praefcke GJ, Evans PR, McMahon HT. 2002. Curvature of clathrin-coated pits driven by epsin. *Nature* 419: 361-6.

Fouquet JP, Kann ML. 1992. Species-specific localization of actin in mammalian spermatozoa: fact or artifact? *Microsc Res Tech.* 20:251-8.

Gaidarov I, Santini F, Warren RA, and Keen JH. 1999. Spatial control of coated-pit dynamics in living cells. *Nat Cell Biol* 1:1-7.

Gerard A, Nya AE, Egloff M, Domingo M, Degrelle H, Gerard H. 1991. Endocytosis of human sex steroid-binding protein in monkey germ cells. *Ann N Y Acad Sci* 637:258-76.

Gerard H, Gerard A, En Nya A, Felden F, Gueant JL. 1994. Spermatogenic cells do internalize Sertoli androgen-binding protein: a transmission electron microscopy autoradiographic study in the rat. *Endocrinol* 134:1515-27.

Griffiths G, Warren G, Stuhlfauth I, Jockusch BM. 1981. The role of clathrin-coated vesicles in acrosome formation. *Eur J Cell Biol* 26:52-60.

Griswold MD. 1993. Protein secretion by Sertoli cells: General considerations. *In* The Sertoli Cell. Russell LD and Griswold MD, editors. Cache River Press, Clearwater, Florida, pp195-200.

Grover A, Sairam MR, Smith CE, Hermo L. 2004. Structural and functional modifications of sertoli cells in the testis of adult follicle-stimulating hormone receptor knockout mice. *Biol Reprod* 71:1117-29.

Grover A, Smith CE, Gregory M, Cyr DG, Sairam MR, Hermo L. 2005. Effects of FSH receptor deletion on epididymal tubules and sperm morphology, numbers, and motility. *Mol Reprod Dev* 72:135-144.

Hecht NB.1998. Molecular mechanisms of male germ cell differentiation. *Bioessays* 20:555-61.

Hermo L, Rambourg A, Clermont Y. 1980. Three-dimensional architecture of the cortical region of the Golgi apparatus in rat spermatids. *Am J Anat* 157: 357-73.

Hussain NK, Yanabhai M, Bhakar AL, Metzler M, Ferguson SSG, Hayden MR, McPherson PS, Kay BK. 2003. A role for epsin N-terminal homology/AP180 N-terminal homology (ENTH/ANTH) domains in tubulin binding. *J Biol Chem* 278: 28823-28830.

Hyun TS, Li L, Oravec-Wilson KI, Bradley SV, Provot MM, Munaco AJ, Mizukami IF, Sun H, Ross TS. 2004. Hip1-related mutant mice grow and develop normally but have accelerated spinal abnormalities and dwarfism in the absence of HIP1. *Mol Cell Biol* 24: 4329-4340.

Igdoura SA, Herscovics A, Lal A, Moremen KW, Morales CR, Hermo L. 1999. Alpha-mannosidases involved in N-glycan processing show cell specificity and distinct subcompartmentalization within the Golgi apparatus of cells in the testis and epididymis. *Eur J Cell Biol* 78: 441-52.

Itoh T, Koshiha S, Kigawa T, Kikuchi A, Yokoyama S, Takenawa T. 2001. Role of the ENTH domain in phosphatidylinositol-4,5-bisphosphate binding and endocytosis. *Science* 291: 1047-1051.

Kalchman MA, Koide HB, McCutcheon K, Graham RK, Nichol K et al. 1997. HIP1, a human homologue of *S. cerevisiae* Sla2p, interacts with membrane-associated huntingtin in the brain. *Nat Genet* 16:44-53.

Kang-Decker N, Mantchev GT, Juneja SC, McNiven MA, van Deursen JMA. 2001. Lack of acrosome formation in Hrb-deficient mice. *Science* 294: 1531-1533.

Kierszenbaum AL, Rivkin E, Tres LL. 2003. Acroplaxome, an F-actin-Keratin-containing plate, anchors the acrosome to the nucleus during shaping of the spermatid head. *Mol Biol Cell* 14: 4628-4640.

Kierszenbaum AL and Tres LL. 2004. The acrosome-acroplaxome-manchette complex and the shaping of the spermatid head. *Arch Histol Cytol* 67: 271-284.

Leblond CP, Clermont Y. 1952. Spermiogenesis of rat, mouse, hamster and guinea pig as revealed by the periodic acid-fuchsin sulfurous acid technique. *Am J Anat* 90:167-215.

Legendre-Guillemain V, Metzler M, Charbonneau M, Gan L, Chopra V, Philie J, Hayden MR, McPherson PS. 2002. HIP1 and HIP12 display differential binding to F-actin, AP2, and clathrin. Identification of a novel interaction with clathrin light chain. *J Biol Chem* 277: 19897-19904.

Legendre-Guillemain V, Wasiak S, Hussain NK, Angers A, McPherson PS. 2004. ENTH/ANTH proteins and clathrin-mediated membrane budding. *J Cell Science* 117: 9-18.

Legendre-Guillemine V, Metzler M, Lemaire J-F, Philie J, Gan L, Hayden MR, and McPherson PS. 2005. Huntingtin interacting protein 1 (HIP1) regulates clathrin assembly through direct binding to the regulatory region of the clathrin light chain. *J Biol Chem* 280: 6101-6108.

Lufkin T, Lohnes D, Mark M, Dierich M, Gorry P, Gaub M-P, Le Meur M, Chambon P. 1993. High postnatal lethality and testis degenerations in retinoic acid receptor α mutant mice. *Proc Natl Acad Sci USA* 90 :7225-7229.

Meistrich ML. Nuclear morphogenesis during spermiogenesis.1993. *In* Molecular biology of the male reproductive system. De Krester D, editor. Academic Press, New York, pp 67-97.

Mendoza-Lujambio I, Burfeind P, Dixkens C, Meinhardt A, Hoyer-Fender S, Engel W, Neesen J. 2002. The Hook 1 gene is non-functional in the abnormal spermatozoon head shape (azh) mutant mouse. *Hum Mol Genet* 11 : 1647-1658.

Metzler M, Gertz A, Sarkar M, Schachter H, Schrader JW, Marth JD. 1994. Complex asparagines-linked oligosaccharides are required for morphogenic events during post-implantation development. *EMBO J.* 13:2056-2065.

Metzler M, Legendre-Guillemain V, Gan L, Chopra V, Kwok A, McPherson PS, Hayden MR. 2001. HIP1 functions in clathrin-mediated endocytosis through binding to clathrin and adaptor protein 2. *J Biol Chem* 276: 39721-39276.

Mishra SK, Agostinelli NR, Brett TJ, Mizukami I, Ross TS, Traub LM. 2001. Clathrin- and AP-2 binding sites in HIP1 uncover a general assembly role for endocytic accessory proteins. *J Biol Chem.* 276: 46230-46236.

Monesi V. 1965. Synthetic activities during spermatogenesis in the mouse RNA and protein. *Exp Cell Res* 39:197-224.

Morales CR, Clermont Y, Hermo L. 1985. Nature and function of endocytosis in Sertoli cell of the rat. *Am J Anat* 173: 203-217.

Morales C and Clermont Y. 1993. Structural changes of the Sertoli cell during the cycle of the seminiferous epithelium. In *The Sertoli Cell*. Russell LD and Griswold MD, editors. Cache River Press, Clearwater, Florida, pp 305-330.

Morales CR, Zhao Q, El-Alfy M, Suzuki K. 2000. Targeted disruption of the mouse prosaposin gene affects the development of the prostate gland and other male reproductive organs. *J Androl* 21: 765-775.

Moreno RD, Ramalho-Santos J, Sutovsky P, Chan EK, Schatten G. 2000. Vesicular traffic and golgi apparatus dynamics during mammalian spermatogenesis: implications for acrosome architecture. *Biol Reprod* 63:89-98.

O'Brien DA, Gabel CA, Rockett DL, Eddy EM. 1989. Receptor-mediated endocytosis and differential synthesis of mannose 6-phosphate receptors in isolated spermatogenic and sertoli cells. *Endocrinol* 125:2973-84.

Oko R. 1998. Occurrence and formation of cytoskeletal proteins in mammalian spermatozoa. *Andrologia* 30:193-206.

O'Brien DA, Gabel CA, Eddy EM. 1993. Mouse Sertoli cells secrete mannose 6-phosphate containing glycoproteins that are endocytosed by spermatogenic cells. *Biol Reprod* 49:1055-65.

Oko R, Clermont Y. 1991. Origin and distribution of perforatorial proteins during spermatogenesis of the rat: an immunocytochemical study. *Anat Rec* 230:489-501.

Paranko J, Yagi A, Kuusisto M. 1994. Immunocytochemical detection of actin and 53 kDa polypeptide in the epididymal spermatozoa of rat and mouse. *Anat Rec* 240:516-27.

Percival JM, Hughes JA, Brown DL, Schevzov G, Heimann k, Vrhovski B, Bryce N, Stow JL, and Gunning PW. 2004. Targeting of a tropomyosin isoform to short microfilaments associated with the Golgi complex. *Mol Biol Cell* 15:268-290.

Petrie RG Jr, Morales CR. 1992. Receptor-mediated endocytosis of testicular transferring by germinal cells of rat testis. *Cell Tissue Res.* 267:45-55.

Prigent Y, Dadoune JP. 1993. Immunoelectron microscopic distribution of actin in the spermatids and epididymal spermatozoa of the mouse. *Acta Anat (Basel)* 147:133-9.

Raamsdonk JMV, Pearson J, Rogers DA, Bissada N, Vogl AW, Hayden MR, Leavitt BR. 2005. Loss of wild-type huntingtin influences motor dysfunction and survival in the YAC128 mouse model of Huntington disease. *Hum Mol Genet* 14: 1379-1392.

Rao DS, Chang JC, Kumar PD, Mizukami I, Smithson GM, Bradley SV, Parlow AF, Ross TS. 2001. Huntingtin Interacting protein 1 is a clathrin coat binding protein required for differentiation of late spermatogenic progenitors. *Mol Cell Biol* 21: 7796-7806.

Russell LD. 1977. Desmosome-like junctions between Sertoli cells and germ cells in the rat testis. *Am J Anat* 148: 301-312.

Russell LD, Clermont Y. 1977. Degeneration of germ cells in normal, hypophysectomized and hormone treated hypophysectomized rats, *Anat Rec* 187:347-66.

Russell LD, Russell JA, MacGregor GR, Meistrich ML. 1991. Linkage of manchette microtubules to the nuclear envelope and observations of the role of the manchette in nuclear shaping during spermiogenesis in rodents. *Am J Anat* 192:97-120.

Russell LD, Goh JC, Rashed RM, Vogl AW. 1988. The consequences of actin disruption at Sertoli ectoplasmic specialization sites facing spermatids after in vivo exposure of rat testis to cytochalasin D. *Biol Reprod* 39: 105-18.

Russell LD. 1993. Role in Spermiation. In *The Sertoli Cell*. Russell LD and Griswold MD, editors. Cache River Press, Clearwater, Florida, pp 269-303.

Ruz R, Gregory M, Smith CE, Cyr D, Hess RA, Lubhan D, Hermo L. 2005. Effects of lab chow and phytoestrogen-free casein diets on sperm counts, sperm motility, and expression of aquaporin-1,-9 and -10 in the efferent ducts of α ERKO adult mice.

Segretain D, Egloff M, Gerard N, Pineau C, Jegou B. 1992. Receptor-mediated and absorptive endocytosis by male germ cells of different mammalian species. *Cell Tissue Res* 268:471-8.

Senetar MA, Foster SJ, McCanna RO. 2004. Intrasteric inhibition mediates the interaction of the I/LWEQ module proteins Talin 1, Talin 2, Hip1, and Hip12 with actin. *Biochemistry* 43: 15418-15428.

Susi FR, Leblond CP, Clermont Y. 1971. Changes in the Golgi apparatus during spermiogenesis in the rat. *Am J Anat* 130: 251-67.

Syed V, Gomez E, Hecht N. 1999. mRNAs encoding a von Ebner's-like protein and the Huntington disease protein are induced in rat male germ cells by sertoli cells. *J Biol Chem* 274:10737-10742.

Sylvester SR, Griswold MD. 1984. Localization of transferrin and transferring receptors in rat testis. *Biol Reprod* 31:195-203.

Thorne-Tjomslund G, Clermont Y and Hermo L. 1988. Contribution of the Golgi Apparatus Components to the Formation of the Acrosomic System and Chromatoid Body in Rat Spermatids. *Anat Rec* 221: 591-598.

Toshimori K. 2003. Biology of spermatozoa maturation: an overview with an introduction to this issue. *Micros Res Tech* 61:1-6.

Vogl AW, Grove BD, Lew GJ. 1986. Distribution of actin in Sertoli cell ectoplasmic specializations and associated spermatids in the ground squirrel testis. *Anat Rec* 215:331-41.

Vogl AW. 1989. Distribution and function of organized concentrations of actin filaments in mammalian spermatogenic cells and Sertoli cells. *Int Rev Cytol* 119:1-56.

Vogl AW, Pfeiffer DC, Redenbach DM and Grove BD. 1993. Sertoli cell cytoskeleton. In *The Sertoli Cell*. Russell LD and Griswold MD, editors. Cache River Press, Clearwater, Florida, pp 39-86.

Waelter S, Scherzinger E, Hasenbank R, Nordhoff E, Lurz R, Goehler H, Gauss C, Sathasivam K, Bates GP, Lehrach H, Wanker EE. 2001. The huntingtin interacting protein HIP1 is a clathrin and alpha-adaptin-binding protein involved in receptor-mediated endocytosis. *Hum Mol Genet* 10:1807-17.

Wanker EE, Rovira C, Scherzinger E, Hasenbank R, Walter S et al. 1997. HIP1: a huntingtin interacting protein isolated by the yeast two-hybrid system. *Hum Mol Genet* 6: 487-495.

Weber JE, Russell LD. 1987. A study of intercellular bridges during spermatogenesis in the rat. *Am J Anat* 189:1-24.

Yao R, Ito C, Natsume Y, Sugitani Y, Yamanaka H, Kuretake S, Yanagida K, Sato A, Toshimori K, Noda T. 2002. Lack of acrosome formation in mice lacking a Golgi protein, GOPC. *Proc Natl Acad Sci USA* 99: 11211-11216.

Zhao G-Q, Liaw L, Hogan BLM. 1998. Bone morphogenetic protein 8A plays a role in the maintenance of spermatogenesis and the integrity of the epididymis. *Development* 125: 1103-1112.

Chapter III

Summary

Summary

Huntingtin-interacting protein 1-deficiency (HIP1^{-/-}) in mice results in a neurological phenotype, however, homozygous males also show defects in the male reproductive tract. These mice showed decreased testicular weights compared to the wild-type mice along with a significant decrease in the mean profile area of the seminiferous tubules of the testis. LM immunocytochemical studies revealed that HIP1 localized to Sertoli cells, to the Golgi of all germ cells as well as the cytoplasm of elongating spermatids and lightly in the cytoplasm of round spermatids.

We showed by histological examination of the reproductive tract of these knockout males that major abnormalities were found in the testis. HIP1^{-/-} phenotype resulted in a mosaic appearance with some seminiferous tubules having a normal appearance and others showing varying degrees of abnormalities. For those tubules affected, mild to severe forms of degeneration were observed, with the severe tubules showing numerous vacuoles and the loss of spermatids and/or spermatocytes.

It is still unclear as to why variable effects are produced. The best explanation we can give is that other proteins, perhaps HIP1r play partial compensatory mechanisms to maintain low fertility levels in these mice. HIP1r deficient mice are fertile and show no signs of testicular degeneration. HIP1r protein has never been localized to a cell type in the testis and localization of this protein or evaluation of compensatory changes in gene expression in isolated germ cells from the knock out animals might help us explain the HIP1^{-/-} phenotype.

We showed by detailed light and electron microscopic analysis that the late elongating spermatids and the Sertoli cells were the cell types showing the major abnormalities in the testis. In the spermatids, these changes included: partial or complete absence of acrosome or its detachment from the nucleus, structural deformation of the head, bent flagella and retention of cytoplasm enveloping the sperm head. In Sertoli cells, their organelles and the blood-testis barrier were comparable to the wild type.

However, structural abnormalities were noted with respect to the association of elongating spermatids with the ectoplasmic specializations of the Sertoli cells. Spermatogonia, spermatocytes and Leydig cells appeared to be unaffected.

Examination of the knock out epididymis indicated a reduction of normal spermatozoa, and the presence of numerous structurally abnormal sperm with bent tails as well as numerous spherical germ cells in the lumen. This finding supports the testicular finding of abnormal spermatid development of spermatids and the sloughing and the loss of germ cells due to Sertoli cell alterations.

Our findings at the electron microscopy level suggest a role for HIP1 with respect to actin and microtubules since sperm head and tail contain these cytoskeletal components. The abnormalities we saw do not appear to be a consequence of an alteration of endocytic activity with respect to clathrin coated vesicles at the plasma membrane. First, HIP1 was expressed not at the plasma membrane but in the Golgi of germ cells. Second, unfused proacrosomic granules were found in some spherical germ cells in the epididymal lumen, meaning that the major defect is not the formation of clathrin coated vesicles from the Golgi, but the fusion of the proacrosomic vesicles and their tethering to the nuclear envelope.

Next, the structural changes to sperm corroborated our data on sperm motility and sperm counts. Sperm counts were decreased by over 50% in the HIP1^{-/-} mice compared to the wild-type mice. Computer assisted sperm analysis (CASA) indicated that most motility parameters were significantly lower in HIP1^{-/-} mice compared to the wild-type mice except for the number of static sperm which was increased by over 100% in the knock out animal. These differences in turn accounted for the reduced fertility levels between HIP1^{-/-} and wildtype mice.

In conclusion, differences in sperm counts, morphology and motility of HIP1 deficient mice reflect changes in sperm development in the testis and not sperm maturation which occurs in the epididymis, as the latter was structurally normal in

appearance and in size since the epididymal profile areas in HIP1 deficient mice showed no significant change in comparison to wild-type animals.

Future experiments are needed to confirm some of our results. It would be vital to do electron microscopy and do immunolabeling of HIP1 and determine where it localizes to in the Golgi apparatus of germ cells. Immunofluorescence with phalloidin in the HIP1^{-/-} mice will also help explain if actin distribution is affected in the knock out mice. More specifically, it would be beneficial to look at both actin and tubulin distribution in round spermatids in the HIP1 knockout and compare it to controls.